

1996

Gaseous flux and distribution of polycyclic aromatic hydrocarbons across the air-water interface of southern Chesapeake Bay

Kurt E. Gustafson

College of William and Mary - Virginia Institute of Marine Science

Follow this and additional works at: <https://scholarworks.wm.edu/etd>



Part of the [Environmental Sciences Commons](#), [Mechanical Engineering Commons](#), and the [Oceanography Commons](#)

Recommended Citation

Gustafson, Kurt E., "Gaseous flux and distribution of polycyclic aromatic hydrocarbons across the air-water interface of southern Chesapeake Bay" (1996). *Dissertations, Theses, and Masters Projects*. Paper 1539616678.

<https://dx.doi.org/doi:10.25773/v5-yj7r-qa26>

This Dissertation is brought to you for free and open access by the Theses, Dissertations, & Master Projects at W&M ScholarWorks. It has been accepted for inclusion in Dissertations, Theses, and Masters Projects by an authorized administrator of W&M ScholarWorks. For more information, please contact scholarworks@wm.edu.

INFORMATION TO USERS

This manuscript has been reproduced from the microfilm master. UMI films the text directly from the original or copy submitted. Thus, some thesis and dissertation copies are in typewriter face, while others may be from any type of computer printer.

The quality of this reproduction is dependent upon the quality of the copy submitted. Broken or indistinct print, colored or poor quality illustrations and photographs, print bleedthrough, substandard margins, and improper alignment can adversely affect reproduction.

In the unlikely event that the author did not send UMI a complete manuscript and there are missing pages, these will be noted. Also, if unauthorized copyright material had to be removed, a note will indicate the deletion.

Oversize materials (e.g., maps, drawings, charts) are reproduced by sectioning the original, beginning at the upper left-hand corner and continuing from left to right in equal sections with small overlaps. Each original is also photographed in one exposure and is included in reduced form at the back of the book.

Photographs included in the original manuscript have been reproduced xerographically in this copy. Higher quality 6" x 9" black and white photographic prints are available for any photographs or illustrations appearing in this copy for an additional charge. Contact UMI directly to order.

UMI

A Bell & Howell Information Company
300 North Zeeb Road, Ann Arbor MI 48106-1346 USA
313/761-4700 800/521-0600

**GASEOUS FLUX AND DISTRIBUTION OF POLYCYCLIC AROMATIC HYDROCARBONS
ACROSS THE AIR-WATER INTERFACE OF SOUTHERN CHESAPEAKE BAY**

A Dissertation
Presented to
The Faculty of the School of Marine Science
The College of William and Mary

In Partial Fulfillment
Of the Requirements for the Degree of
Doctor of Philosophy

by
Kurt E. Gustafson
1996

UMI Number: 9622286

**Copyright 1996 by
Gustafson, Kurt Eduard**

All rights reserved.

**UMI Microform 9622286
Copyright 1996, by UMI Company. All rights reserved.**

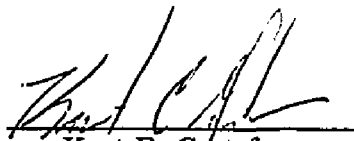
**This microform edition is protected against unauthorized
copying under Title 17, United States Code.**

UMI
300 North Zeeb Road
Ann Arbor, MI 48103

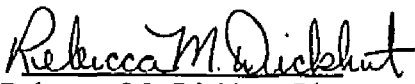
APPROVAL SHEET

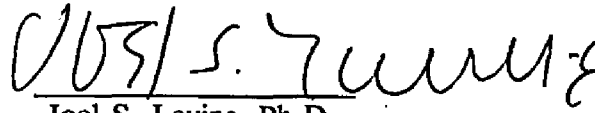
This dissertation is submitted in partial fulfillment of the
requirements for the degree of

Doctor of Philosophy


Kurt E. Gustafson

Approved, April 1996


Rebecca M. Dickhut, Ph.D.
Committee Chairman/Advisor


Joel S. Levine, Ph.D.


William G. MacIntyre, Ph.D.


Laura L. McConnell, Ph.D.


Mark R. Patterson, Ph.D.

TABLE OF CONTENTS

	<u>Page</u>
Acknowledgements.....	v
List of Tables.....	vi
List of Figures.....	vii
List of Appendices.....	ix
Abstract.....	x
Chapter I: Introduction.....	2
Background/Theory.....	2
Quantification of Gaseous Exchange Fluxes.....	7
Gas exchange models.....	7
Affect of the Surface Microlayer on Gas Exchange.....	13
Hypotheses/Objectives.....	16
References.....	18
Chapter II: Sampling Site Descriptions/Locations.....	22
Chapter III: Distribution of Polycyclic Aromatic Hydrocarbons in Southern Chesapeake Bay Surface Water: Evaluation of Three Methods for Determining Freely Dissolved Water Concentrations	27
Abstract.....	27
Introduction.....	27
Device Descriptions.....	30
Sampling.....	34
Sampling Site Descriptions.....	34
Gas Sparging.....	34
SPMDs.....	37
Filtration with Sorption to XAD-2 Resin.....	38
Analytical Methods.....	38
Further Sample Characterization.....	40
Results.....	40
Gas Sparging.....	40
SPMD samplers.....	45
Filtration with Adsorption to Resin.....	54
PAH Concentrations and Distributions.....	55
Summary and Conclusions.....	60
References.....	62

Chapter IV: Particle/Vapor Concentrations and Distributions of PAHs in the Atmosphere of Southern Chesapeake Bay..... 65

Abstract.....	65
Introduction.....	65
Materials and Methods.....	68
Sampling Locations.....	68
Sampling Methods.....	70
Analytical Techniques.....	72
Results and Discussion.....	73
Concentrations.....	73
Distributions.....	82
Atmospheric Redistribution of PAHs.....	90
Conclusion.....	93
References.....	95

Chapter V: Gas Exchange Fluxes for Polycyclic Aromatic Hydrocarbons Across the Air-Water Interface of Southern Chesapeake Bay..... 98

Abstract.....	98
Introduction.....	98
Quantification of Gaseous Exchange Fluxes.....	100
Gas Exchange Models.....	100
Sampling Sites.....	104
Sampling Strategy.....	108
Analytical Procedures.....	109
Results and Discussion.....	111
Gas Exchange Behavior of PAHs.....	112
Controlling Factors Governing Gaseous Flux.....	115
Sensitivity Analysis.....	122
Integrated Net Annual Fluxes.....	122
Conclusion.....	126
References.....	128

Chapter VI: Summary..... 133

Appendices..... 143

Acknowledgements

I would like to thank my major advisor Rebecca Dickhut for her guidance and financial support as well as the opportunity to participate in many interesting research projects.

I would also like to acknowledge my advisory committee: Drs. Levine, MacIntyre, McConnell, and Patterson for their helpful comments and discussions.

I would like to thank Libby MacDonald for her invaluable assistance over the duration of both my M.A. and Ph.D. research projects.

I would like to thank Dr. Schaffner and Michelle Thompson for allowing me to share ship time aboard the R/V Bay Eagle and for instructing me in the "fine art" of box-coring.

I also thank Kewen Liu for his advice (it does not matter), support (Confucius say), and assistance sampling (on dry land) during our research studies which were part of the same NOAA/EPA grant.

I would like to acknowledge the support of other close friends and fellow researchers in the "Chem-Lab," especially: Sid Mitra for his friendship and for questioning everything I did to slow me down- it just helped me to discover problems sooner; Jennifer Bush for her invaluable assistance in the lab and the "three-man" dice, which all of us in the lab made good use of; Mike Gaylor for his assistance, advice and sense of humor; Heather Brooks for her support and friendship; Kyrie Bernstein for her assistance with florisil chromatography; Ginger Edgecomb for her friendship and assistance; Kimani Kimbrough for his friendship and for shooting his samples and running out of the lab to leave the rest of us exposed; Ami VanDeventer for her friendship, strange veterinary stories and having developed our mass-spec method; Caryn Huszai for her friendship and for paving the way for the rest of Rebecca's students to get a "real" job; and Pat Calutti for her friendship and assistance in the lab.

I must acknowledge the rest of the VIMS staff that assisted me during my studies at VIMS from the secretaries to vessels to the artroom; especially Jim Duggan for going way beyond what was expected from him to help maintain the air samplers and other laboratory equipment.

I thank my "non-VIMS" friends who allowed me to escape from my studies to just hang out or go to concerts or dinner, and for "hoping all that education pays off." I thank those friends who joined me fishing, sailing, mountain biking, skiing, surfing or just hanging out at the beach.

Lastly, I would like to acknowledge the love and support of my Mom, Dad, Sisters, and Grandparents.

This work is a result of research sponsored by NOAA Office of Sea Grant, U.S. Department of Commerce to the Virginia Graduate Marine Science Consortium and the Virginia Sea Grant College Program under federal grant number NA90AA-D-SG803.

LIST OF TABLES

Table	Page
3.1	Surrogate PAH Recoveries from Surface Water Samples..... 41
3.2	Contribution of PAH Desorption from Filter Retained Particles to Adsorbent Traps..... 44
3.3	Triolein-Water Partition Coefficients (K_{TW}) for Selected PAHs..... 48
3.4	Dissolved PAH Concentrations Determined by SPMD and XAD-2 for May 10-14, 1994 at Haven Beach..... 50
3.5	Dissolved PAH Concentrations Determined by SPMD and XAD-2 for June 26-29, 1994 at Haven Beach..... 51
3.6	Mean Values and Ranges of PAH Concentrations for the Dissolved and Particulate Phases in Surface Waters of the Southern Chesapeake Bay..... 56
4.1	Surrogate PAH Recoveries for Atmospheric Samples..... 74
4.2	Mean Values and Ranges of PAH Concentrations for the Vapor and Aerosol/Particulate Phases in the Atmosphere of Southern Chesapeake Bay..... 75
4.3	Regression Coefficients for Plots of PAH Particle/Vapor Distributions vs Vapor Pressure..... 83
4.4	Regression Coefficients for plots of PAH Particle/Vapor Distributions vs Inverse Temperature..... 87
5.1	Locations of Gas Exchange Sampling Sites..... 106
5.2	Analytical Procedures\Quality Control Results..... 110
5.3	Sensitivity Analysis: Windspeed and Temperature Effects on Integrated Daily Fluxes for Selected PAHs in Southern Chesapeake Bay..... 123
5.4	Net Annual Gas Exchange Fluxes of Selected PAHs Across the Air-water Interface of Southern Chesapeake Bay..... 125

LIST OF FIGURES

Figure	Page
1.1 Air/Water Transfer Processes.....	3
1.2 Two-film Model of the Air-Water Interface.....	5
1.3 Three-film Model of the Air-Water Interface.....	15
2.1 Map of Sampling Sites in the Southern Chesapeake Bay.....	23
3.1 Schematic of Systems Evaluated for Measuring Freely Dissolved.....	31
3.2 Surface Water Sampling Locations in the Southern Chesapeake Bay....	35
3.3 Comparison of Dissolved PAH Concentrations Determined by Sparging Relative to XAD-2 as a function of their log K_{ow}	43
3.4 PAH Uptake Kinetics and Triolein-water Partition Coefficients for SPMDs.....	46
3.5 SPMD K_{TWS} for Selected PAHs Correlated to the Contaminants log K_{ow}	47
3.6 Mean Concentrations and Ranges of Selected PAHs in the Dissolved and Particulate Phases of Surface Waters in the Southern Chesapeake Bay.....	57
3.7 Relation of Field Measured PAH Particulate-Dissolved Partition Coefficients (K_{OC}) to the Contaminants K_{ow}	59
4.1 Atmospheric Sampling Locations in Southern Chesapeake Bay.....	69
4.2 Σ PAH Concentrations in the Vapor and Particulate Phases of the Atmosphere of Southern Chesapeake Bay.....	76
4.3 Fluoranthene Vapor and Particulate Concentrations in the Atmosphere of Southern Chesapeake Bay.....	78
4.4 Benzo(b)fluoranthene Vapor and Particulate Concentrations in the Atmosphere of Southern Chesapeake Bay.....	79

4.5	Mean Air Temperatures During Atmospheric Sampling in the Southern Chesapeake Bay Region.....	80
4.6	Correlation of PAH Particle-Vapor Partitioning Disequilibria at Haven Beach to Mean Air Temperature.....	86
4.7	Ratios of Particulate Concentrations for PAHs with Similar Liquid Vapor Pressures but Different Photochemical Reactivities.....	92
5.1	Sampling Locations for Determination of PAH Gaseous Exchange Across the Air-water Interface of Southern Chesapeake Bay.....	105
5.2	Hydrologic and Meteorologic Data for the Southern Chesapeake Bay...	113
5.3	Gas Exchange Behaviors of Selected PAHs Across the Air-water Interface of Southern Chesapeake Bay.....	114
5.4	Controlling Factors Governing Gaseous Fluxes.....	117
5.5	Phenanthrene Gas Exchange Fluxes Across the Air-water Interface of Southern Chesapeake Bay.....	118
5.6	Pyrene Gas Exchange Fluxes Across the Air-water Interface of Southern Chesapeake Bay.....	120
5.7	Fluxes and Concentrations of Chrysene Across the Air-water Interface of the Elizabeth River.....	121
5.8	Comparison of Air-water Transfer Fluxes for PAHs to the Southern Chesapeake Bay.....	127

LIST OF APPENDICES

A	Acenaphthylene Aqueous Solubility as a function of Temperature.....	143
B	Temperature Correlations for Chrysene Liquid Vapor Pressure.....	144
C	Setschenow Constants for PAHs and a Correlation as a Function of Molecular Weight.....	145
D	Equations for PAH Vapor Pressures, Aqueous Solubilities, and Henry Law Constants.....	146
E	Auxiliary Atmospheric Data.....	149
F	Auxiliary Surface Water Data.....	155
G	Instantaneous Gaseous Flux Data for PAHs Across the Air-water Interface of Southern Chesapeake Bay.....	161

ABSTRACT

Gaseous fluxes of polycyclic aromatic hydrocarbons (PAHs) across the air-water interface of Southern Chesapeake Bay were calculated for the period January 1994 through May 1995 using a modified two-film model. Additionally, the distributions of PAHs between the vapor and aerosol phase in the atmosphere, and between the freely dissolved and suspended particulate phase in the water column were investigated. Net instantaneous gaseous fluxes of PAHs were determined to vary in direction and magnitude both spatially and temporally across the air-water interface of Southern Chesapeake Bay at four sites ranging from remote to urban and highly industrialized. The magnitude of gas exchange fluxes was of the same order as wet and dry atmospheric depositional fluxes. Spatial variations in gaseous fluxes resulted from differences in the air-water concentration gradients between sites. Temporal variations in gas exchange fluxes resulted from seasonal changes in both water temperatures and vapor concentrations. Atmospheric PAH vapor concentrations increased exponentially with temperature at the non-rural sites suggesting volatilization from contaminated surfaces (soils, roads, vegetation) during warmer weather; whereas, PAH vapor concentrations at the rural site decreased with time. All sites experienced increased loadings of particulate-associated PAHs during winter. Mean total atmospheric PAH concentrations ranged from 7.87 ng/m³ at a rural (Haven Beach) site to 92.8 ng/m³ at an urban (Elizabeth River) site. Plots of the logarithm of the particle-vapor partitioning coefficient ($C_p/TSP \cdot C_v$) versus inverse temperature indicate different particle characteristics or atmospheric partitioning processes at the urban and rural sites. Three methods (gas sparging, semipermeable membrane devices, filtration with sorption of the dissolved contaminant fraction to XAD-2 resin) for determining freely dissolved contaminant concentrations in estuarine waters were investigated. Mean total PAH concentrations in surface waters ranged from 24.2 ng/l at a mainstem bay site to 91.1 ng/l at the industrialized Elizabeth River site. Dissolved-particulate partitioning of PAHs approximated equilibrium theory at all sites and sampling periods. The results of this study support the hypothesis that gas exchange is a major transport process affecting concentrations and exposure levels of PAHs in the southern Chesapeake Bay Region.

**GASEOUS FLUX AND DISTRIBUTION OF POLYCYCLIC
AROMATIC HYDROCARBONS ACROSS THE AIR-WATER
INTERFACE OF SOUTHERN CHESAPEAKE BAY**

CHAPTER I: INTRODUCTION

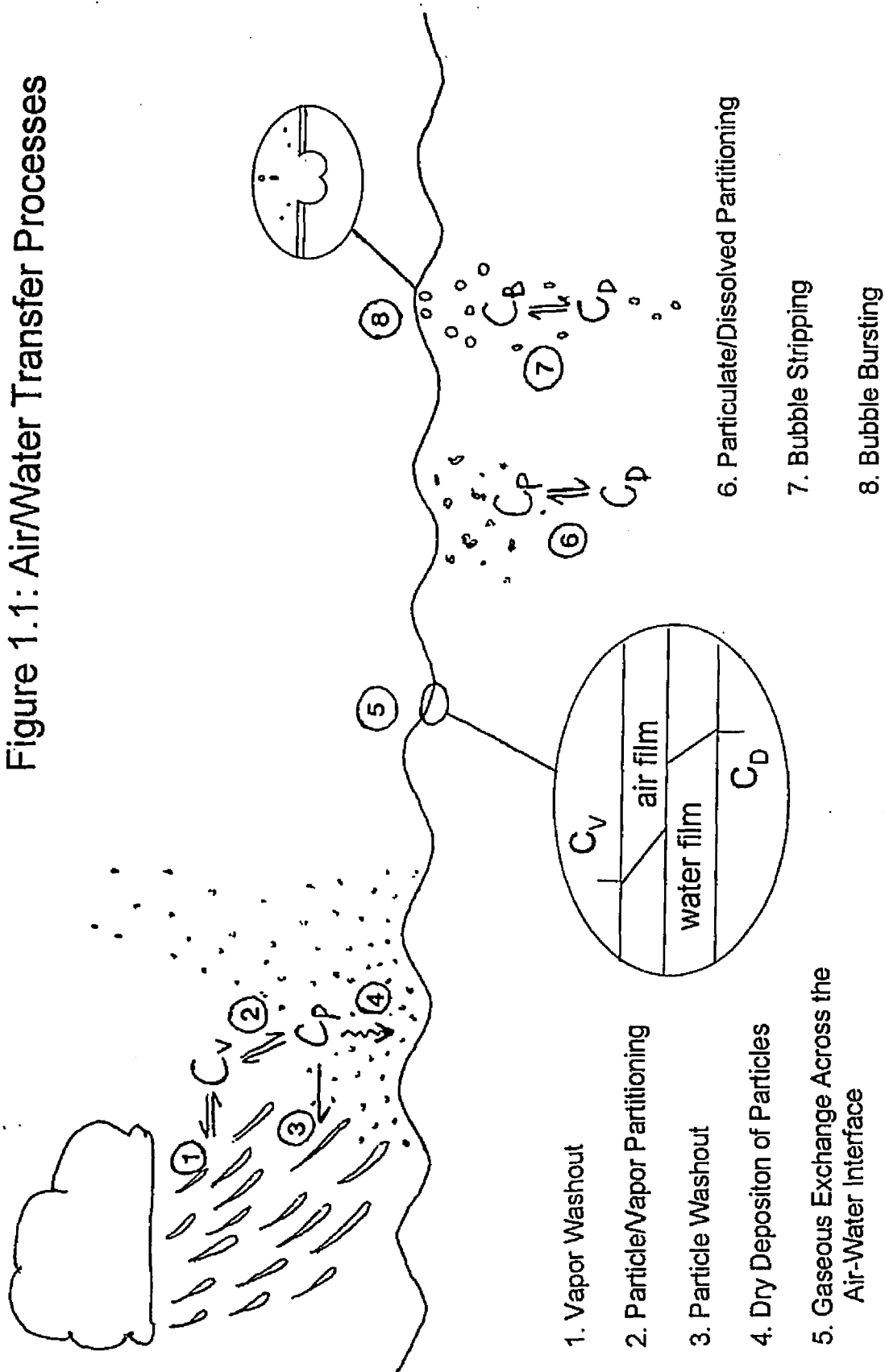
Background/Theory:

Semivolatile organic contaminants (SOCs), *e.g.* polycyclic aromatic hydrocarbons (PAHs), polychlorinated biphenyls (PCBs), and organochlorine pesticides may cycle between air and water with periods of net upward flux during dry weather followed by periods of intense downward flux during rainfall (Mackay *et al.*, 1986; Baker and Eisenreich, 1990). Further, it has been suggested that persistent, semivolatile, hydrophobic pollutants are transferred throughout the world via successive deposition and reemission- a "grasshopper" scenario (Ottar, 1981).

The physical-chemical properties of many trace organic contaminants indicate that SOC's will be long lived in the environment, cycling between the atmosphere and water (Mackay *et al.*, 1986) thus increasing their effective residence times in the total environment. The original substances and their transformation products eventually will be deposited to the Earth's surface and may impinge on communities or ecosystems hundreds or even thousands of kilometers removed from the original point of release (Schroeder and Lane, 1988). Thus, the importance of quantifying air-water exchange processes for SOC's is evident.

Air-water transfer processes for chemicals include volatilization and absorption of gases, dry deposition with particles, wet deposition by rain or snow, *i.e.* particle and vapor "washout", spray transfer, and bubble scavenging (Andren, 1983)(Figure 1). Gas exchange (volatilization-absorption) is a dominant process governing air-

Figure 1.1: Air/Water Transfer Processes



- 1. Vapor Washout
- 2. Particle Vapor Partitioning
- 3. Particle Washout
- 4. Dry Deposition of Particles
- 5. Gaseous Exchange Across the Air-Water Interface
- 6. Particulate/Dissolved Partitioning
- 7. Bubble Stripping
- 8. Bubble Bursting

water transfer of chemicals in non-storm conditions via both molecular and turbulent diffusive transfer. Diffusive air-water transfer of gaseous chemicals through stagnant films at the interface is driven by the gradient between equilibrium concentrations at the interface and bulk reservoirs (Figure 2). The rate of diffusive mass transfer is dependent upon the molecular diffusivities of the compound in air and water and upon surface roughness and film thickness which are determined by windspeed.

In order to compile a legitimate mass balance and determine exposure levels for SOCs in an aquatic system, it is necessary to consider all of the major air-water exchange processes (Mackay *et al.*, 1986). In the Chesapeake Bay watershed, researchers conducting the Chesapeake Bay Atmospheric Deposition (CBAD) study have determined the wet and dry depositional fluxes of selected SOCs and trace elements to Chesapeake Bay (Baker *et al.*, 1994; Leister and Baker, 1994; Dickhut and Gustafson, 1995). This research quantitatively measures the volatile-absorptive fluxes of selected SOCs across the air-water interface at four main sites in Southern Chesapeake Bay over the course of a year and a half. Spatial and temporal variability in SOC concentrations in the atmosphere and surface waters, and the influence of interfacial conditions (*i.e.* temperature and windspeed) on air-water gaseous exchange of SOCs in lower Chesapeake Bay have been evaluated. Subsequently, the existence and time scale of the "grass hopper" or "global distillation" and "cold condensation" theories has been evaluated for both PAH atmospheric concentration and gaseous exchange flux data from Southern Chesapeake Bay; the influence of the surface microlayer on volatile-absorptive exchange of SOCs across the air-water interface has also been considered. The diffusive fluxes determined in this study will provide

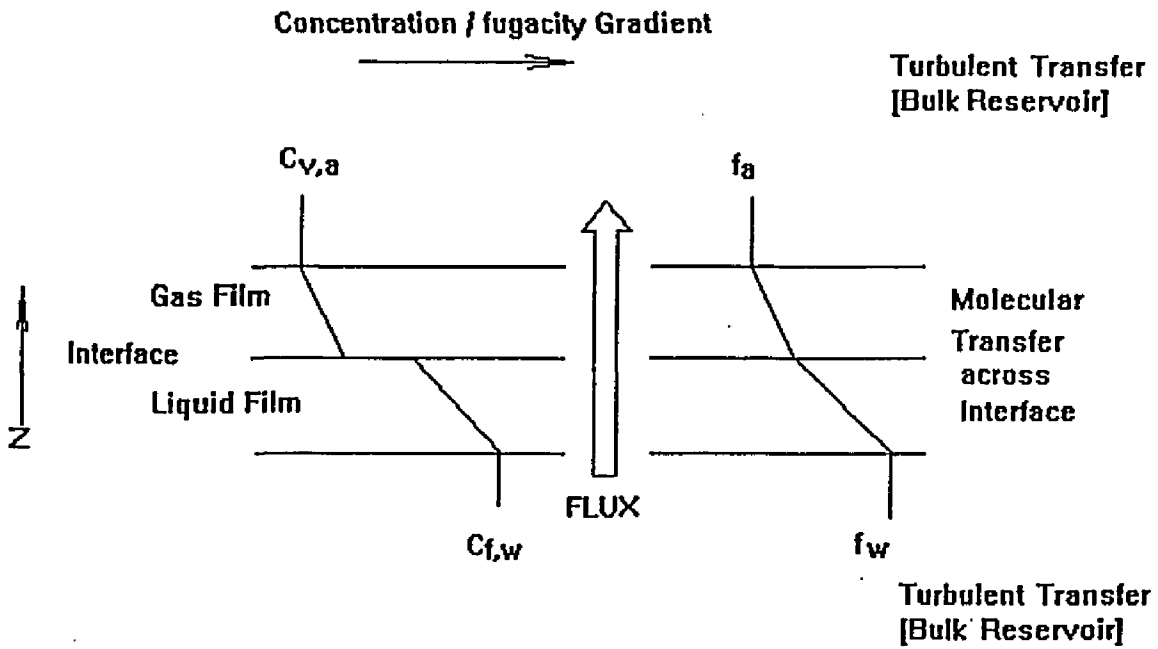


Figure 2: Liss and Slater Two-film model of the Air/Water Interface

insight into the importance of gaseous exchange at the air-water interface in contributing to loadings of toxicants to aquatic ecosystems such as Chesapeake Bay.

Any quantitative assessment of air-water exchange processes must consider the chemical speciation in both the atmosphere and water column. The distribution of a chemical between vapor and particulate-aerosols, and, water and suspended particulates determines the amount of chemical available for air-water transfer through a particular vector. In order to use the two-film model to assess gaseous exchange of contaminants to/from the Chesapeake Bay, it is necessary to determine the truly dissolved and gaseous fractions of the chemical contaminant as only the vapor-phase and truly-dissolved species are available for gaseous exchange across the air-water interface.

In addition to the measurement of gaseous contaminant fluxes in this study, the investigation of the distributions of a contaminant between the vapor and aerosol phase in the atmosphere, and, between the freely dissolved and suspended particulate phase in the water column will provide insight into transport and distribution processes for contaminants in estuarine systems such as the Chesapeake Bay. Determination of the major air-water transfer processes for contaminants is necessary such that net fluxes of chemicals to and from the bay and exposure levels can be accurately modeled. Moreover, implementation of environmental legislation, and risk management of both ecosystem and human health in the Chesapeake Bay region requires an understanding and quantification of air and water quality.

Quantification of Gaseous Exchange Fluxes

Gas Exchange Models. Quantification of the evaporation or absorption rate (volatile transport) of chemicals across the air-water interface relies primarily on the two layer (film) model presented by Liss and Slater (1974). The basic assumption of this model is that the two fluid phases are separated by stagnant layers, a liquid film and a gaseous film, through which transport occurs via molecular diffusion driven by the concentration (or fugacity) gradient of the chemical between the bulk reservoirs (Figure 2). This framework was extended by Mackay and Leinonen (1975), wherein they presented calculations for the transport of low solubility compounds including selected saturated and aromatic hydrocarbons, pesticides, and PCBs expressed in terms of mass transfer coefficients instead of diffusion coefficients and boundary layer thicknesses. Transport by molecular diffusion across two boundary layers has also been adopted by Doskey and Andren (1981), and Bopp (1983), in separate PCB air-water transfer models, and by Eisenreich *et al.*, (1981), Baker and Eisenreich (1991), Hornbuckle *et al.*, (1993), Achman *et al.*, (1993) and McConnell *et al.*, (1993) in modeling organic contaminants in the Great Lakes ecosystem.

According to Fick's first law of diffusion in the one-dimensional form in a homogeneous phase,

$$F = -D(dc/dy) \tag{1}$$

where F is the flux of chemical (mass/length²*time), D is the molecular diffusion

coefficient of the chemical in the medium, and dc/dy is the concentration gradient in the Y direction (Liss and Slater, 1974). Under steady state conditions, the concentration gradient (dc/dy) is constant, therefore equation (1) can be simplified to:

$$F = -D(\Delta C/\Delta Y) = -k\Delta C \quad (2)$$

where k , the chemical specific mass transfer coefficient, is equal to $D/\Delta Y$; and ΔC is the difference in concentration across the diffusive exchange distance. The mass transfer coefficient has the dimensions of velocity (length/time) and is a measure of flux of gas per unit area. The reciprocal of the mass transfer coefficient is a measure of the "resistance" (r) to diffusive transfer and has the dimensions of time/length.

Applying equation (2) to the two-film model (Figure 2), and assuming volatile flux of a chemical across the air-water interface is a steady state process:

$$F = k_a(C_{v,ai} - C_{v,a}) = k_w(C_{f,w} - C_{f,wi}) \quad (3)$$

where $C_{v,a}$ and $C_{v,ai}$ are the concentrations of the vapor in the atmosphere and at the air-water interface, respectively, k_a and k_w are the chemical specific mass transfer coefficients in the air and water films, respectively, and $C_{f,wi}$ and $C_{f,w}$ are the freely dissolved chemical concentrations at the air-water interface and in the surface water, respectively. Since the flux equation has been expressed in terms of chemical concentrations rather than activities, ideal behavior has already been assumed; therefore, it follows that Henry's law is valid and the chemicals' concentrations at

equilibrium can be expressed as:

$$C_{v,ai}/C_{f,wi} = K_{aw} = H/RT \quad (4)$$

Here K_{aw} is the dimensionless air-water partition coefficient which is equal to the Henry's law constant (H) divided by the gas constant (R) and the absolute temperature (T). From equation (3):

$$C_{v,ai} = F/k_a + C_{v,a} \quad , \quad C_{f,wi} = C_{f,w} - F/k_w \quad (5)$$

Substituting equation (4) into (5) and solving for F yields:

$$F = (C_{f,w} - C_{v,a}RT/H)/(1/k_w + RT/Hk_a) \quad (6)$$

Letting k_{ol} denote the overall air-water mass transfer coefficient or total resistance to transfer (r_{tot}):

$$1/k_{ol} = 1/k_w + RT/Hk_a \quad (7)$$

then the volatile flux (F_{vol}) or equation (6) can be simplified to:

$$F_{vol} = k_{ol}(C_{f,w} - C_{v,a}/K_{aw}) \quad (8)$$

Fugacity gradients as formulated by Mackay (1979), are also used for modeling air-water transfer processes. In terms of fugacity:

$$F_{vol} = (k_{ol}/H)(f_w - f_a) \quad (9)$$

where f_w and f_a are the water and gas phase fugacities ($f_a = p$), respectively.

Fugacity, defined as the escaping tendency of a chemical from a designated phase such as air or water (Mackay, 1979), is linearly related to concentration:

$$C_{f,w} = f_w Z_w \quad \text{and} \quad C_{v,a} = f_a Z_a \quad (10)$$

where $Z_w = 1/H$ and $Z_a = 1/RT$ are the fugacity capacities of the water and air, respectively.

Mass transfer coefficients control the rate of diffusive transport across interfaces and for air-water systems have been related to the Schmidt numbers of a chemical in water (Sc_w) and air (Sc_a) and wind speed at a reference height of 10 meters (U_{10}) by Mackay and Yeun (1983):

$$k_a = 0.001 + 0.0462(U^*)(Sc_a)^{-0.67} \quad (11)$$

$$k_w = 1.0(10)^{-6} + 34.1(10)^{-4}(U^*)(Sc_w)^{-0.5} \quad (12)$$

$$k_w = 1.0(10)^{-6} + 144(10)^{-4}(U^*)^{2.2}(Sc_w)^{-0.5} \quad (13)$$

where equation (12) applies for $U^* > 0.3$ m/s, equation (13) applies for $U^* < 0.3$ m/s, and $U^* = U_{10}(6.1 + 0.63U_{10})^{0.5}(10)^{-2}$. The air and water mass transfer coefficients (k_a and k_w) are related to molecular diffusion via the Schmidt numbers (Bird *et al.*, 1960):

$$Sc_w = \mu_w / (\rho_w D_{sw}) \quad (14)$$

$$Sc_a = \mu_a / (\rho_a D_{sa}) \quad (15)$$

where D_{sa} and D_{sw} are the molecular diffusivities of a chemical solute in air and water, respectively, and the ρ 's and μ 's are the densities and dynamic viscosities of the bulk phases, respectively.

For calculation of mass transfer coefficients, knowledge of windspeeds, viscosity and density of the bulk phases as well as molecular diffusivities of the compound of interest at the environmental temperatures and salinities must be known. The temperature of each phase (air and water) in the stagnant film layers (Figure 2) is needed. However, the surface skin temperatures have been determined to be only some tenths of a degree celsius cooler than the underlying water due to energy losses from long-wave infrared radiation and evaporation (Paulson and Parker, 1972; Hornbuckle *et al.* 1995). Therefore, in this study, surface water temperatures were used for calculating parameters (i.e. density, viscosity, diffusivity, Henry law constants) necessary to determine gaseous fluxes. Molecular diffusivities for PAHs in air (D_{sa}) and water (D_{sw}) have been calculated according to the methods of Gustafson

and Dickhut (1994a, 1994b):

$$D_{sa} = (0.186 * 10^{0.00283T}) / V^{0.213} \quad (16)$$

where T is temperature (°C), and V is the molar volume of the PAH, and,

$$D_{sw} = 4.864 * 10^{-3} / (\mu^{0.905} V^{1.32}) \quad (17)$$

where μ is the aqueous viscosity. Bulk phase viscosities and densities have been calculated according to the equations of Millero *et al.* (1976), Riley *et al.* (1975), Horne (1969), and Weast (1987) using field measured temperatures and salinities.

Henry's law constants are necessary for determining air-water partition coefficients of the compounds of interest. Henry's law constants which are compound specific have been calculated using sub-cooled liquid aqueous solubilities and vapor pressures according to the methods of Sonnefeld *et al.* (1983) and May *et al.* (1978, 1983) (Appendix D) at environmental temperatures and surface water salinities. For benzo(b)fluoranthene, benzo(k)fluoranthene, benzo(a)pyrene, indeno(1,2,3-cd)pyrene, and benzo(g,h,i)perylene both solubility and vapor pressure data as a function of temperature are not available; nonetheless, measured Henry law constants at several temperatures for freshwater have been reported (Th.E.M. ten Hulscher *et al.*, 1992). The logarithms of reported Henry law values have been linearly related to inverse temperatures and the resulting predictive equations utilized in this study (Appendix D). Chrysene sub-cooled liquid vapor pressures have been estimated using PAH

solubility-vapor pressure correlations (see Appendix B). Aqueous solubilities of acenaphthylene were measured using a generator column method and uv absorbance detection. Acenaphthylene solubilities in aqueous solution determined as a function of temperature, and a predictive equation, are reported in Appendix A.

Correction of PAH solubilities at environmental salinities is based upon employing the Setschenow equation:

$$\log(S_0/S_s) = K_s C_s \quad (18)$$

where S_0 is the solubility in fresh water, S_s is the solubility in saline solution, K_s is the Setschenow constant for the compound of interest, and C_s is the molar salt concentration of the saline solution (sea water). From Sverdrup *et al.*, (1942) using the 10 most abundant constituents and assuming salinity is conservative over the range measured in this study 15-27 ppt, molar salt concentrations can be directly related to field measured salinities. Reported Setschenow constants for PAHs (Rossi and Thomas, 1981; May *et al.*, 1978; Whitehouse, 1985; Schwarz, 1977; Eganhouse and Calder, 1976) have been linearly related to the molecular weight of the compound (Appendix C). Selected Setschenow constants from literature values and values determined from the predictive equation were used in this study to correct Henry law constants determined from aqueous solubilities for field measured salinities.

Affect of the Surface Microlayer on Gas Exchange. The two film model considers only the existence of air and water stagnant layers at the surface of a water body (Figure 2). However, it is well established that surface films, generally organic

in nature, form at the air-water interface (Hunter and Liss, 1981; Norkrans, 1980). According to Mackay (1982), this surface film or microlayer adds additional resistance to mass transfer of gaseous substances between the atmosphere and a water body (Figure 3). The volatile flux, in terms of resistances, can be viewed as:

$$F_{vol} = (f_w - f_a)/(r_w + r_f + r_a) \quad (19)$$

where r_w , r_f , and r_a are the water layer, surface film, and air layer resistances to mass transfer, respectively. These resistances are generally defined by (Mackay, 1982):

$$r = \Delta Y/DZ \quad \text{or} \quad r = 1/kZ \quad (20)$$

where ΔY is the thickness of the stagnant layer, D is the molecular diffusivity of the chemical in the media, and, Z and k are defined above. If there is no surface film, equation 19 reduces to equation 9 (or equation 8).

Mackay (1982) postulates that the diffusive resistance of surface films will be small for SOCs, as these substances will be quite soluble in the organic layer resulting in a large Z_f value and, consequently, a low r_f . However, it is also possible that the organic nature of surface films will also affect D as the viscosity and solvent self-association factor are likely different for surface film and surface water. Diffusivities may potentially be significantly lower for surface film than surface water media resulting in higher diffusive resistances for surface film media and a concurrent lowering of SOC diffusive flux across the air-water interface.

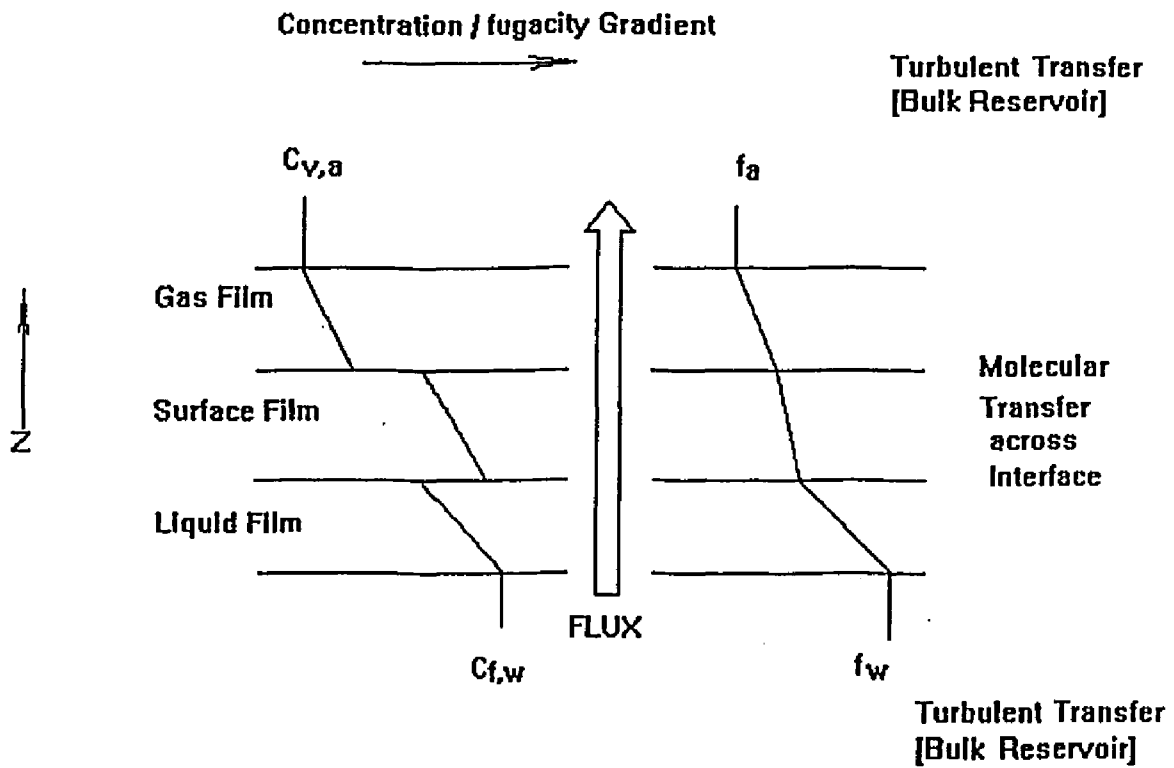


Figure 3: Three-film model of the Air/Water Interface

Hypotheses\Objectives

The main hypothesis of this research was that the volatile-absorptive diffusive exchange of SOCs (*i.e.* PAHs, PCBs, and organochlorine pesticides) would be of the same order of magnitude as atmospheric wet and dry depositional fluxes to the Southern Chesapeake Bay. This was supported by CBAD atmospheric deposition data and surface water concentration data of selected PAHs for February 1991 taken during a cruise on the lower Chesapeake Bay during that month (Dickhut and Gustafson, 1995). Consequently, volatile-absorptive fluxes were expected to significantly influence the net atmospheric loadings of SOCs to lower Chesapeake Bay. The working hypotheses of the proposed research were:

(1) atmospheric and surface water concentrations of SOCs would vary spatially and seasonally due to variation in air-water interfacial conditions, influencing both the magnitude and direction of the volatile-absorptive flux of SOCs,

(2) the presence of a surface microlayer would alter the diffusive exchange of SOCs across the air-water interface,

(3) the "grasshopper" or "global distillation" scenario for contaminant transport would be important to determining atmospheric loadings of SOCs to Chesapeake Bay and would act on time scales as small as the duration of storm events as well as seasonal cycles.

The primary objective of the proposed research was to assess the volatile-absorptive exchange of semivolatile organic contaminants (SOCs) across the air-water interface of southern Chesapeake Bay. The overall objectives were to:

(1) design, fabricate, and validate systems for measuring "freely-dissolved" SOC concentrations in surface water and microlayer samples,

(2) directly measure the concentrations of selected SOCs in the atmosphere and surface waters of the southern Chesapeake Bay region, and to assess the spatial and temporal variability in SOC concentrations in the atmosphere and surface waters of the southern Chesapeake Bay,

(3) evaluate the influence of the surface microlayer and air-water interfacial conditions (*i.e.* windspeed and temperature) on the diffusive flux of SOCs,

(4) determine the existence and timescale for the "grasshopper" scenario with selected SOCs in southern Chesapeake Bay.

The various working hypotheses and objectives were examined by methods outlined in the following chapters. The main hypothesis was evaluated via concurrent measurement of wet depositional fluxes of SOCs to lower Chesapeake Bay and estimation of dry depositional SOC fluxes through measurement of atmospheric particle concentrations of SOCs and application of appropriate modeling equations.

References

- Achman, D.R., K.C. Hornbuckle, and S.J. Eisenreich. 1993. Volatilization of Polychlorinated Biphenyls from Green Bay, Lake Michigan. *Environ. Sci. Technol.* 27:75-87.
- Andren, A.W. 1983. Processes determining the flux of PCBs across air/water interfaces. Chapter 8 in Mackay, D., S. Patterson, S.J. Eisenreich and M.S. Simmons (eds), *Physical behavior of PCBs in the Great Lakes*, Ann Arbor Science, 127-140.
- Baker, J.E., D. Burdige, T.M. Church, G. Cutter, R.M. Dickhut, D.L. Leister, J.M. Ondov, and J.R. Scudlark. 1994. Chesapeake Bay Atmospheric Deposition Study: Phase II final report submitted to the EPA Chesapeake Bay Program Office.
- Baker, J.E. and S.J. Eisenreich. 1990. Concentrations and fluxes of polycyclic aromatic hydrocarbons and polychlorinated biphenyls across the air-water interface of Lake Superior. *Environ. Sci. Technol.* 24:342-352.
- Bird, R.B., W.E. Stewart and E.N. Lightfoot. 1960. *Transport phenomena*, John Wiley and Sons, New York, p. 512.
- Bopp, R.F. 1983. Revised parameters for modeling the transport of PCB components across an air water interface. *J Geophysical Res.* 88:2521-2529.
- Dickhut, R.M., K.E. Gustafson. 1995. Atmospheric inputs of selected polycyclic aromatic hydrocarbons and polychlorinated biphenyls to southern Chesapeake Bay. *Mar. Pollut. Bull.* 30:385-396.
- Doskey, P.V. and A.W. Andren. 1981. Modeling the flux of atmospheric polychlorinated biphenyls across the air/water interface. *Environ. Sci. Technol.* 15:705-711.
- Eganhouse, R.P. and J.A. Calder. 1976. The solubility of medium molecular weight aromatic hydrocarbons and the effects of hydrocarbon co-solutes and salinity. *Geochim. Cosmochim. Acta.* 40:555-561.
- Eisenreich, S.J., B.B. Looney, and J.D. Thornton. 1981. Airborne organic contaminants in the Great Lakes ecosystem. *Environ. Sci. Technol.* 15:30-38.
- Gustafson, K.E. and R.M. Dickhut. 1994a. Molecular Diffusivity of Polycyclic Aromatic Hydrocarbons in Aqueous Solution. *J. Chem. Eng. Data.* 39:281-285.

- Gustafson, K.E. and R.M. Dickhut. 1994b. Molecular Diffusivity of Polycyclic Aromatic Hydrocarbons in Air. *J. Chem. Eng. Data.* 39:286-289.
- Hornbuckle, K.C., D.R. Achman, S.J. Eisenreich. 1993. Over-water and over-land polychlorinated biphenyls in Green Bay, Lake Michigan. *Environ. Sci. Technol.* 27:87-96.
- Hornbuckle, K.C., C.W. Sweet, R.F. Pearson, D.L. Swackhamer, and S.J. Eisenreich. 1995. Assessing annual water-air fluxes of polychlorinated biphenyls in Lake Michigan. *Environ. Sci. Technol.* 29:869-877.
- Horne, R.A. 1969. *Marine Chemistry; the structure of water and the chemistry of the hydrosphere.* New York. Wiley-Interscience. pp. 568.
- Hunter, K.A. and P.S. Liss. 1981. Organic sea surface films. In *Marine Organic Chemistry*, Duursma, E.K. and R. Dawson, ed., Elsevier: New York, Chap. 9.
- Leister, D.L. and J.E. Baker. 1994. Atmospheric Deposition of Organic Contaminants to the Chesapeake Bay. *Atmos. Environ.* 28:1499-1520.
- Liss, P.S. and P.G. Slater. 1974. Flux of gases across the air-sea interface. *Nature* 247:181-184.
- Mackay, D. 1982. Effects of surface films on air-water exchange rates. *J. Great Lakes Res.* 8:299-306.
- Mackay, D. 1979. Finding fugacity feasible. *Environ. Sci. Technol.* 13:1218-1223.
- Mackay, D. and P.J. Leinonen. 1975. Rate of evaporation of low-solubility contaminants from water bodies to atmosphere. *Environ. Sci. Technol.* 9:1178.
- Mackay, D., S. Paterson and W.H. Schroeder. 1986. Model describing the rates of transfer processes of organic chemicals between the atmosphere and water. *Environ. Sci. Technol.* 20:810-816.
- Mackay, D. and A.T.K. Yeun. 1983. Mass transfer coefficient correlations for volatilization of organic solutes from water. *Environ. Sci. Technol.* 17: 211-217.
- May, W.E., S.P. Wasik, and D.H. Freeman. 1978. Determination of the Solubility Behavior of Some Polycyclic Aromatic Hydrocarbons in Water. *Anal. Chem.* 50:997-1000.

- May, W.E., S.P. Wasik, M.M. Miller, Y.B. Tewari, J.M. Brown-Thomas, and R.N. Goldberg. 1983. Solution thermodynamics of some slightly soluble hydrocarbons in water. *J. Chem. Eng. Data* 28:197-200.
- McConnell, L.L., W.E. Cotham, and T.F. Bidleman. 1993. Gas exchange of hexachlorocyclohexane in the Great Lakes. *Environ. Sci. Technol.* 27: 1304-1311.
- Millero, F.J., A. Gonzalez, and G.K. Ward. 1976. The density of seawater solutions at one atmosphere as a function of salinity. *J. Mar. Res.* 34:61-93.
- Norkrans, B. 1980. Surface microlayers in aquatic environments. In *Advances in Microbial Ecology Volume 4*; Alexander, A. ed. Plenum Press: New York. pp 51-85.
- Ottar, B. 1981. The transfer of airborne pollutants to the arctic region. *Atmos. Environ.* 15: 1439-1445.
- Paulson, C.A. and T.W. Parker. 1972. *J. Geophys. Res.* 77. 491-495.
- Riley, J.P., G. Skirrow, and K. Chester. 1975. *Chemical Oceanography*. 2nd ed. New York. Academic Press. p. 576.
- Rossi, S.J. and W.H. Thomas. 1981. Solubility Behavior of Three Aromatic Hydrocarbons in Distilled Water and Natural Seawater. *Environ. Sci. Technol.* 15:715-716.
- Schroeder, W.H. and D.A. Lane. 1988. The fate of toxic airborne pollutants. *Environ. Sci. Technol.* 22:240-246.
- Schwartz, F.P. 1977. Determination of Temperature Dependence of Solubilities of Polycyclic Aromatic Hydrocarbons in Aqueous Solutions by a Fluorescence Method. *J. Chem. Eng. Data.* 22:273-276.
- Sonnefeld, W.J., W.H. Zoller, and W.E. May. 1983. Dynamic coupled-column liquid chromatographic determination of ambient vapor pressures of polynuclear aromatic hydrocarbons. *Anal. Chem.* 55:275-280.
- Sverdrup, H.U., M.W. Johnson, and R.H. Fleming. 1942. *The oceans, their physics, chemistry, and general biology*. New York. Prentice-Hall, Inc. pp. 1087.
- Ten Hulscher, Th.E.M., L.E. Van Der Velde, and W.A. Bruggeman. 1992. Temperature Dependence of Henry's Law Constants for Selected Chlorobenzenes, Polychlorinated Biphenyls and Polycyclic Aromatic Hydrocarbons. *Env. Tox. Chem.* 11:1595-1603.

Weast, R.C. (ed.) 1987. CRC Handbook of Chemistry and Physics. Boca Raton, FL. CRC Press.

Whitehouse, B.G. 1985. Observation of Abnormal Solubility Behavior of Aromatic Hydrocarbons in Seawater. Mar. Chem. 17:277-284.

CHAPTER II: Sampling Site Descriptions\Locations

Sampling Sites. To determine gas exchange fluxes for PAHs across the air-water interface of the southern Chesapeake Bay, measurements of both freely dissolved water and atmospheric vapor concentrations reflecting those at the air-water interface must be known. Concentrations for selected PAHs in air and surface waters were measured at four main sites in the southern Chesapeake Bay (Figure 1) over the period January 1994 through the end of May 1995.

High-volume air samplers (General Metal Works, model GPYN1123) were placed adjacent to the shore (Haven Beach < 100 m, at all other sites < 10 m) at four locations in the southern Chesapeake Bay (Figure 1). The Haven Beach atmospheric sampling site (37°26.16' N, 76°15.25' W) was a rural site, the air sampler was located 100m from the shore of Chesapeake Bay in a high marsh area, as well as > 50 m from the nearest road which has limited traffic (i.e. dead end) and > 200 m from the nearest residence. The closest regional sources of contaminants to the Haven Beach site include shipping traffic on the mainstem bay, and a refinery and coal/oil-fired power plant which are located approximately 30 km to the southwest. The Haven Beach site also served as a sampling site for the Chesapeake Bay Atmospheric Deposition Study which quantified wet and dry atmospheric depositional fluxes of SOCs to the southern bay region.

The air sampler at the York River site was located at the Virginia Institute of Marine Science (37°14.75' N, 76°30.0 W). At this site, the sampler was placed on

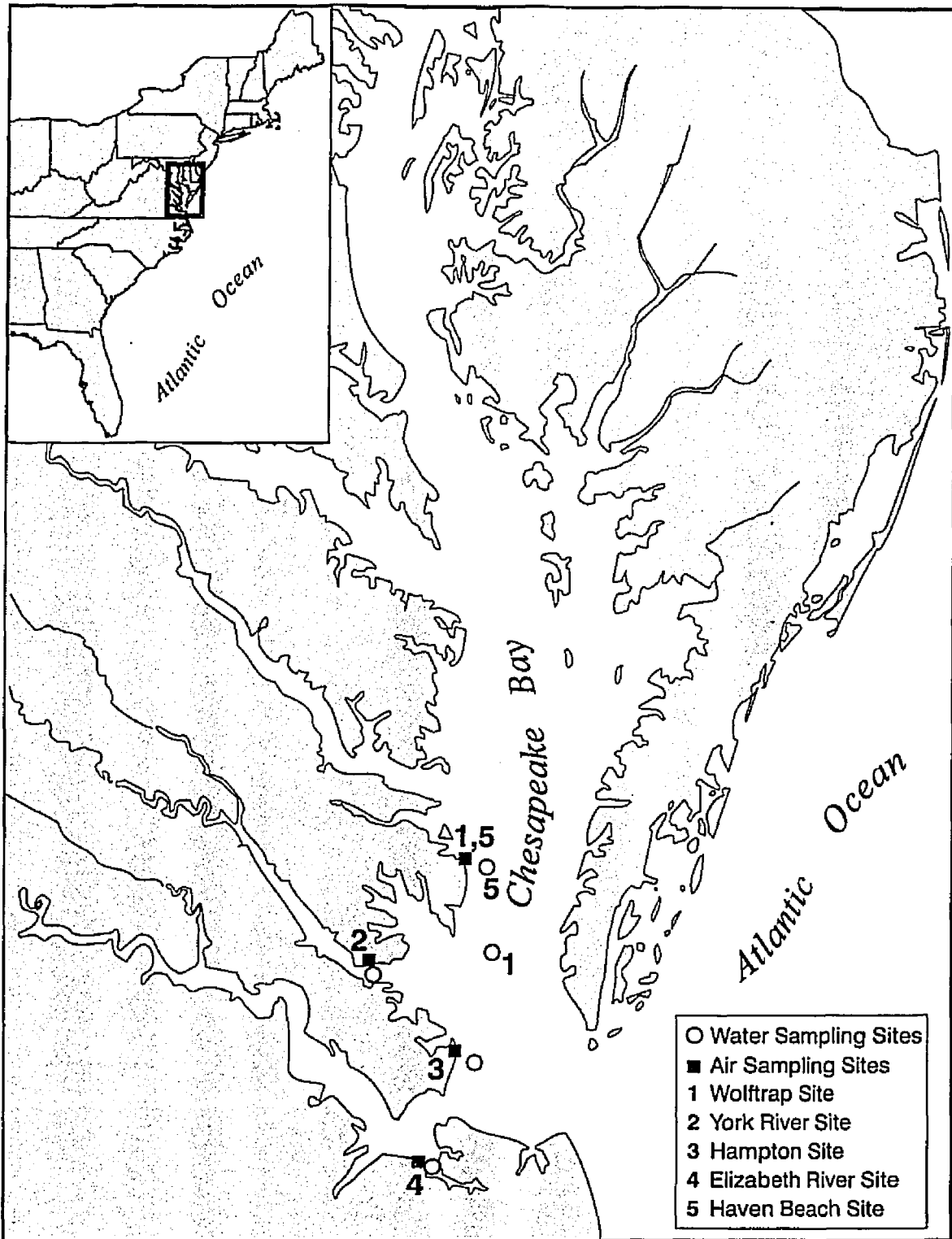


Figure 2.1: Atmospheric and Surface Water Sampling Locations in the Southern Chesapeake Bay Region.

the windward side (during sampling periods) at the end of one of the institute's research piers on the York River (approximately 50 m from shore). The York River site was considered a semi-urban site, approximately 5 km northwest of an oil refinery and coal/oil-fired power plant and 1 km east of a major vehicular river crossing.

The Hampton atmospheric sampling site (37°4.6' N, 76°16.4 W) was located less than 10 m from the shore of the Chesapeake Bay at Grandview Beach\Dandy Point. The Hampton site was considered an urban site lying in the eastern most section of the city of Hampton (pop. 138,000) and within 5 km of the cities of Newport News (pop. 179,000) and Norfolk (pop. 245,000).

The Elizabeth River atmospheric sampling site was located at the Portsmouth Coast Guard Station (36°53.2' N, 76°21.2 W). The air sampler was located on a remote section of the base 2 m from the shore of the Elizabeth River. The Elizabeth River site is considered representative of contaminated rivers-estuaries. The site is in close proximity (< 5 km) to Lambert's Point coal terminals, Norfolk Naval Station, and Portsmouth Naval Shipyard; in addition, the site is located centrally within the Hampton Roads Metropolitan area (pop. 1.5 million).

Surface water samples were collected simultaneously with paired atmospheric samples at five sites on the southern Chesapeake Bay (Figure 1). The principal study site located in the Wolftrap region of the southern Chesapeake Bay (37°16.53 N, 76°12.0 W) is removed from local sources of contamination (land based) and is close to the Haven Beach atmospheric and CBAD sampling site where SOC wet and dry

atmospheric depositional inputs to the Bay were quantified. Surface water sampling at the Wolftrap site occurred from aboard the VIMS R/V Bay Eagle. Additionally, a second Wolftrap region site (Haven Beach) was located approximately 1500 m from shore of Haven Beach (37°25.7' N, 76°13.1' W). The Haven Beach site was selected for method development due to its accessibility by small boat or canoe from the site where atmospheric samples were collected during water sampling for both Wolftrap regional sites.

A Hampton roads region study site on Chesapeake Bay was located approximately 1000 m off of Grandview beach (37°5.0' N, 76°13.3' W). It was hypothesized that this region would be characterized by larger absorptive-volatile fluxes (as compared to the rural site) as the surrounding region is heavily populated, and therefore, will contribute largely to atmospheric levels of SOCs.

Additionally, the Elizabeth River was selected as a study site as it is an intensely industrialized waterway representative of contaminated rivers-estuaries and likely to include surface films in the form of slicks. The Elizabeth River surface water sampling site was located at the mouths of the river's western and southern branches (36°52.0' N, 76°19.6'W).

Finally, the York river was chosen as an additional site as part of a joint project (see Liu, 1994) to examine the effect of the sea surface microlayer on gaseous diffusive transfer. The York River study site is located in the center of the river approximately 1000 m downstream from the Virginia Institute of Marine Science (37°14.5' N, 76°29.0' W). Sea surface microlayer sampling was conducted at both the

York River and Elizabeth River sites during atmospheric and surface water sampling (Liu 1994).

Field sampling was conducted intensively (*i.e.* to assess diurnal through seasonal variability) at the Wolftrap site, and less intensively (*e.g.* to examine spatial variability) at the three remaining sites. Microlayer samples were collected at the York and Elizabeth River sites during atmospheric and surface water sampling periods with the objective of assessing the effects of the surface microlayer on gaseous exchange. The "grasshopper" scenario was examined from instantaneous gas flux, wet and dry atmospheric depositional flux, and atmospheric concentration data from the southern Chesapeake Bay region.

References

- Liu, K. 1994. Ph. D. Prospectus submitted to the Faculty of the School of Marine Science, The College of William and Mary.

Chapter III: Distribution of Polycyclic Aromatic Hydrocarbons in Southern Chesapeake Bay Surface Water: Evaluation of Three Methods for Determining Freely Dissolved Water Concentrations

Abstract:

Gas sparging, semipermeable membrane devices (SPMDs), and filtration with sorption of dissolved polycyclic aromatic hydrocarbons (PAHs) to XAD-2 resin, were evaluated for determining freely dissolved PAH concentrations in estuarine waters of the southern Chesapeake Bay at sites ranging from rural to urban and highly industrialized. Gas sparging had significant sampling artifacts due to particle scavenging by rising bubbles and SPMDs were kinetically limited for 4-ring and larger PAHs relative to short-term temporal changes in water concentrations. Filtration with sorption of the dissolved contaminant fraction to XAD-2 resin was found to be the most accurate and feasible method for determining freely dissolved PAH concentrations in estuarine water. PAH dissolved and particulate concentrations, and distribution coefficients were measured using the filtration\XAD-2 method. PAH surface water concentrations in the southern Chesapeake Bay are higher than those reported for the northern bay; concentrations in the Elizabeth River were elevated relative to all other sites. A gradient for particulate PAHs was observed from urban to remote sites. No seasonal trends were observed in dissolved or particle-bound fractions at any site. PAH dissolved-particulate distributions in surface waters of the Chesapeake Bay are near equilibrium at all locations and seasons.

Introduction

The fate and transport of semivolatile organic contaminants (SOCs) in the environment depends on their physical-chemical phase distribution. In natural waters, only the freely dissolved fraction is related to chemical potential and contributes to diffusive fluxes. However, it is well known that SOC's sorb to suspended particles as well as to dissolved organic matter, and the existence of this bound fraction in natural waters decreases the partitioning and mass transfer of SOC's to other phases (Landrum et al. 1984). Therefore, it is necessary to accurately measure the phase distribution of

SOCs in natural waters in order to quantify contaminant transport and evaluate chemical behavior in aquatic systems.

Several methods have been developed to distinguish between bound and freely dissolved fractions of organic compounds. Techniques that have been used to determine freely dissolved or bioavailable fractions of organic contaminants in fresh waters include gas-phase partitioning (or gas sparging) (Murray et al., 1991; Sproule et al., 1991; Yin and Hassett, 1986; Yin and Hassett, 1989), equilibrium dialysis (Black et al., 1982; Huckins et al., 1990; Lebo et al., 1992; Prest et al., 1992; Sodergren, A., 1987) and filtration with subsequent sorption of the dissolved fraction in the filtrate to resin columns such as Amberlite^R XAD-2 resin (Capel and Eisenreich, 1985; Achman et al., 1993; Baker and Eisenreich 1990; Dickhut and Gustafson, 1995). However, estuarine systems such as Chesapeake Bay generally contain higher levels of suspended matter as well as particulate and dissolved organic carbon than do freshwater lakes. For example, total suspended particulates (TSP) in the Great Lakes ranges from .03 to 4.97 mg/L (Achman 1993, Yin and Hassett 1989, Eadie and Robbins 1987, Capel and Eisenreich 1985, Baker and Eisenreich 1989) whereas in the Chesapeake Bay, TSP ranges from 3.2 to 25.86 mg/L (Ko and Baker 1995, this work). Likewise, total organic carbon (TOC), dissolved and particulate (DOC + POC) range from 1.63 to 5.51 mg/L in the Great Lakes (Yin and Hassett 1989, Baker and Eisenreich 1989); whereas in the Chesapeake Bay, DOC and POC range from 3.03 to 7.88 mg/L and .309 to 2.74 mg/L, respectively (this work). Thus, each of the methods for measuring freely dissolved concentrations may be

impacted if colloidal and dissolved organic carbon (DOC) bound contaminants are not adequately separated from the sample.

The objective of this study was to determine the most accurate and feasible method for measuring freely dissolved SOC concentrations in estuarine surface waters for the purpose of quantifying air-water gas exchange in Chesapeake Bay. The SOCs examined in this study were selected polycyclic aromatic hydrocarbons (PAHs). PAHs are a class of organic contaminants composed of numerous compounds which span a range of physical-chemical properties (e.g. solubility, vapor pressure, octanol-water partition coefficient- K_{ow}). Moreover, the toxicity of many PAHs and their metabolites has been well established. In this chapter, three methods for measuring freely dissolved SOC concentrations in estuarine systems: gas-phase partitioning, equilibrium dialysis, and filtration with adsorption to resin, are described and evaluated. Further, PAH freely dissolved and particle-associated concentrations have been determined at five sites in lower Chesapeake Bay during the period January 1994 through May 1995 using the filtration/sorption to Amberlite^R XAD-2 resin method. Spatial and temporal variations in operationally defined particulate and dissolved concentrations are discussed as are measured particle-water distribution coefficients (K_{oc}).

Device Descriptions

Three separate systems were developed and tested for determining freely dissolved SOC concentrations (Figure 1). A floating sparger designed to emulate the devices described by Sproule et al. (1991) was designed which consists of a cylindrical chamber of inert material (marine grade stainless steel) 5 cm in diameter by 115 cm high, inlet and outlet passages for water and air, and a solid sorbent trap on the air outlet to capture SOC's stripped from the water by the air. Water flow through the system was maintained using a submersible pump (Aquarium Systems) and air flow was supplied via teflon tubing from ultra high purity air cylinders on board ship. Subsequently, an inline 47mm stainless steel filter holder with a Gelman Type A/E glass fiber filter (GFF) was employed to prevent particles, which may be scavenged and ejected by the air bubbles, from entering the analytical trap.

An overview of the theory and equations for mass transfer within the sparger chamber are given in detail by Sproule et al. (1991). Briefly, air is introduced into the bottom of the chamber with water continuously being pumped in through the top flowing counter-current to the air. If the dimensions of the chamber (i.e. bubble path length) are sufficient to allow the SOC of interest to reach equilibrium between the water and air phases, and the air and water flow rates through the system are adjusted such that the water is negligibly depleted of SOC's (i.e. no stripping of SOC's from particles occurs), then the fugacity of the compound in water (f_w) equals the fugacity or partial pressure of the compound in the air exiting the chamber. Further, if the

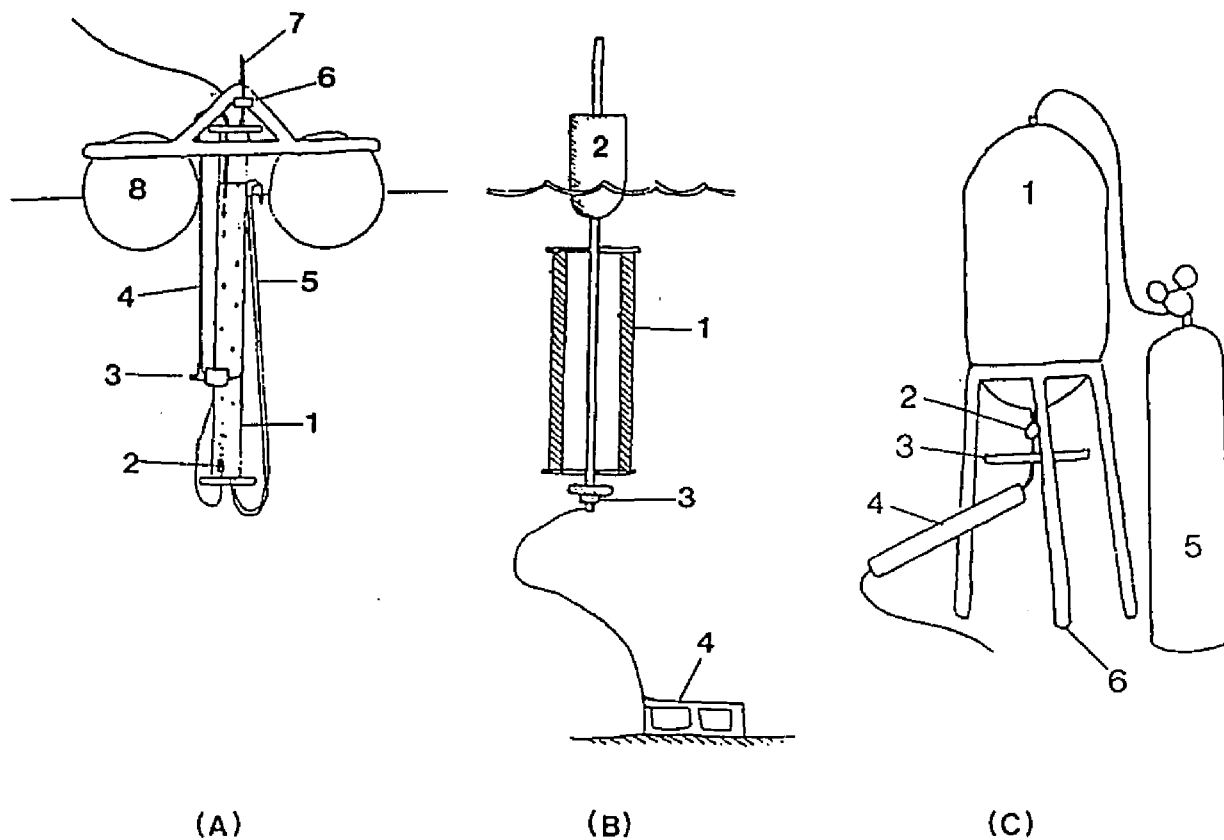


Figure 3.1: Freely Dissolved Contaminant Sampling Devices [A] Gas Sparging system- (1) sparging chamber, (2) air diffuser, (3) submersible pump at .5 m depth, (4) water inlet, (5) water outlet, (6) in-line air filter, (7) adsorbent trap, (8) float; **[B] Semipermeable membrane device-** (1) 1 m SPMDs, (2) float, (3) weight, (4) anchor; **[C] filtration/resin sorption system-** (1) 35 L holding tank, (2) metering valve, (3) 142 mm filter holder, (4) 35 cm long x 2.2 cm I.D. XAD-2 resin column, (5) ultra high purity air tank, (6) stand.

air-water partition coefficient (K_{AW}) of the SOC of interest is known, then the freely dissolved water concentration ($C_{f,w}$) can be calculated from the measured concentration of SOC in the air exiting the chamber ($C_{a,e}$):

$$C_{f,w} = C_{a,e}/K_{AW} \quad (1).$$

However, knowledge of K_{AW} (or Henry's law constant, H) is not necessary for direct determination of surface water fugacities as:

$$C_{a,e} = C_{f,w}K_{AW} = C_{f,w} * H/RT = f_w/RT \quad (2)$$

where T is temperature (K) and R is the gas constant.

Similarly, semipermeable membrane devices (SPMDs) operate on the principle of thermodynamic partitioning of organic contaminants across a membrane surface between water and an organic phase. If sampling time and conditions are sufficient to achieve equilibrium partitioning, the freely dissolved water concentration (i.e. that fraction which can pass through the membrane) is determined by analyzing the concentration of the organic phase (C_{SPMD}). Applying a compound specific partition coefficient (K_{TW}) between water and the organic (e.g. triolein) phase:

$$C_{f,w} = C_{SPMD}/K_{TW} \quad (3);$$

however, for sampling durations or conditions insufficient for equilibrium to be obtained, a kinetic model based upon laboratory uptake experiments (see next section) can be developed.

In this study, low density lay-flat tubing (Cope Plastics, Inc., St. Louis) was used as a semipermeable membrane. Low density polyethylene membranes appear to have cavities or transient holes in the range of 5 to 10 Å (Huckins et al. 1990, Lebo 1992), and therefore, only freely dissolved organic compounds of low molecular weight can diffuse into SPMD-enclosed lipids. Contaminants larger than the exclusion limit (600 da) or sorbed to suspended particles, colloids, or organic matter are not SPMD available.

The SPMDs were prepared to 1 m lengths as follows. The lay-flat tubing was cut and extracted with hexane. The clean tubing was heat sealed at one end and loaded with 1 g of Triolein purchased from (Sigma, 95% purity). The triolein was squeezed toward the other end of the tubing to form a thin film on the inside of the tubing walls and the second end was heat sealed. The constructed SPMDs were kept in tightly sealed pre-cleaned jars in the refrigerator until deployment at sampling sites. SPMD samplers were constructed from large styrofoam bullet floats with PVC pipe frames and stainless steel arm supports, a weight was added to the bottom of the frame to maintain the upright position of the sampler in the water in the presence of strong winds and waves (Figure 1).

Finally, the most common method for determining dissolved SOC concentrations is to filter water samples (e.g. surface or precipitation) through a glass

fiber filter (GFF) to remove the particulate matter, and subsequently pass the effluent through a resin column such as Amberlite^R XAD-2 (Rohm and Haas, Co.) to isolate the dissolved fraction (Capel and Eisenreich 1985, Achman 1993, Baker and Eisenreich 1990, Dickhut and Gustafson 1995, Leister and Baker 1994). The system employed in this study consisted of a 35 L stainless steel holding vessel connected to a 142 mm stainless steel filter head (Millipore, Inc.) with Gelman type A/E (1 μ m wet pore size) GFF, and a 35 cm long x 2.2 cm I.D. stainless steel column containing XAD-2 resin (Rohm and Haas) (Figure 1).

Sampling

Sampling Site Descriptions. Samples were collected and/or experiments were conducted at 5 sites in the southern Chesapeake Bay ranging from rural to urban and highly industrialized (Figure 2). The two rural sites are the Haven Beach (37°25.7'N, 76°13.1'W) and Wolftrap (37°16.53'N, 76°12.0'W) sites located in the mainstem bay off of rural Mathews County, VA. A semiurban site was located on the York River (37°14.5'N, 76°29.0'W) near the Virginia Institute of Marine Science (VIMS). Urban sites were selected off of the city of Hampton at Grandview Beach in the mainstem bay (37°5.0'N, 76°13.3'W), and in the industrialized Elizabeth River (36°52.0'N, 76°19.6'W) which is a site representative of contaminated rivers and estuaries.

Gas Sparging. Two sparger systems were deployed October 7, 1993 tethered from the anchor line upcurrent of the VIMS R/V Langley at the Wolftrap site in

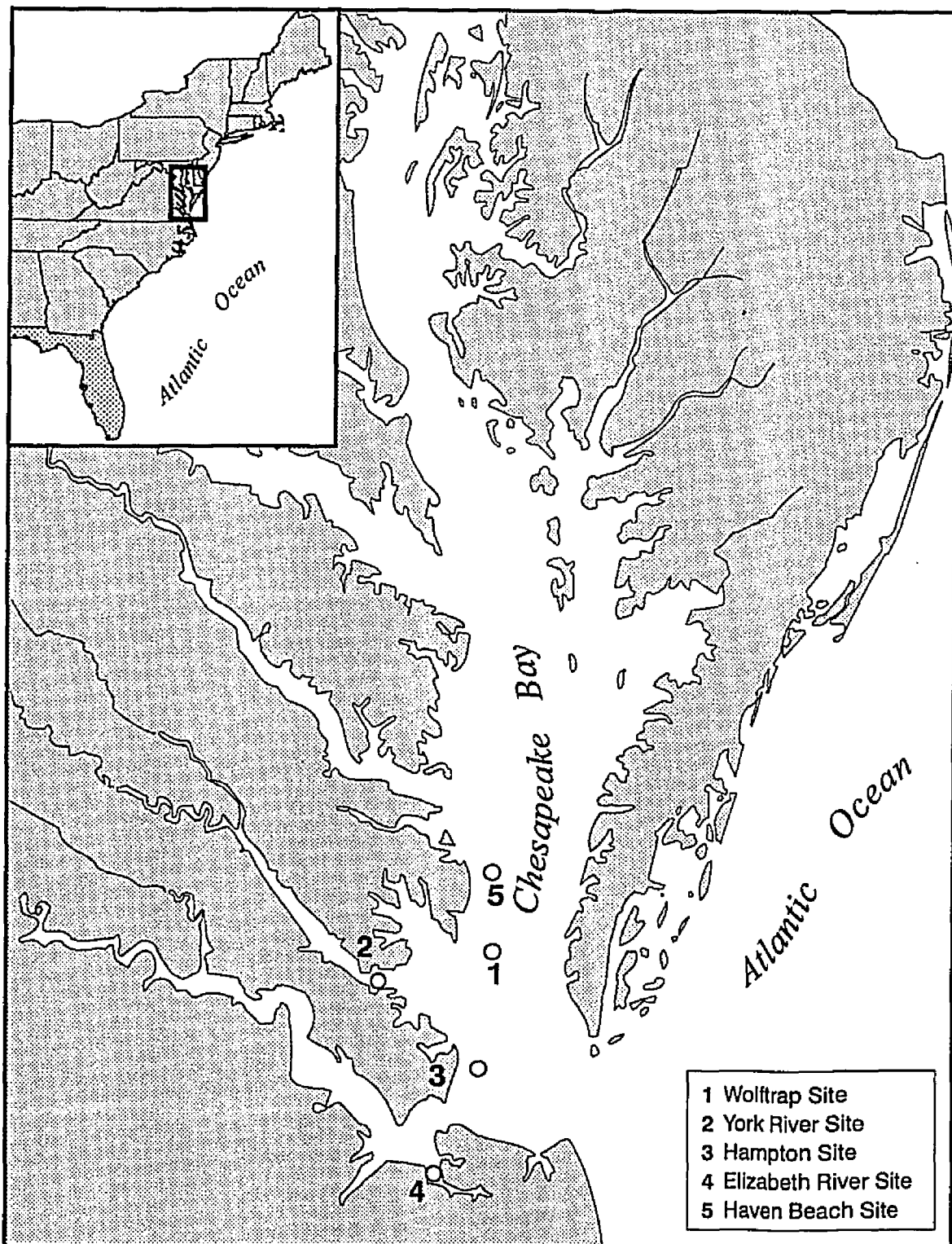


Figure 3.2: Surface Water Sampling Locations in Southern Chesapeake Bay.

southern Chesapeake Bay (Figure 2). Ultra high purity air was introduced through the bottom of the sparger through a diffuser with 140-175 μm pore size glass frit. Water was introduced through the top of the sampler counter-current to the air by a submersible pump (Maxi-jet 750, Aquarium Systems Inc.) at a flow rate of >350 ml/min. The outlet air exited through two (5.3 mm i.d. x 10 cm) stainless steel sorbent traps each packed with .25 g Tenax (Figure 1). The air flow through the traps averaged 200 ± 20 ml/min, and was monitored throughout the sampler deployment (3.5 h) to calculate the total air volume expelled through each trap.

Subsequent tests of the sparger system took place at the York River site (Figure 2) and in the laboratory. As part of the extended evaluation of the sparger, a 47 mm GFF was included in the airstream of the system to remove particulates ejected from the water during sampling. The sparger was deployed in the York River for a sample time of 2.5 h with air flow rates maintained at 400 ± 20 ml/min (approximately 200 ml/min per trap) and average total air sample volumes ($n=11$) of $61,800 \pm 3,200$ ml. Subsequent to field sampling, the filter was installed in a clean sparger in the lab to examine the potential contribution of SOC_s desorbed from the ejected particles to the measured dissolved concentrations of PAH_s. The sparging chamber was filled with purified water and the water inlet and outlet orifices sealed. Air flow rates were maintained at 400 ml/min through the two trap system for a sampling time of 2.5 h. The contribution of PAH desorption from filter retained particles to adsorbent concentrations was evaluated by analyzing and comparing compound concentrations on sorbent traps from the clean sparger to those measured in the river.

Breakthrough of analyte from the adsorbent traps was assessed by sparging 18 L of PAH spiked water in a 20 L carboy. Flow rates were similar to those used in the field (200 ml/min) and the sparging time was increased from 2.5 h to 4 h. The air exiting the sorbent trap was sparged through a 30 cm column of hexane in a graduated cylinder to collect breakthrough analytes. For all PAHs, breakthrough levels were not detectable.

SPMDs. SPMD uptake kinetics and triolein-water partition coefficients were measured in the lab by spiking a mixed PAH standard (naphthalene, acenaphthylene, fluorene, phenanthrene, anthracene, fluoranthene, pyrene) into 4 L amber solvent bottles containing 3 L of Milli-Q purified water and a small SPMD (7 cm long coated with .08 g triolein) suspended from the cap using stainless steel tubing. The bottles, capped and sealed to prevent evaporative losses of the more volatile PAHs, were stirred vigorously on a stir-plate for the entire sampling period. Simultaneous water and SPMD concentrations were measured at two concentration levels at time intervals ranging from 1 to 30 days.

SPMD sampling devices (Figure 1) were deployed via canoe off of Haven Beach (Mathews Co., VA) in Chesapeake Bay (Figure 2) in approximately 8 m of water during several sampling periods in 1994. SPMDs were withdrawn from clean jars using stainless steel forceps and attached to the sampler support frame. The SPMDs were left in the field for sampling intervals between 3 and 12 days. Upon retrieval, the membrane surfaces were wiped with pre-cleaned glass wool wetted with purified water to remove any particulates or algae sorbed to the membrane surface.

The SPMDs were submersed in methanol in clean glass jars and held in a refrigerator at 4 °C until extraction.

Filtration with Sorption to XAD-2 Resin. Water samples for filtration and sorption of the freely dissolved fraction to XAD-2 resin were collected at various times including during SPMD and sparger experiments. The 35 L holding tank (precleaned by sequential rinsing with soap and water, acetone, hexane, dichloromethane, hexane, acetone, and Milli-Q water) was filled by pumping water from 1 m depth through tygon tubing using a 12 V submersible pump. Between 1-2 sample volumes were passed through the pump system prior to sample collection to equilibrate the pump and tubing with ambient contaminant levels and minimize sorptive losses. The water was filtered by pressurizing the system using ultra high purity air and eluting the sample at 200 ml/min through a GFF and 35 cm long x 2.2 cm I.D. stainless steel column containing XAD-2 resin. After sampling, the filter and resin fractions were submersed in methanol in clean jars and held in a refrigerator at 4 °C until extraction.

Analytical Methods. The various sample media were prepared as follows. Glass fiber filters were ashed at 450 °C for 4 h. Amberlite XAD-2 resin was Soxhlet extracted for 24 h each with methanol, acetone, hexane, dichloromethane (DCM-twice), hexane, acetone, and methanol, respectively. Prior to column packing, the resin was rinsed several times with purified water to remove any residual methanol. Glasswool was cleaned by Soxhlet extraction with DCM for 48 h and dried in an oven at 60 °C in clean glass jars covered with aluminum foil. Lay-flat tubing was pre-

cleaned by submersion in hexane for 24 h prior to SPMD construction. Tenax sorbent traps were packed and precleaned by elution with 30 ml each of methanol, acetone, and hexane; residual solvent was evaporated from the traps using ultra high purity air.

After collection, the XAD-2 and GFF samples were spiked with a surrogate standard containing deuterated PAHs (naphthalene, anthracene, benzo[a]anthracene, benzo[a]pyrene, benzo[ghi]perylene) and Soxhlet extracted with organic solvents for 48 h. The SPMDs were Soxhlet extracted for 24 h in hexane. XAD-2 and GFF extracts were concentrated to 1 ml by rotoevaporation and subjected to silica cleanup to remove interfering compounds as described in detail elsewhere (Dickhut and Gustafson 1995). The SPMD hexane extract was concentrated to 1 ml using rotoevaporation and a stream of purified N₂, and subjected to solid-liquid chromatography clean-up on silica (Bio-Sil A, 100-200 mesh) to remove compounds that interfered with PAH analysis. The silica clean-up method (Dickhut and Gustafson, 1995) used for all sample matrices, was modified slightly by overlaying the silica column with 1.25 cm of anhydrous Na₂SO₄ instead of sand. The sorbent traps from the sparger system (Tenax columns) were extracted by eluting analytes from the columns with 40 ml hexane. The extract was concentrated to 1 ml and subjected to silica clean-up as described above.

Prior to analysis for PAHs, the extracts were spiked with an internal standard mixture consisting of additional deuterated PAHs (acenaphthene, phenanthrene, chrysene, perylene), and reduced to a volume of 100 ul under a stream of purified N₂.

The samples were subsequently analyzed for selected PAHs using gas chromatography/mass spectrometry (GC/MS) on a Hewlett Packard 5890A Series II GC and 5971A MS operated in the selective ion monitoring mode (Dickhut and Gustafson, 1995). Average recoveries from the various sample media were between 52.0 and 75.3% for d-8 naphthalene, and 85.2 and 115.0% for d-10 anthracene, d-12 benzo[a]anthracene, and d-12 benzo[a]pyrene (Table 1).

Further Sample Characterization. Total suspended particulates (TSP) were measured by filtering approximately 1 L of water through a pre-ashed and weighed 47mm GFF, which was subsequently dried at 70 °C for 24 h. TSP was determined as the gain in mass on the pre-tared filter per unit volume of water filtered; reported values are averages of three replicate samples. TSP concentrations ranged from 3.1 ± 0.2 to 25.9 ± 0.2 mg/l. Particulate and dissolved organic carbon (POC, DOC) analyses were performed on a Carlo Erba model NA 1500 and a Shimadzu model TOC-500, respectively, by the institute's nutrient analysis lab. POC and DOC values ranged from 0.31 to 2.74 mg/l and 3.03 to 7.88 mg/l, respectively. Salinities, which ranged from 14.0 to 27.0 ppt, were determined with a conductivity meter.

Results

Gas-Sparging. Paired experiments with both gas sparging and filtration with sorption of SOCs to resin were conducted to determine freely dissolved PAH concentrations in Chesapeake Bay surface water. Freely dissolved concentrations

Table 1: Average sample recoveries for various water sampling media

deuterated standard	Sample media*	Recovery mean \pm std (%)
d-8 naphthalene	XAD-2 (n=59)	61.8 \pm 10.8
d-10 anthracene		86.1 \pm 12.8
d-12 benzo[a]anthracene		97.1 \pm 8.1
d-12 benzo[a]pyrene		85.6 \pm 7.9
d-8 naphthalene	SPMDs (n=16)	75.3 \pm 6.7
d-10 anthracene		94.8 \pm 5.5
d-12 benzo[a]anthracene		96.1 \pm 9.7
d-12 benzo[a]pyrene		93.3 \pm 2.8
d-8 naphthalene	Tenax (n=13)	52.0 \pm 12.1
d-10 anthracene		85.2 \pm 6.0
d-12 benzo[a]anthracene		115.0 \pm 7.5
d-12 benzo[a]pyrene		92.2 \pm 4.3
d-8 naphthalene	Water Filter (GFFs) (n=51)	68.5 \pm 11.7
d-10 anthracene		99.1 \pm 19.1
d-12 benzo[a]anthracene		98.6 \pm 10.9
d-12 benzo[a]pyrene		87.6 \pm 8.0

*n is the number of samples and blanks quantified.

determined from sparging were calculated using equation 1 and H values determined from the ratio of the subcooled liquid vapor pressure (Sonnefeld et al. 1983, Appendix B) and Setschenow corrected solubility (May et al. 1983, Ross and Thomas 1981, May and Wasik 1978, Whitehouse 1985, Schwartz 1977, Eganhouse and Calder 1975, Appendices A,C) for the compound of interest at the temperature and salinity of the water. PAH concentrations determined by sparging relative to those determined from GFF/XAD-2 filtration, increased exponentially as the $\log K_{ow}$ of the PAH increased (Figure 3). Therefore, a sampling artifact in the sparging system was suspected.

The large increase in measured freely dissolved concentrations of PAHs with gas-sparging relative to GFF/XAD-2 filtration was hypothesized to be due to particles being scavenged from the water by rising bubbles which are swept through the air stream into the sorbent trap as proposed by Friesen et al. 1993. To examine this hypothesis, an inline 47 mm stainless steel filter holder with GFFs was added to remove particles from the airstream before they entered the analytical trap. The inline filter removed particles from the airstream, but PAH desorption from the filter retained particles was substantial, contributing significantly to measured freely dissolved SOC concentrations (Table 2). PAH desorption from filter retained particles in the clean sparger ranged from 2% (naphthalene) to a factor of 2 (fluoranthene and pyrene) greater than the concentrations determined from a sorbent trap in the field (Table 2). Although a larger fraction of low molecular weight, volatile PAHs were desorbed from particles relative to the high molecular weight

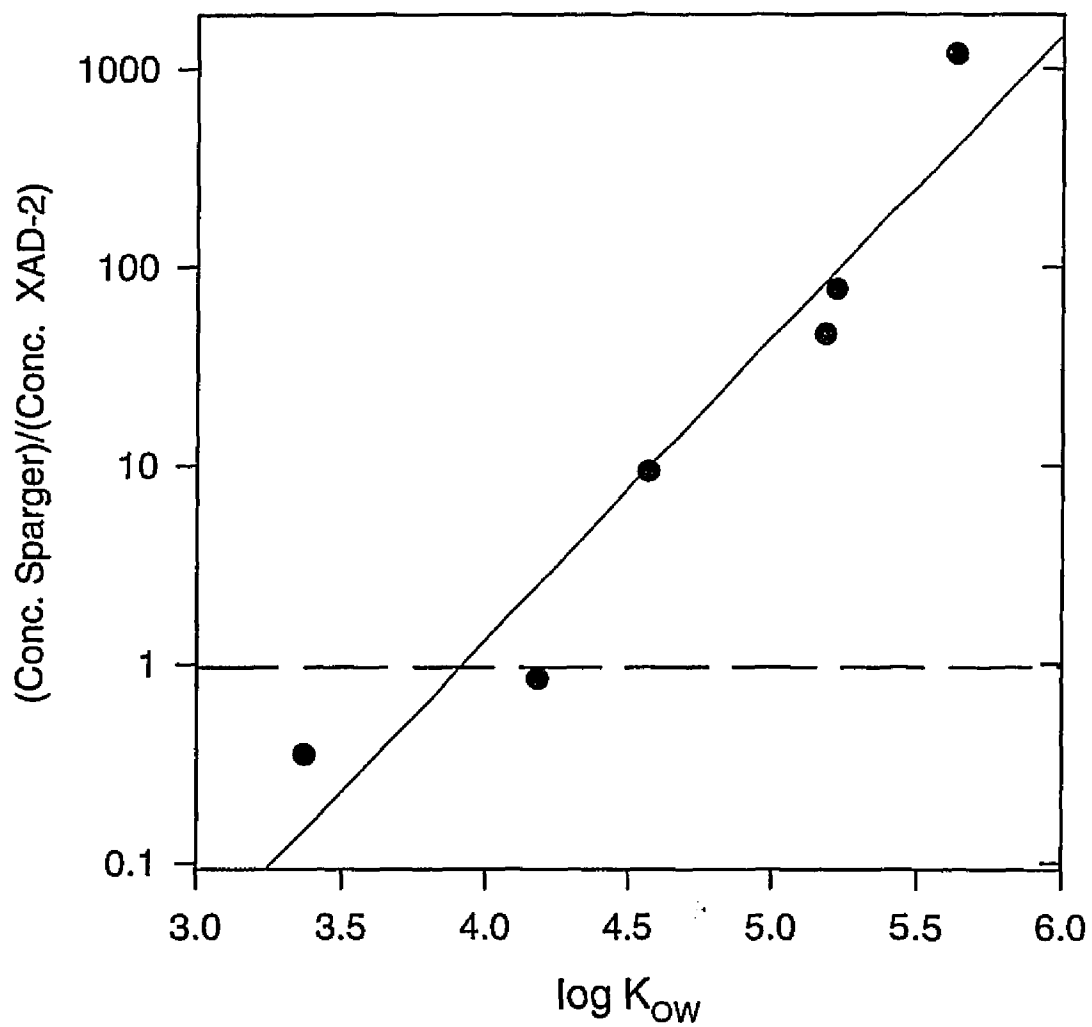


Figure 3.3 : Comparison of Dissolved Concentrations Determined by Sparging Relative to XAD-2 for Selected PAHs as a function of their log K_{ow}s; ---- Ideal Line Given Comparable Methods

Table 2: Contribution of PAH desorption from filter retained particles to sorbent traps.

PAH	sorbent trap-field (ng)	sorbent trap-lab (ng)	desorption contribution ¹ (%)	GFF after desorption (ng)
naphthalene	583	11.5	2	6.94
acenaphthylene	17.2	.85	5	7.70
acenaphthene	173	6.17	4	3.47
fluorene	13.4	3.14	23	.90
phenanthrene	6.07	4.35	72	4.15
anthracene	1.17	.97	83	n.d.
fluoranthene	.87	1.76	202	2.57
pyrene	.55	1.06	193	2.25
benzo[a]anthracene	.80	n.d.	n/a	n.d.
chrysene	n.d.	n.d.	n/a	n.d.
benzo[b]fluoranthene	n.d.	n.d.	n/a	1.65
benzo[k]fluoranthene	n.d.	n.d.	n/a	n.d.
benzo[e]pyrene	n.d.	n.d.	n/a	.86
benzo[a]pyrene	n.d.	n.d.	n/a	n.d.
i[123cd]p ²	n.d.	n.d.	n/a	.51
dibenzo[a,h]anthracene	n.d.	n.d.	n/a	n.d.
benzo[ghi]perylene	n.d.	n.d.	n/a	.64

n.d. = not detected

n/a = not applicable

¹ amount desorbed relative to adsorbent trap-field (%)

² i[123cd]p is ideno[1,2,3-cd]pyrene

compounds, the overall contribution of particle desorption to the measured freely dissolved concentration was low for volatile PAHs due to high truly dissolved concentrations of these compounds. High desorption contributions may be due in part to the fact that the sparger in the laboratory constantly blew clean air across a contaminated filter which created a chemical potential gradient higher than present during field sampling. In the field, air exiting the water column is partially saturated with compounds leading to a lower chemical potential difference between the compound associated with filter retained particles and the intervening air stream, and thus, less desorption. Nonetheless, desorption of semivolatile compounds from ejected particles during gas sparging likely creates a significant artifact in measuring freely dissolved concentrations of SOCs with this method.

SPMD samplers. Uptake kinetic studies with SPMDs containing triolein indicate that at least 72 h sampling time under turbulent conditions is required to achieve equilibrium partitioning (Figure 4). Triolein-water partition coefficients were calculated by averaging the experimentally determined K_{TW} values (after 72 h) and were not corrected for salinity. The K_{TW} 's for selected PAHs and their standard deviations, which averaged 16.6%, are quantitatively related ($r^2 = .96$) to the octanol-water partition coefficient of the compounds (Table 3, Figure 5). Thus, a linear equation between $\log K_{TW}$ and $\log K_{OW}$ may be used to predict SPMD concentration factors of other PAHs, provided there are no kinetic limitations with SPMD sampling of 5-6 ring compounds.

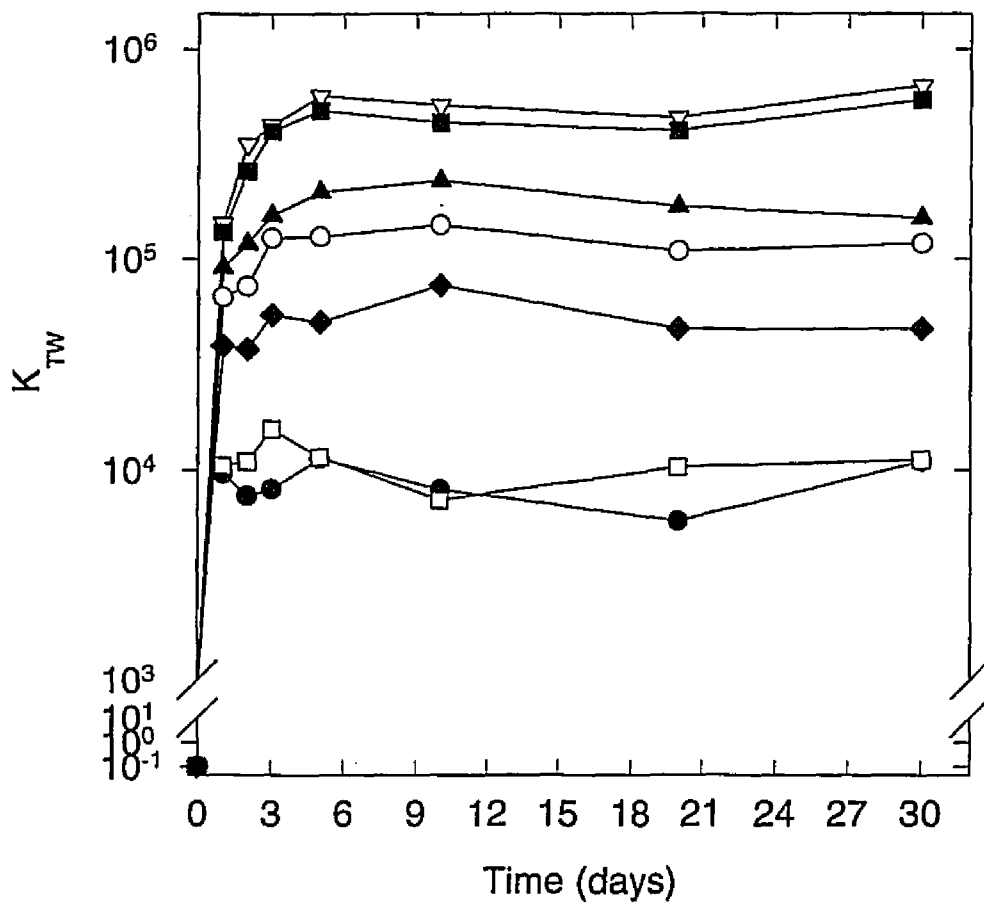


Figure 3.4: Semipermeable Membrane Triolein-Water Partition Coefficients and Uptake Kinetics for Selected PAHs:—●— naphthalene,—▽— pyrene,—□— acenaphthylene,—○— phenanthrene,—◆— fluorene,—▲— anthracene,—■— fluoranthene,

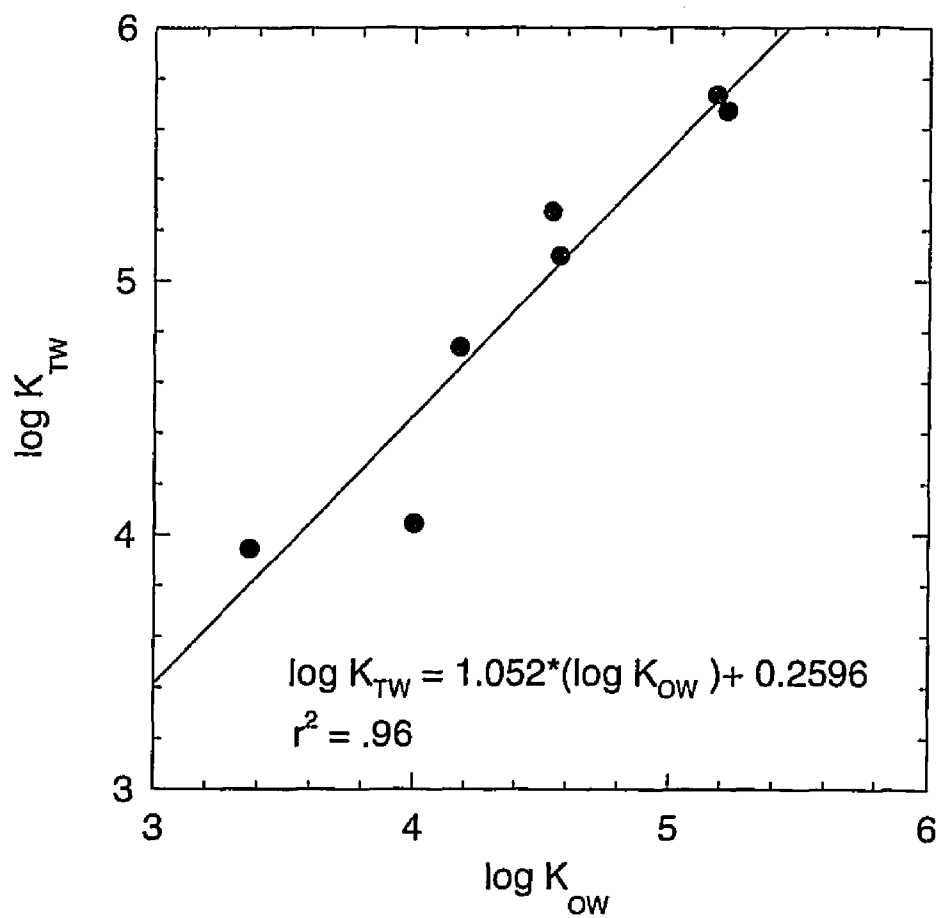


Figure 3.5: SPMD Triolein-Water Partition Coefficients (K_{TW}) for Selected PAHs Correlated to the Contaminants' K_{ow} s

Table 3: Triolein-water partition coefficients (K_{TW}) for selected PAHs

PAH	Partition Coefficient	log K_{TW}	Published* log K_{ow}
naphthalene	8770 ± 1840	3.94	3.37
acenaphthylene	11000 ± 2290	4.04	4.0
fluorene	54400 ± 10600	4.74	4.18
phenanthrene	125000 ± 11900	5.10	4.57
anthracene	187000 ± 30200	5.27	4.54
pyrene	541000 ± 85300	5.73	5.18
fluoranthene	467000 ± 63400	5.67	5.22

*from Mackay et al. 1992

regression equation: $\log K_{TW} = 1.052 * \log K_{ow} + 0.260$; $r^2 = .96$

Two SPMD samplers were deployed at the Haven Beach site on May 10, 1994; one sampler (2 SPMDs) was retrieved 4 days later and the second sampler was left in the field for 12 days. The SPMDs exposed in the field for a 12 days showed signs of algal growth on the outer membrane surface. Furthermore, the 12 day samples were not quantifiable by GC/MS due to the presence of a large interfering peak that remained with the PAH fraction after silica clean-up. PAH dissolved surface water concentrations determined from the four day exposure of the SPMDs were compared to those determined by filtration and sorption of SOCs to XAD-2 for a water sample collected on the first day of SPMD deployment. The dissolved concentrations determined by the two methods were comparable only to within a factor of 4 for the majority of the PAHs analyzed, but deviated more than a factor of 10 for the larger PAHs (Table 4).

A second SPMD deployment was conducted from June 26 to 29, 1994. Dissolved PAH water concentrations were measured using GFF/XAD-2 filtration on June 26, 28, and 29; a rain event (1.0 cm) occurred June 27 during the SPMD deployment. Again, freely dissolved PAH concentrations determined by the two methods were comparable within a factor of four with deviations exceeding a factor of ten for the larger PAHs (Table 5).

From the field trials, the average relative standard deviation associated with dissolved PAH concentrations determined by replicate SPMDs was <10%; whereas, the variability in the XAD-2 concentrations over three days averaged 30%. Thus, each of these methods for measuring dissolved SOC concentrations appear to be

Table 4: Freely dissolved water concentrations determined by SPMDs May 10-14, 1994 and GFF/XAD-2 May 10, 1994 at Haven Beach Site

PAH ¹	XAD-2 (ng/l)	SPMD #1 (ng/l)	SPMD #2 (ng/l)	SPMD ² % rel std	SPMD/XAD-2 Ratio ³
naphthalene	18.8	5.22	5.03	1.9	-3.7
acenaphthylene	.102	.233	.177	13.7	2.01
acenaphthene*	.206	1.08	.874	10.4	-4.74
fluorene	.607	1.01	.947	.3	1.61
phenanthrene	.963	1.15	1.03	5.5	1.13
anthracene	.064	.082	.056	18.8	1.08
fluoranthene	.632	.328	.345	2.5	-1.89
pyrene	.264	.104	.102	1.0	-2.56
b[a]a*	.016	.0016	.0015	4.9	-10.3
chrysene*	.008	.0062	n.d.	n/a	n/a
b[b]f	.024	.0017	.0014	8.1	-12.9
b[k]f	n.d.	.0014	n.d.	n/a	n/a
b[e]p*	.020	.0022	.0015	16.6	-10.8
b[a]p*	.011	.0004	n.d.	n/a	n/a
i[1,2,3-cd]p*	n.d.	n.d.	n.d.	n/a	n/a
d[3,h]a*	.033	n.d.	n.d.	n/a	n/a
b[ghi]p*	n.d.	n.d.	n.d.	n/a	n/a

avg. = 7.6

¹ Abbreviations for PAHs are as follows: b[a]a is benzo[a]anthracene; b[b]f, benzo[b]fluoranthene; b[k]f, benzo[k]fluoranthene; b[e]p, benzo[e]pyrene; b[a]p, benzo[a]pyrene; i[1,2,3-cd]p, ideno[1,2,3-cd]pyrene; d[a,h]a, dibenzo[a,h]anthracene; b[ghi]p, benzo[ghi]perylene

* Triolein-water partition coefficients were determined from the regression eq in Table 3.

² Relative standard deviation (%) for replicate SPMDs

³ Ratio of SPMD/XAD-2 measured concentrations, if the ratio was < 1, the negative inverse of the ratio is reported.

n.d. is not detected

n/a is not available

Table 5: Freely dissolved water concentrations determined by SPMDs June 26-29, 1994 and GFF/XAD-2 filtration June 26,28,29 at Haven Beach

PAH [†]	SPMD #1 (ng/l)	SPMD #2 (ng/l)	SPMD RSD [†] (%)	XAD 6-26-94 (ng/l)	XAD 6-28-94 (ng/l)	XAD 6-29-94 (ng/l)	XAD ¹ avg (ng/l)	XAD ² RSD (%)	SPMD/XAD-2 ³ Ratio (%)
naphthalene	3.10	2.45	11.8	9.25	17.3	6.061	10.9	43.4	-3.84
acenaphthylene	.156	.153	1.0	.050	.061	.045	.052	12.3	2.97
acenaphthene*	.447	.547	10.0	.145	.190	.144	.160	13.4	3.11
fluorene	.497	.747	20.1	.305	.415	.368	.363	12.4	1.72
phenanthrene	.766	.833	4.2	.647	1.02	.745	.804	19.7	1.0
anthracene	.034	.036	2.9	.089	.086	.036	.070	34.9	-2.0
fluoranthene	.174	.170	1.2	.858	.335	.365	.519	46.2	-3.03
pyrene	.083	.084	.6	.431	.187	.218	.279	38.9	-3.33
b[a]a*	.0017	.0016	3.5	n.d.	.0381	n.d.	n/a	n/a	n/a
chrysene*	.0059	.0061	3.3	.0968	.0478	.1201	.0882	34.1	-14.7
b[b]f	.0042	.0048	5.9	.0567	.0749	.0545	.0620	14.7	-13.8
b[k]f	n.d.	n.d.	n/a	.0354	.149	.0339	.0727	74.0	n/a
b[e]p*	.0010	.0010	1.2	.0384	.0273	.0395	.0351	15.7	-35.1
b[a]p*	n.d.	n.d.	n/a	.0281	.0221	.0421	.0308	27.2	n/a
i[1,2,3-cd]p*	n.d.	n.d.	n/a	n.d.	n.d.	n.d.	n.d.	n/a	n/a
d[a,h]a*	n.d.	n.d.	n/a	n.d.	n.d.	n.d.	n.d.	n/a	n/a
b[ghi]p*	n.d.	n.d.	n/a	n.d.	n.d.	n.d.	n.d.	n/a	n/a

avg = 5.5

avg = 30

[†] Abbreviations for PAHs are as follows: b[a]a, benzo[a]anthracene; b[b]f, benzo[b]fluoranthene; b[k]f, benzo[k]fluoranthene; b[e]p, benzo[e]pyrene; b[a]p, benzo[a]pyrene; i[1,2,3-cd]p, indeno[1,2,3-cd]pyrene; d[a,h]a, dibenzo[a,h]anthracene; b[ghi]p, benzo[ghi]perylene
* denotes SPMD concentration calculated using triolein-water partition coefficients from regression eq in Table 3.

[†] SPMD RSD (% relative standard deviation) for replicate SPMDs.

¹ Average dissolved concentration determined by GFF/XAD-2 filtration over the SPMD exposure period.

² XAD RSD (% relative standard deviation) for concentrations determined by GFF/XAD-2 filtration June 26, 28, 29, 1994; RSD for replicate measurements by GFF/XAD-2 filtration was 5.4%

³ SPMD/XAD-2 ratios calculated with average GFF/XAD-2 concentrations over June 26-29 and average of 2 SPMD replicates; when ratios were less than 1, negative values indicate the reciprocal ratio
n.d. is not detected.
n/a is not available.

reasonably precise given that the measured concentrations were averaged over several days. However, the large negative SPMD/XAD-2 ratios reported in Tables 4 and 5 for the larger PAHs indicate that the dissolved concentrations of these compounds measured using SPMDs are much lower than those measured using XAD-2, and that the larger PAHs may not achieve equilibrium between the triolein and the surface water during the SPMD deployment (4 d). Incomplete equilibrium may be due to a lack of turbulence in the estuary. In the absence of turbulence, high molecular weight SOCs may be depleted locally in the vicinity of the SPMDs due to the high affinity of these compounds for the SPMD lipid phase. This phenomena would slow the rate of mass transfer of the SOCs into the SPMD, and would impact the distribution of high molecular weight compounds, with larger partition coefficients and lower diffusivities, more than the lighter SOCs. It was expected that turbulence in estuarine surface waters subject to tidal and wind driven currents would be sufficient to attain equilibrium of SOCs between freely dissolved components and the SPMD after 3 days of exposure. This may not be the case.

A kinetic model was developed from laboratory studies to evaluate dissolved water concentrations determined from SPMDs for larger PAHs which may not have attained steady-state during the exposure period. The natural logarithm of the compound specific triolein-water partition coefficient can be plotted as a function of exposure time for the uptake portion of the curve. The freely dissolved water concentration determined from the SPMD during the uptake period is then a function

of an 'effective' partition coefficient ($\exp(b^1*t + b^0)$); thus:

$$C_{f,w} = C_{SPMD}/(\exp(b^1*t + b^0)) \quad (4)$$

where b^1 and b^0 are compound specific regression coefficients obtained from a plot of $\ln K_{TW}$ vs t .

The 'effective' partition coefficient increased dissolved water concentrations for the larger PAHs determined by SPMDs using eq 3. However, the increase in concentrations (c.a. 10%) did not significantly increase the SPMD/XAD-2 ratios as the exposure time in the field was near the exposure time determined in the lab for achievement of steady-state and hence, the effective partition coefficient approached the equilibrium partition coefficient. The kinetic model should have corrected for a compounds inability to reach steady-state based on an insufficient exposure period given constant water concentrations and turbulent conditions over the exposure period. Neither of these conditions may be environmentally realistic. Concentrations determined by the GFF/XAD-2 method exhibited a 30% variance over a three day period. Additionally, turbulence in the water column of Chesapeake Bay is largely wind and tide induced; during periods of low wind speed, tidal mixing may not be sufficient to overcome diffusion-limited conditions.

Another potential factor contributing to larger freely dissolved concentrations measured with GFF/XAD-2 filtration compared to SPMDs may be association of DOC-bound SOCs with the XAD-2 resin, thus artificially inflating the $C_{f,w}$ values

determined by the filtration/sorption method. The sorption capacity of XAD-2 for dissolved organic matter was investigated by quantifying dissolved organic carbon (DOC) in a water sample before and after the XAD-2 column in the sampling train. DOC levels were 3.2 mg/l after the filter and before the XAD-2 column and 3.63 mg/l after the XAD column (Wolftrap Site 1-11-94), indicating a 13% rise, not loss, of DOC in the XAD column. Thus DOC does not appear to be retained by the XAD-2 column.

Filtration with sorption to resin. Water samples were collected for filtration and sorption of the freely dissolved fraction to XAD-2 resin during SPMD and air-sparging experiments, as well as monthly from January 1994 through May 1995 at Wolftrap, and every other month from July 1994 to May 1995 at the Hampton, Elizabeth River, and York River sites. Potential sampling artifacts for filtration with subsequent sorption of freely dissolved PAHs to resin were assessed via several experiments. Using replicate GFF/XAD-2 systems, the average error for measurement of dissolved concentrations was 5.4% for all PAHs detected. The sorption of PAHs to the sampling train surface, PAH blank levels, and the efficiency of the XAD-2 resin for isolating SOCs were tested by spiking deuterated PAHs into 35 L of purified water. Recoveries for the deuterated PAHs via this method and the entire analytical process were measured as 74% for d_{10} -anthracene, 98% for d_{12} -benzo[a]anthracene, and 59% for d_{12} -benzo[a]pyrene. The average recovery of 77% is similar to that determined by others (Daignault et al. 1988) verifying the use of XAD-2 resin and this system for quantification of SOCs in water. Analyses of field

and lab blank levels of analyte compounds attributable to sampling artifacts were typically less than 5% those in the actual samples. Finally, the sorption of DOC and associated PAHs by XAD-2 is expected to be negligible as noted above.

PAH Concentrations and Distributions. Total (particulate and dissolved) mean concentrations for 17 PAHs ranged from 24.1 to 91.1 ng/L with the largest percentage of the total levels occurring in the dissolved phase at all sites (Table 6). The total PAH concentrations reported here for the southern Chesapeake are higher than those reported by Ko and Baker (1995) for surface waters of the northern bay; however, a larger number of PAHs were also quantified in this study. Moreover, a larger site-to-site compared to seasonal variability in PAH surface water concentrations in Chesapeake Bay (Figure 6) was observed in this study.

Mean particle-associated PAH concentrations at the Elizabeth River site were significantly different (at the .05 level) from those at all other sites (Figure 6). Further, mean particulate concentrations of the heavier molecular weight PAHs (e.g. pyrene, benzo[e]pyrene) at the York River site were significantly different (at the .05 level) from concentrations measured at the Wolftrap site (Figure 6). For the dissolved PAH fraction, analyses of variance at the $\alpha = .05$ level yielded slightly different results. Mean dissolved PAH concentrations at the Elizabeth River site were significantly different from dissolved PAH concentrations measured at all other sites with the exception of the lighter molecular weight PAHs (e.g. fluorene, phenanthrene) at the Wolftrap site. Dissolved concentrations at the York River site were significantly different from concentrations at all other sites except Hampton. The

Table 6: Mean Values and Ranges of PAH Concentrations (ng/l) for the Dissolved and Particulate Phases in Surface Waters of Southern Chesapeake Bay

PAH ¹	Wolftrap Site						Elizabeth River Site					
	Dissolved (n=17)			Particulate			Dissolved (n=6)			Particulate		
	min.	max.	mean	min.	max.	mean	min.	max.	mean	min.	max.	mean
naphthalene	9.71	27.4	16.3	n.q.	n.q.	n.q.	9.32	24.6	16.4	1.44	2.04	1.70
acenaphthylene	<.003	.802	.291	.006	.039	.021	.244	.772	.546	.024	.086	.049
acenaphthene	.225	1.12	.669	<.003	.161	.040	2.79	11.3	5.56	.159	.539	.304
fluorene	.616	4.01	2.57	.045	.481	.145	1.10	4.25	2.32	.240	.623	.414
phenanthrene	1.11	6.00	3.90	.169	1.28	.401	1.70	7.37	4.11	.883	2.31	1.41
anthracene	<.003	.199	.089	.016	.092	.042	.362	1.23	.799	.250	.639	.411
fluoranthene	.154	.709	.280	.089	.359	.180	4.71	47.3	22.1	1.59	10.2	4.07
pyrene	.110	.381	.229	.084	.666	.188	2.65	17.4	10.6	1.64	8.57	3.49
b(a)a	<.003	.051	.013	.019	.141	.077	.150	1.13	.701	.555	2.57	1.27
chrysene	<.003	.081	.044	.041	.197	.112	.464	2.64	1.65	.899	3.95	2.09
b(b)f	<.003	.049	.019	.046	.262	.130	.100	.552	.363	1.16	4.28	2.40
b(k)f	<.003	.031	.006	<.003	.225	.110	<.003	.172	.069	.853	3.52	1.84
b(e)p	<.003	.053	.017	.033	.207	.106	.102	.435	.325	.902	2.90	1.83
b(a)p	<.003	.047	.008	.026	.183	.093	.023	.163	.094	.723	2.37	1.28
i(1,2,3-cd)p	<.003	.055	.007	<.003	.258	.111	<.003	.066	.028	.689	2.44	1.30
d(a,h)a	<.003	.016	.004	<.003	.068	.016	<.003	.012	.006	.123	.518	.280
b(g,h,i)p	<.003	.052	.008	.020	.262	.114	<.019	.076	.041	.693	2.36	1.29
total 17 PAHs			24.5			1.89			65.7			25.4

PAH ¹	York River Site						Hampton Site					
	Dissolved (n=9)			Particulate			Dissolved (n=6)			Particulate		
	min.	max.	mean	min.	max.	mean	min.	max.	mean	min.	max.	mean
naphthalene	11.72	21.2	15.9	.620	1.55	.950	8.051	27.1	16.1	.613	2.19	1.19
acenaphthylene	.141	.571	.361	.011	.050	.023	.077	.476	.259	.008	.045	.021
acenaphthene	.580	2.77	1.43	.035	.136	.073	.189	.649	.391	.020	.093	.047
fluorene	.655	2.70	1.16	.064	.182	.111	.224	1.40	.759	.050	.121	.079
phenanthrene	1.08	4.78	2.22	.236	.779	.491	.469	3.15	1.65	.206	.513	.317
anthracene	.082	.392	.166	.033	.207	.093	.042	.078	.057	.025	.094	.049
fluoranthene	.421	1.45	.858	.203	1.41	.711	.229	.688	.430	.221	.548	.354
pyrene	.245	.945	.529	.189	1.68	.641	.127	.340	.222	.159	.483	.295
b(a)a	<.003	.084	.033	.113	.586	.250	<.003	.034	.010	.075	.254	.147
chrysene	.044	.276	.123	.163	.780	.450	<.003	.060	.035	.121	.399	.235
b(b)f	.017	.122	.048	.245	1.08	.508	<.003	.033	.020	.136	.491	.274
b(k)f	<.003	.062	.023	.189	.782	.387	<.003	.024	.010	.102	.416	.225
b(e)p	.014	.067	.033	.149	1.03	.387	<.003	.078	.021	.097	.365	.214
b(a)p	<.003	.028	.009	.136	.813	.330	<.003	.041	.010	.091	.357	.193
i(1,2,3-cd)p	<.003	.011	.004	.113	.946	.361	<.003	.024	.006	.122	.476	.248
d(a,h)a	<.003	.005	.003	<.003	.170	.064	<.003	.003	.003	.026	.069	.041
b(g,h,i)p	<.003	.012	.006	.140	1.23	.413	<.003	.003	.110	.417	.239	
total 17 PAHs			22.9			6.24			20.0			4.17

¹Abbreviations for PAHs: b(a)a, benzo(a)anthracene; b(b)f, benzo(b)fluoranthene; b(k)f, benzo(k)fluoranthene; b(e)p, benzo(e)pyrene; b(a)p, benzo(a)pyrene; i(1,2,3-cd)p, indeno(1,2,3-cd)pyrene; d(a,h)a, dibenzo(a,h)anthracene; b(g,h,i)p, benzo(g,h,i)perylene
< = below detection limit; limit of detection given
n.q. = not quantifiable

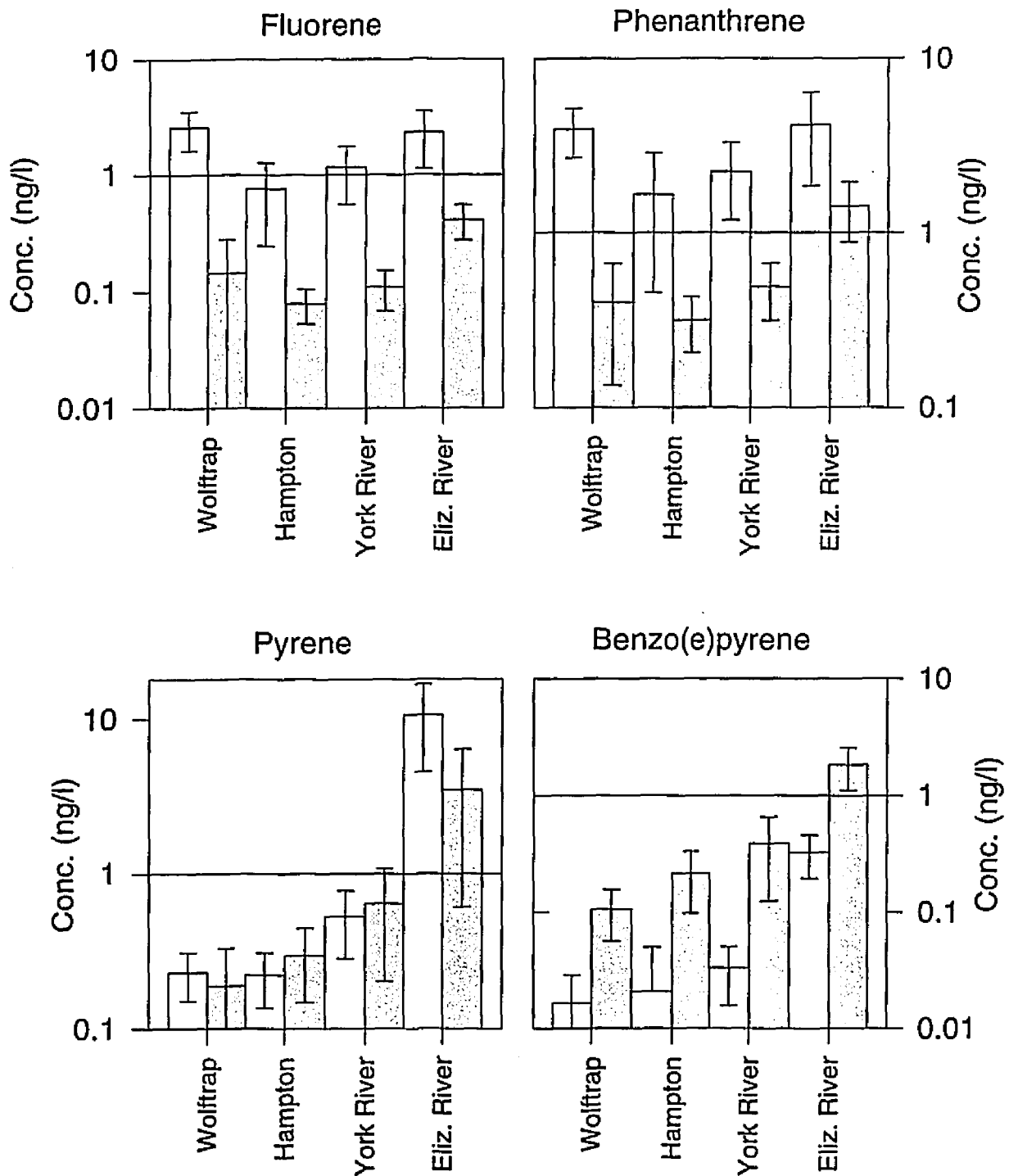


Figure 3.6: Mean Concentrations (+/- std) of PAHs in Surface Waters of Southern Chesapeake Bay

Dissolved
 Particulate

mean dissolved PAH concentrations at the Hampton and Wolftrap sites were significantly different for the lighter molecular weight PAHs.

The Elizabeth River exhibited considerably elevated dissolved and particulate PAH concentrations; the waters of the Elizabeth River were especially enriched in dissolved fluoranthene and pyrene as well as particle-associated PAHs (Figure 6, Table 6). In addition, the York River site showed an increased loading of the particle-bound PAHs relative to the bay sites (Table 6, Figure 6). The data exhibit an obvious gradient in surface water PAH concentrations of the heavy molecular weight compounds from source regions in the river basins to mainstem Chesapeake Bay (Figure 6).

Organic carbon normalized distribution coefficients (K_{OC}) were determined for 29 water samples for which PAH concentrations, TSP, and POC were measured. The $\log K_{OC}$ values were plotted versus reported $\log K_{OW}$ (Mackay et al. 1992) where:

$$K_{OC} = (C_p * POC) / (TSP * C_{f,w})$$

and C_p is the measured particle-associated PAH concentrations (Figure 7).

Equilibrium partitioning theory suggests that the slope of the $\log K_{OC}$ vs $\log K_{OW}$ relationship should be ~ 1 for the distribution of a group of SOCs between the particle-associated and freely dissolved phases. The average slope obtained from plots of $\log K_{OC}$ vs $\log K_{OW}$ for all sampling sites/times was $.92 \pm .14$ with an intercept value of $1.41 \pm .66$ ($n=29$). These results suggest that PAH dissolved-particle distributions in surface waters of southern Chesapeake Bay are near

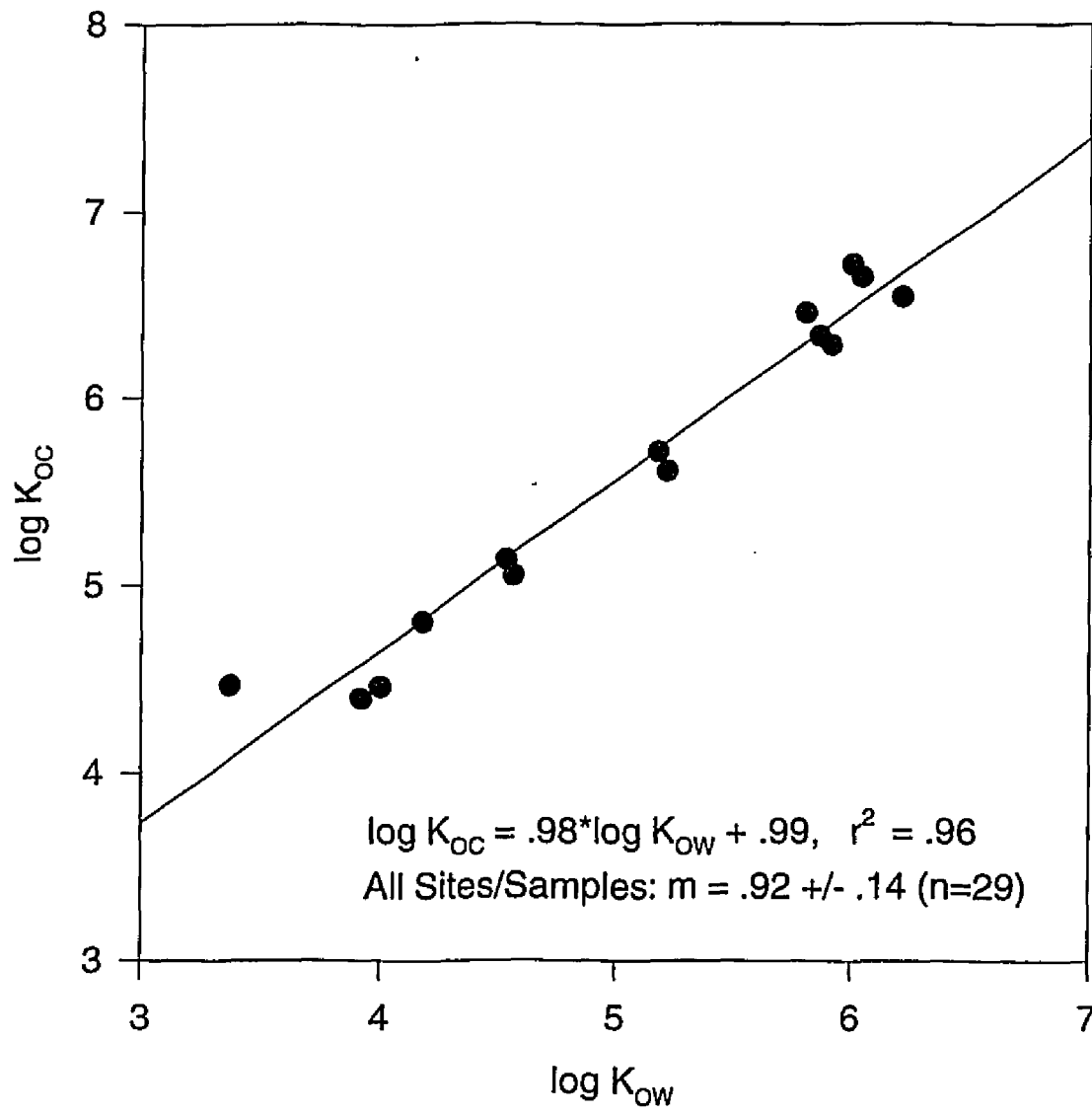


Figure 3.7: Dissolved-Particulate Distribution Coefficients (K_{oc}) for PAHs Correlated to the Contaminants K_{ow} (York River 8-12-94)

equilibrium. Further, the relationship between K_{OC} and K_{OW} implies that filtration with sorption of the dissolved fraction to XAD-2 resin is unbiased with respect to contribution of a third phase. If colloids or DOC-associated PAHs were contributing to the dissolved fraction measured by XAD-2, the K_{OC} - K_{OW} relationship would deviate from a slope of 1 as K_{OW} increased, because heavier PAHs with larger K_{OW} s would be more influenced by sorption to DOC or colloids to the resin relative to compounds with smaller K_{OW} s. Although this behavior has been observed for particulate-dissolved distribution coefficients of SOCs in many cases (Baker et al 1991, Achman et al. 1993), it is clearly not the case for PAHs in the Chesapeake Bay water samples collected in this study (Figure 7).

Summary and Conclusions

Freely dissolved PAH concentrations have been measured in Chesapeake Bay surface waters via three methods. Dissolved concentrations measured by air sparging and SPMDs were significantly different than those measured by filtration with subsequent sorption of the freely dissolved fraction to XAD-2 resin. Higher freely dissolved concentrations relative to GFF/XAD-2 filtration and evidence for particle-mediated transport of PAHs was observed in the gas sparging experiments. In contrast, freely dissolved PAH concentrations determined by in situ SPMDs were within a factor of four, and typically lower than, concentrations determined by XAD-2. Sample cleanup of interfering compounds in SPMDs is also problematic.

Furthermore, PAHs require at least 72 h to achieve equilibrium partitioning with SPMDs under turbulent conditions, thus the ability to determine short-term temporal variability is lost. Therefore, filtration with sorption to XAD-2 resin at present is the most feasible and accurate method to determine freely dissolved SOC concentrations in estuarine waters. The major disadvantage with XAD-2 resin, however, is the extensive clean-up required to achieve acceptable blank levels of analytes.

PAH surface water concentrations measured in the southern Chesapeake Bay are higher than those reported for the northern bay. Further, PAH concentrations in the Elizabeth River were significantly higher than concentrations measured at all other sites, supporting the conclusion that this tributary has been greatly impacted by human activities and is representative of a contaminated estuary. Additionally, particle-bound PAH concentrations were also elevated at the York River site; hence, both tributary sites exhibited higher particle-bound PAH loadings than the mainstem bay sites. No seasonal trends were observed in either the dissolved or particle-bound PAH fraction at any sites. Nonetheless, PAH dissolved-particle distributions in surface waters of southern Chesapeake Bay were near equilibrium for all locations and seasons.

References

- Achman, D.R., K.C. Hornbuckle, and S.J. Eisenreich. 1993. Volatilization of Polychlorinated Biphenyls from Green Bay, Lake Michigan. *Environ. Sci. Technol.* 27:75-87.
- Baker, J.E. and S.J. Eisenreich. 1989. PCBs and PAHs as tracers of particulate dynamics in large lakes. *J. Great Lakes Res.* 15(1):84-103.
- Baker, J.E. and S.J. Eisenreich. 1990. Concentrations and fluxes of polycyclic aromatic hydrocarbons and polychlorinated biphenyls across the air-water interface of Lake Superior. *Environ. Sci. Technol.* 24:342-352.
- Baker, J.E., S.J. Eisenreich, and D.L. Swackhammer. 1991. Field measured associations between polychlorinated biphenyls and suspended solids in natural waters: an evaluation of the partitioning paradigm. In *Organic Substances and sediments in water, Vol. 2*, R.A. Baker ed. Lewis Publishers, Chelsea Michigan.
- Black, J.J., T.F. Hart, Jr., P.J. Black. 1982. A novel integrative technique for locating and monitoring polynuclear aromatic hydrocarbon discharges to the aquatic environment. *Environ. Sci. Technol.* 16:247-250.
- Capel, P.D., and S.J. Eisenreich. 1985. PCBs in Lake Superior, 1978-1980. *J. Great Lakes Res.* 11(4):447-461.
- Daignault, S.A., D.K. Noot, D.T. Williams, and P.M. Huck. 1988. A review of the use of XAD resins to concentrate organic compounds in water. *Water Resour.* 22:803-813.
- Dickhut, R.M., K.E. Gustafson. 1995. Atmospheric inputs of selected polycyclic aromatic hydrocarbons and polychlorinated biphenyls to southern Chesapeake Bay. *Mar. Pollut. Bull.* 30:385-396.
- Eadie, B.J. and J.A. Robbins. 1987. In-Sources and fates of aquatic pollutants. Hites, R.A. and S.J. Eisenreich, Eds., *Advances in Chemistry Series 216*. American Chemical Society. Washington, DC. 319-364.
- Eganhouse, R.P. and J.A. Calder. 1976. The solubility of medium molecular weight aromatic hydrocarbons and the effects of hydrocarbon co-solutes and salinity. *Geochim. Cosmochim. Acta.* 40:555-561.

- Friesen, K.J., W.L. Fairchild, M.D. Loewen, S.G. Lawrence, M.H. Holoka, and D.C.G. Muir. 1993. Evidence for particle-mediated transport of 2,3,7,8-tetrachlorodibenzofuran during gas sparging of natural water. *Environ. Tox. Chem.* 12:2037-2044.
- Huckins, J.N., M.W. Tubergen, and G.K. Manuweera. 1990. Semipermeable membrane devices containing model lipid: A new approach to monitoring the bioavailability of lipophilic contaminants and estimating their bioconcentration potential. *Chemosphere.* 20:533-552.
- Ko, F. and J.E. Baker. 1995. Partitioning of hydrophobic organic contaminants to resuspended sediments and plankton in the mesohaline Chesapeake Bay. *Mar. Chem.* 49:171-188.
- Landrum, P.F., S.R. Nihart, B.J. Eadie, and W.S. Gardner. 1984. *Environ. Sci. Technol.* 18:187-192.
- Lebo, J.A., J.L. Zajicek, J.N. Huckins, J.D. Petty, and P.H. Peterman. 1992. Use of semipermeable membrane devices for in situ monitoring of polycyclic aromatic hydrocarbons in aquatic environments. *Chemosphere.* 25:697-718.
- Leister, D.L. and J.E. Baker. 1994. Atmospheric Deposition of Organic Contaminants to the Chesapeake Bay. *Atmos. Environ.* 28:1499-1520.
- Mackay, D., W.Y. Shiu, and K.C. Ma. 1992. Illustrated handbook of physical-chemical properties and environmental fate for organic chemicals. Vol. II. Lewis Publishers. Chelsea, Michigan.
- May, W.E., S.P. Wasik, and D.H. Freeman. 1978. Determination of the Solubility Behavior of Some Polycyclic Aromatic Hydrocarbons in Water. *Anal. Chem.* 50:997-1000.
- May, W.E., S.P. Wasik, M.M. Miller, Y.B. Tewari, J.M. Brown-Thomas, and R.N. Goldberg. 1983. Solution thermodynamics of some slightly soluble hydrocarbons in water. *J. Chem. Eng. Data* 28:197-200.
- Murray, M.W. and A.W. Andren. 1991. Preliminary evaluation of the potential of gas purging for investigating the air-water transfer of PCBs. In *Organic Substances and Sediments in Water: Volume 2, Processes and Analytical*. CRC Press: Boca Raton, FL. pp 3-13.

- Prest, H.F., W.M. Jarman, S.A. Burns, T. Weismuller, M. Martin, and J.N. Huckins. 1992. Passive water sampling via semipermeable membrane devices (SPMDS) in concert with bivalves in the Sacramento/San Joaquin river delta. *Chemosphere*. 25:1811-1823.
- Rossi, S.J. and W.H. Thomas. 1981. Solubility Behavior of Three Aromatic Hydrocarbons in Distilled Water and Natural Seawater. *Environ. Sci. Technol.* 15:715-716.
- Schwartz, F.P. 1977. Determination of Temperature Dependence of Solubilities of Polycyclic Aromatic Hydrocarbons in Aqueous Solution by a Fluorescence Method. *J. Chem. Eng. Data*. 22:273-276.
- Sodergren, A. 1987. Solvent-filled dialysis membranes simulate uptake of pollutants by aquatic organisms. *Environ. Sci. Technol.* 21:855-859.
- Sonnefeld, W.J., W.H. Zoller, and W.E. May. 1983. Dynamic coupled-column liquid chromatographic determination of ambient vapor pressures of polynuclear aromatic hydrocarbons. *Anal. Chem.* 55:275-280.
- Sproule, J.W., W.Y. Shiu, D. Mackay, W.H. Schroeder, R.W. Russell, and F.A.P.C. Gobas. 1991. Direct in situ sensing of the fugacity of hydrophobic chemicals in natural waters. *Environ. Toxicol. Chem.* 10:9-20.
- Whitehouse, B.G. 1985. Observation of Abnormal Solubility Behavior of Aromatic Hydrocarbons in Seawater. *Mar. Chem.* 17:277-284.
- Yin, C. and J.P. Hassett. 1986. Gas-partitioning approach for laboratory and field studies of mirex fugacity in water. *Environ. Sci. Technol.* 20:1213-1217.
- Yin, C. and J.P. Hassett. 1989. Fugacity and Phase Distribution of Mirex in Oswego River and Lake Ontario waters. *Chemosphere*. 19:1289-1296.

Chapter IV: Particle/Vapor Concentrations and Distributions of PAHs in the Atmosphere of Southern Chesapeake Bay

Abstract:

Atmospheric PAH concentrations were measured at four sites characterized as 'rural' (Haven Beach), 'semiurban' (York River), 'urban' (Hampton), and 'industrialized' (Elizabeth River) areas as part of a study to quantify gaseous exchange fluxes across the air water interface of Southern Chesapeake Bay. Aerosol particle-associated PAH concentrations were similar at all sites; however, PAH vapor concentrations in the urban areas were as much as a factor of 50 greater than those at the rural site. Mean total PAH concentrations ranged from 7.87 ng/m³ at the rural site to 92.8 ng/m³ at the urban site. Daily total PAH concentrations ranged from 1.60 to 198 ng/m³. Exponential increases in PAH vapor concentrations with temperature were observed at the non-rural sites, suggesting volatilization from contaminated surfaces (soils, vegetation, roads) during warmer weather; whereas PAH vapor concentrations at the rural Haven Beach site exhibited little seasonal variability. Aerosol particle-associated PAH levels were similar at all sites and increased in winter due to the temperature dependence of particle-vapor partitioning, increased sources from combustion of fossil fuel and wood for home heating, and cold condensation of vapors to background aerosols as air masses are dispersed from source areas to remote regions. Plots of $\log K_d$ vs $\log P_{sat,SCL}$ indicate PAH partitioning is not at equilibrium in rural areas of Southern Chesapeake Bay. In addition, plots of $\log K_d$ vs. $1/T$ for individual PAHs indicate different particle characteristics or partitioning processes influence particle-vapor distributions at the urban and rural sites.

Introduction:

Atmospheric inputs of contaminants have been noted as a prominent source of pollutants to various aquatic ecosystems (McVeety and Hites, 1988; Eisenreich *et al.* 1981; Schreitmuller and Ballschmiter, 1995; Bidleman *et al.* 1989; Atlas, *et al.*, 1981). The physical characteristics of Chesapeake Bay; a large surface area to mean water volume ratio and 75-100 cm of precipitation annually, make the atmosphere

likely to be a significant source of contaminants to this large estuary (Leister and Baker, 1994), which is an important habitat for many fisheries. Development and implementation of environmental legislation, and risk management of both ecosystem and human health in the Chesapeake Bay region requires an understanding and quantification of air and water quality. Moreover, determination of the major air-water transfer processes for contaminants is necessary such that net fluxes of chemicals to and from the bay and exposure levels can be accurately modeled.

Air-water transfer processes include wet and dry atmospheric deposition, spray transfer, bubble stripping and bursting, and gaseous exchange. Municipal and industrial point sources of contaminants are scattered along the shores of the Chesapeake Bay and its tributaries; however, urban and industrial centers are concentrated along the northwest and southern shores. Anthropogenic sources of PAHs to the atmosphere include: automobile exhaust and degradation of tires; industrial emissions from catalytic cracking, air-blowing of asphalt, and coking coal; domestic heating emissions from coal, oil, gas, and wood; refuse incineration and biomass burning (Nikolaou *et al.*, 1984). Thus, emissions into the urban atmosphere and the subsequent aerial transport and deposition of pollutants as air masses move across the Chesapeake Bay may significantly impact contaminant levels in the bay and its fisheries.

Wet and dry deposition are expected to be higher near urban sources than in rural areas of the bay (Leister and Baker 1994, Cotham and Bidleman 1995). Nonetheless, vapor and particle washout will act as sources of pollutants to the water

throughout the bay. In contrast, volatile-absorptive gas exchange of semivolatile organic contaminants (SOCs) across the air-water interface occurs as a result of disequilibria between freely dissolved water concentrations and atmospheric vapor concentrations, and thus may act as an input or efflux mechanism throughout the bay depending on the spatial and temporal variability of the air-water fugacity gradient of SOCs. Therefore, in order to determine gaseous fluxes of SOCs, including polycyclic aromatic hydrocarbons (PAHs) across the air-water interface of a water body such as Chesapeake Bay, it is necessary to have accurate measurements of atmospheric vapor concentrations and have a quantitative understanding of environmental factors controlling the levels and distributions of semivolatile pollutants in air which is in contact with the Bay.

The overall objectives of this investigation were to quantify and assess spatial and temporal variation in PAH gaseous exchange fluxes across the air-water interface of Southern Chesapeake Bay. In this chapter, trends in the atmospheric concentrations of PAHs in the southern Chesapeake Bay region during the period January 1994 through June 1995 are described and seasonal and spatial variability in atmospheric PAH vapor and particulate concentrations and distributions are assessed.

Materials and Methods:

Sampling Locations. To determine PAH gaseous exchange fluxes across the air-water interface, measurements of atmospheric vapor concentrations reflecting those at the air-water interface must be known. High-volume air samplers were placed adjacent to the shore (Haven Beach < 100 m, all other sites < 10 m) at four locations in Southern Chesapeake Bay (Figure 1). At the rural Haven Beach site (37°26.16' N, 76°15.25' W), the air sampler was located 100 m from the shore of Chesapeake Bay in a high marsh area, as well as >50 m from the nearest road which has limited traffic (i.e. dead end) and >200 m from the nearest residence. The closest regional sources of contaminants to the Haven Beach site include shipping traffic on the mainstem bay, in addition to a refinery and coal/oil-fired power plant which are located approximately 30 km to the southwest. The air sampler at the York River site was located at the Virginia Institute of Marine Science (37°14.75' N, 76°30.0' W). At this site, the sampler was placed on the windward side (during sampling periods) at the end of one of the Institute's research piers on the York River (approximately 50 m from shore). The York River site was considered a semi-urban site approximately 5 km northwest of an oil refinery and coal/oil-fired power plant, and 1 km east of a major vehicular river crossing. The Hampton site (37°4.6' N, 76°16.4' W) was located less than 10 m from the shore of the Chesapeake Bay at Grandview Beach, and was considered an urban site lying in the eastern most section of the city of Hampton (pop. 138,000) and within 5 km of the cities of Newport News

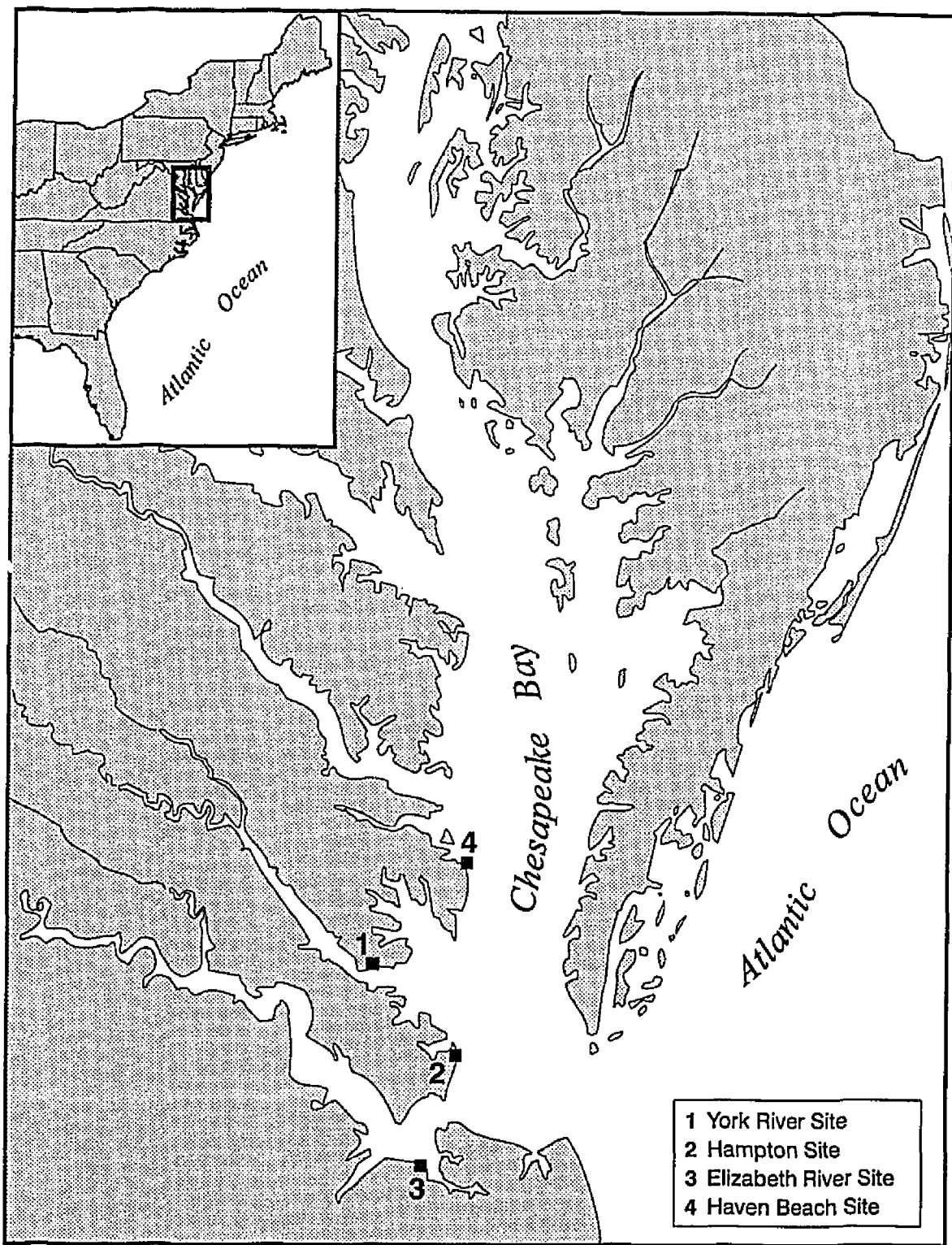


Figure 4.1: Atmospheric Sampling Locations in the Southern Chesapeake Bay Region.

(pop. 179,000) and Norfolk (pop. 245,000). The Elizabeth River site was located at the Portsmouth Coast Guard Station (36°53.2' N, 76°21.2'W); the air sampler was located on a remote section of the base 2 m from the shore of the river. The Elizabeth River site is in an industrialized area in close proximity (< 5 km) to Lambert's Point coal terminals, Norfolk Naval Station, and Portsmouth Naval Shipyard; in addition, the site is located centrally within the Hampton Roads Metropolitan area (pop. 1.5 million).

Sampling Methods. Atmospheric samples, vapor and particulate, were collected using a high volume air sampler (General Metal Works model GPYN1123) which employs precombusted glass fiber filters to remove atmospheric particulates and two polyurethane foam (PUF) plugs in series to collect vapor phase SOCs (Burdick and Bidleman, 1981; You and Bidleman, 1984; Keller and Bidleman, 1984; Bidleman *et al.* 1984; Baker, *et al.* 1994; Dickhut and Gustafson, 1995). The air sampler was equipped with a flow controller to maintain a constant flow rate during sampling regardless of particle loading. Particulate samples were fractionated using 8 in. x 10 in. Gelman type A/E glass fiber filters; the subsequent air was passed through two 8 cm diameter x 7.6 cm long PUF plugs in series which sorbed the SOC vapor fraction. Air sample times ranged from 4 h at the industrialized Elizabeth River site to 12 h at the rural Haven Beach site. Air volumes sampled ranged from 172 to 665 m³ collected at flow rates ranging from .51 to .75 m³/min. Sample media were collected as soon as possible after termination of air sampling to minimize desorptive losses of chemicals due to changes in air temperatures; PUF plugs and GFFs were stored in a freezer at -20 °C until extraction.

Sample media for PAHs were prepared as follows. Glass fiber filters were ashed at 450 °C for 4 h and wrapped in aluminum foil. PUF plugs were Soxhlet extracted for 24 h each with acetone followed by petroleum ether, dried in an oven at 60 °C for 2 h, and stored in precleaned glass jars covered with aluminum foil and sealed.

Potential sampling artifacts including sorption of vapor to filters during sampling may inflate measurements of particle-associated concentrations and reduce vapor concentrations. Sorption of vapors to filters was previously assessed (Dickhut and Gustafson, 1995) by use of a second (back-up) filter in the sampling system; sorption of PAH vapors to the back filters was <15% the measured amount on the front (primary) filter for all PAHs less volatile than fluorene. Back-up filter concentrations of PAHs more volatile than fluorene were often similar to those on the front filter, thus aerosol data for these compounds were not included in the data analysis. Volatile PAHs however, are abundant in the vapor phase and the amount of these SOCs sorbed to the GFFs were insignificant compared to the measured vapor phase concentrations. Aerosol concentrations of the less volatile PAHs were not corrected for filter sorption since back-up filter concentrations were typically <5% those on the primary filter (Dickhut and Gustafson, 1995).

Breakthrough of gaseous PAHs from the PUF plugs in the air sampler was also previously assessed by evaluation of front and back PUF plug concentrations (Dickhut and Gustafson, 1995). For PAHs less volatile than fluorene, no more than 30% of the total measured vapor concentration was found to be associated with the

back PUF plug, whereas for PAHs more volatile than fluorene, occasionally more than 50% of the vapor concentration was associated with the back plug. Nonetheless, since sample sizes and flow rates used in this study were lower than those assessed by Dickhut and Gustafson (1995) and within the range recommended by You and Bidleman (1984), it is expected that little breakthrough of vapors past these two PUF plugs in series occurred. Furthermore, the PUF plugs used in this study were longer than those used by others (Hoff *et al.*, 1992; Leister and Baker, 1994), whereas sample flow rates were similar and volumes lower for collection of air samples for SOC analysis. Therefore, measured PAH gas phase concentrations are expected to be representative of actual ambient levels.

Analytical Techniques. Atmospheric total suspended particulate (TSP) concentrations were determined as the change in mass of the preweighed GFF per unit volume of air sampled. GFFs were weighed on a Mettler PM400 top loading balance. Samples (PUF plugs and GFFs) were analyzed for 17 PAHs by extracting the analytes into appropriate organic solvents (*e.g.* acetone, petroleum ether, dichloromethane) using a Soxhlet apparatus after the addition of five deuterated PAH surrogate standards. The extracts were then concentrated using rotoevaporation followed by evaporation under purified nitrogen, solvent exchanged into hexane, and cleaned using solid-liquid chromatography on silica gel prior to PAH analysis. PAHs were analyzed directly by gas chromatography (GC) with electron impact mass spectrometry (MS) and quantified relative to the closest eluting PAH surrogate. Additional details of the methodology are provided elsewhere (Dickhut and Gustafson,

1995). Average recoveries for surrogate deuterated PAHs from the PUF plugs and GFFs are listed in Table 1.

PAH detection limits for air samples were calculated from instrumental detection limits and individual sample volumes. Detection limits ranged from .12 to .79 pg/m³ with a mean value of .30 pg/m³. Blank values (field and laboratory) averaged 3.8% and 2.9% of mean individual PAH sample values which ranged from .35 to 4990 ng, and 1.71 to 38.7 ng, per sample for PUF and GFF matrices, respectively.

Results and Discussion:

Concentrations. Thirty-seven air samples were collected in the southern Chesapeake Bay region during 1994-1995. Annual mean PAH concentrations (vapor and particulate) ranged from 7.87 ng/m³ at the rural Haven Beach site to 92.8 ng/m³ at the urban Hampton site (Table 2). Daily total PAH concentrations ranged from 1.60 to 198 ng/m³ at the same sites, respectively. These measured values are comparable to those reported elsewhere for similar rural and urban sites (Leister and Baker, 1994; Keller and Bidleman, 1984; Hoff and Chan, 1987; Gardner *et al.*, 1995; Foreman and Bidleman, 1990). Further, differences in atmospheric levels of PAHs at the various sites were due to variations in the gas phase concentrations (Fig. 2).

Total atmospheric PAH concentrations were dominated by several of the more volatile compounds including phenanthrene, fluorene, and acenaphthylene (Table 2).

Table 1: Surrogate Deuterated PAH Recoveries for Air Sampling Media

Deuterated PAH	Sample Matrix	Mean Recovery (%)	Relative Std. Dev. (%)	N* 70% < N < 130%	
d-8 naphthalene	PUF plugs	49.0	13.1	64	9
d-10 anthracene		89.3	18.5	63	56
d-12 benzo(a)anthracene		100.0	20.7	65	61
d-12 benzo(a)pyrene		87.2	19.8	65	61
d-8 naphthalene	GFF	56.1	12.9	52	7
d-10 anthracene		92.6	22.1	52	47
d-12 benzo(a)anthraene		103.1	9.5	52	52
d-12 benzo(a)pyrene		79.3	13.5	52	45

* Number of Samples.

Table 2: Mean Values and Ranges of PAH Concentrations (pg/m³) in the Atmosphere of Southern Chesapeake Bay

PAH	<u>Haven Beach Site</u>						<u>Elizabeth River Site</u>					
	Vapor			Particulate			Vapor			Particulate		
	min.	max.	mean	min.	max.	mean	min.	max.	mean	min.	max.	mean
naphthalene	69.3	15700	1940	N.Q.	769	n.q.	434.05	8950	3910	N.Q.	232	n.q.
acenaphthylene	<.19	2250	283	<.19	8.28	n.q.	118.05	6250	1670	4.17	38.8	n.q.
acenaphthene	38.8	1550	342	<.17	5.48	n.q.	1738.77	13700	5830	<.45	78.3	n.q.
fluorene	224	3050	1170	2.28	15.9	n.q.	2788.34	11200	6620	7.02	20.7	n.q.
phenanthren	516	6900	2510	10.5	205	70.5	6013.35	25200	14700	43.1	302	139
anthracene	<.15	293	31.7	<.15	11.3	3.65	124.01	1040	614	3.34	36.7	12.7
fluoranthene	98.0	651	380	2.34	228	78.0	677.71	4580	2510	20.5	534	202
pyrene	62.9	968	410	1.51	200	64.6	500.74	2520	1580	16.9	632	190
b(a)a	<.15	13.2	2.29	<.15	108	26.5	<.41	284	62.2	6.26	200	62.4
chrysene	<.25	110	28.1	2.21	414	91.2	15.07	1810	362	21.7	865	255
b(b)f	<.17	17.2	4.35	1.96	322	99.1	1.77	19.4	9.21	17.1	434	154
b(k)f	<.15	7.91	1.26	<.15	266	76.1	<.79	17.8	5.73	8.89	333	114
b(e)p	<.18	40.6	4.86	1.27	255	75.1	<.41	15.7	5.67	13.2	387	125
b(a)p	<.15	6.36	.68	.83	174	43.1	<.41	67.0	14.2	6.54	271	83.6
i(1,2,3-cd)p	<.15	<.75	<.23	<.19	229	57.8	<.41	6.84	3.27	10.7	365	116
d(a,h)a	<.15	.60	.25	<.19	31.7	9.28	<.41	9.77	2.08	<.79	43.6	17.6
b(g,h,i)p	<.15	32.3	4.31	<.19	223	64.6	<.41	10.8	6.37	18.2	514	160
total			7110			760			37900			1630

PAH	<u>York River Site</u>						<u>Hampton Site</u>					
	Vapor			Particulate			Vapor			Particulate		
	min.	max.	mean	min.	max.	mean	min.	max.	mean	min.	max.	mean
naphthalene	427	6870	2440	N.Q.	211	n.q.	536	6780	3200	N.Q.	94.7	n.q.
acenaphthylene	122	2630	693	1.44	23.6	n.q.	17.5	715	379	1.26	11.4	n.q.
acenaphthene	2290	12800	5520	N.Q.	20.6	n.q.	328	40100	17600	N.Q.	18.2	n.q.
fluorene	3890	16400	8920	N.Q.	33.8	n.q.	1740	40600	17100	N.Q.	21.8	n.q.
phenanthrene	5780	65200	24400	19.9	282	90.8	2460	125000	44800	16.7	167	100
anthracene	152	3230	1130	1.06	19.2	7.20	<.27	6940	1830	.83	15.3	7.51
fluoranthene	1440	8060	4160	24.6	203	97.0	801	12900	4940	12.1	215	111
pyrene	507	3070	1700	15.6	158	81.9	568	5560	1990	10.4	146	80.0
b(a)a	<.28	183	42.5	<.12	75.4	31.6	<.27	25.0	10.1	<.29	78.0	28.5
chrysene	47.4	365	132	14.1	166	89.0	41.5	198	99.1	11.1	192	79.7
b(b)f	3.63	67.5	22.6	13.5	386	140	2.33	16.6	11.2	10.9	260	98.3
b(k)f	<.18	71.4	10.2	9.68	332	111	<.23	7.77	1.76	7.87	208	72.9
b(e)p	1.41	48.0	14.3	9.17	359	120	1.45	24.1	10.0	7.83	171	65.7
b(a)p	<.12	14.6	5.15	6.10	139	58.6	<.23	4.69	1.22	4.95	131	45.8
i(1,2,3-cd)p	<.12	4.94	1.47	7.17	584	142	<.23	8.55	1.68	7.39	193	61.9
d(a,h)a	<.12	2.81	.72	<.12	36.7	12.2		<.44	<.29	<.23	29.5	8.77
b(g,h,i)p	<.12	12.1	4.02	8.64	746	183	<.23	9.16	2.79	10.5	184	65.3
total			49200			1160			92000			825

Abbreviations for PAHs: b(a)a, benzo(a)anthracene; b(b)f, benzo(b)fluoranthene; b(k)f, benzo(k)fluoranthene; b(e)p, benzo(e)pyrene; b(a)p, benzo(a)pyrene; i(1,2,3-cd)p, indeno(1,2,3-cd)pyrene; d(a,h)a, dibenzo(a,h)anthracene; b(g,h,i)p, benzo(g,h,i)perylene.

N.Q. = not quantifiable, less than 3x blank

n.q. = not quantified due to sampling artifacts (see text)

< = not detected, limit of detection given

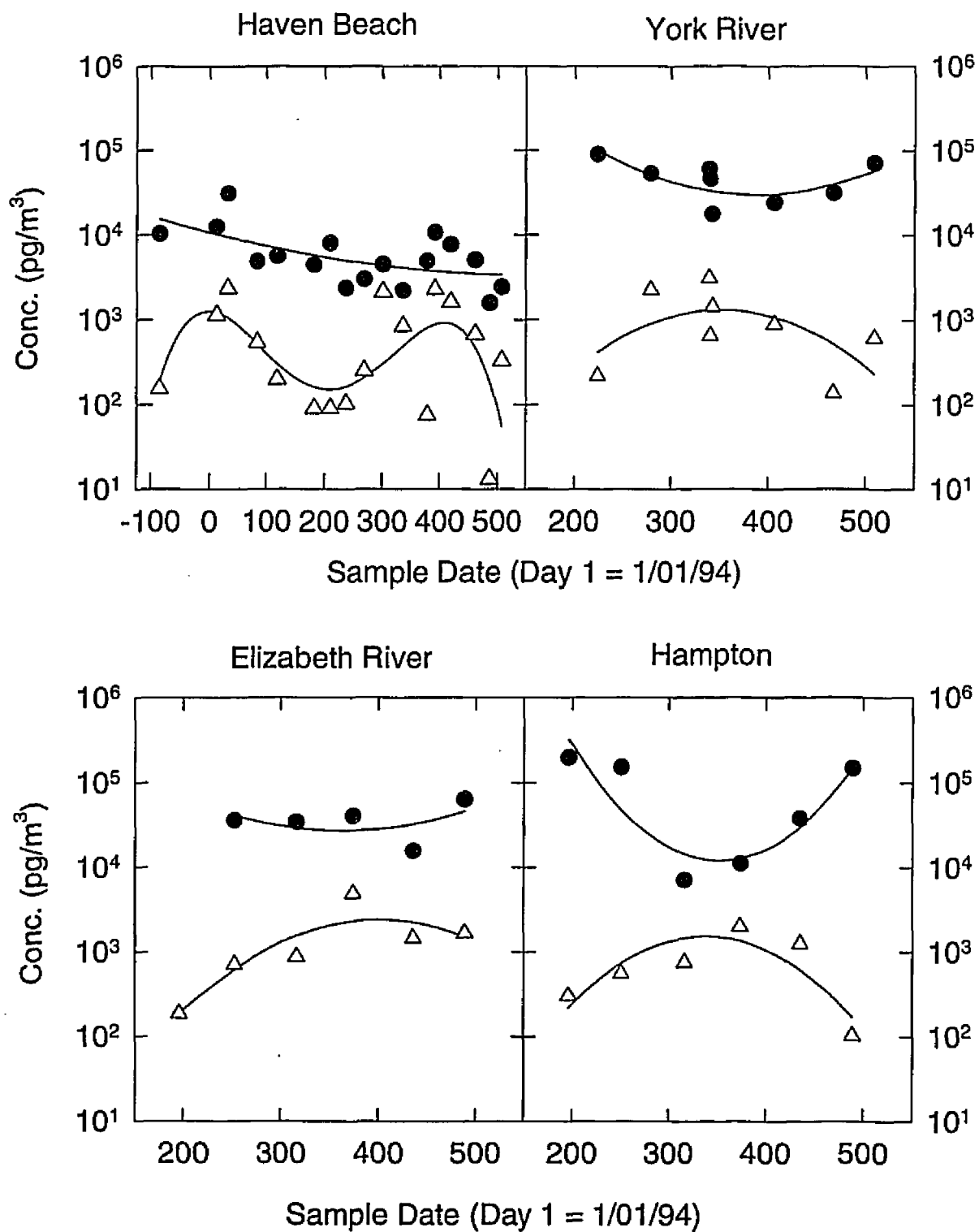


Figure 4.2: Total PAH Concentrations (17 compounds) (● Vapor and △ Particulate) in the Atmosphere of the Southern Chesapeake Bay.

As a result, the highest levels of PAHs in the air exist predominantly in the vapor phase (Figure 2), and the seasonal patterns in total vapor phase and particle-associated PAHs reflects that of the more volatile compounds (Figs. 2-3). In contrast, distributions of the more nonvolatile PAHs favor aerosol particles, even though seasonal patterns of these chemicals in the atmosphere at specific sites are similar to those for the volatile PAHs (Figs. 3-4).

Vapor concentrations were highest at the Hampton site and lowest at the rural Haven Beach site, varying up to 50-fold between sites during summer (Fig. 2-4). PAH vapor concentrations at the non-rural sites (all sites except Haven Beach) exhibit a minimum in winter with an exponential increase in gas phase levels with warmer weather (Fig. 2-5). This rise in PAH concentrations between winter and summer was most pronounced at the Hampton site. No seasonal variability in vapor concentrations was observed at Haven Beach; however, PAH atmospheric vapor concentrations at Haven Beach appear to be decreasing with time (Fig. 2-4). The mean vapor concentration of the PAHs (Σ fluorene through b(ghi)p = 4550 pg/m³) at the Haven Beach site measured in this study was lower than the mean concentration reported for this same site in 1991 (6203 pg/m³) (Baker *et al.* 1994).

Since vapor pressure is exponentially related with temperature by both the well known Antoine and Clausius-Clapeyron equations, the increase of both vapor and total PAH concentrations from winter to summer at the non-rural sites is consistent with volatilization from contaminated surfaces (soils, roads, vegetation) near the sources due to an increase in partial pressures of PAHs. Since PAHs are emitted to the

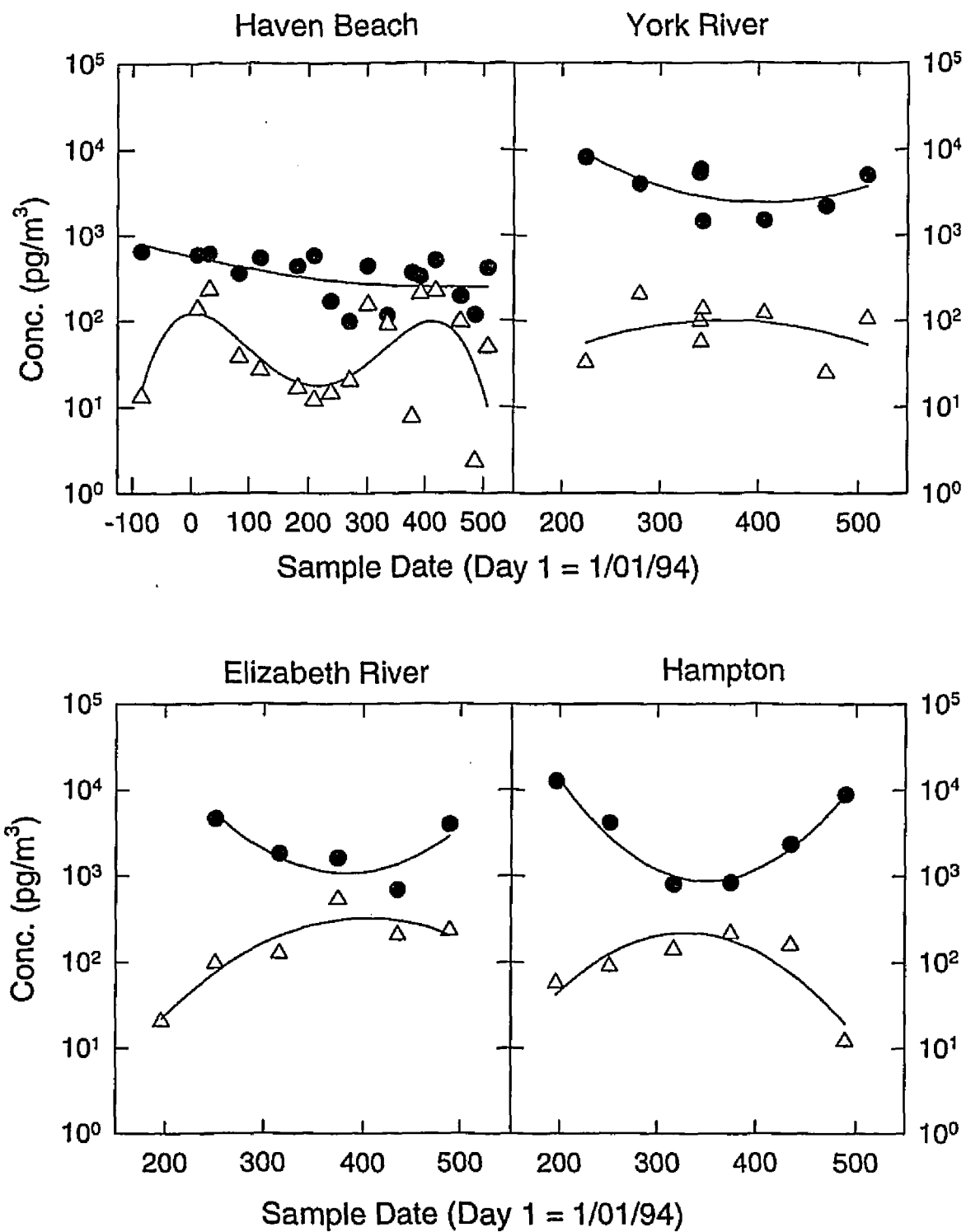


Figure 4.3: Concentrations of Fluoranthene, ● Vapor and Δ Particulate, in the Atmosphere of Southern Chesapeake Bay

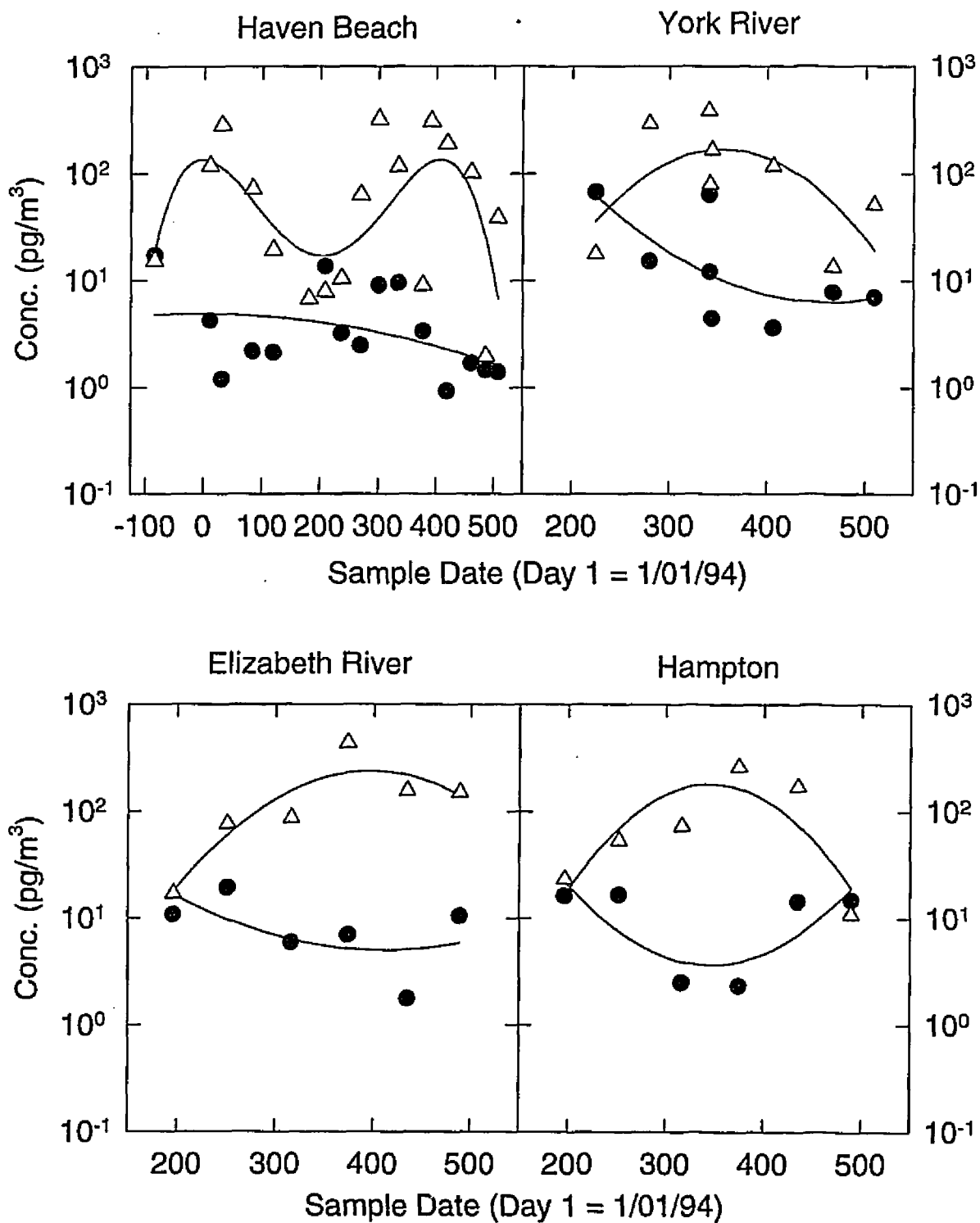


Figure 4.4: Concentrations of Benzo[b]fluoranthene, ● Vapor and △ Particulate, in the Atmosphere of Southern Chesapeake Bay

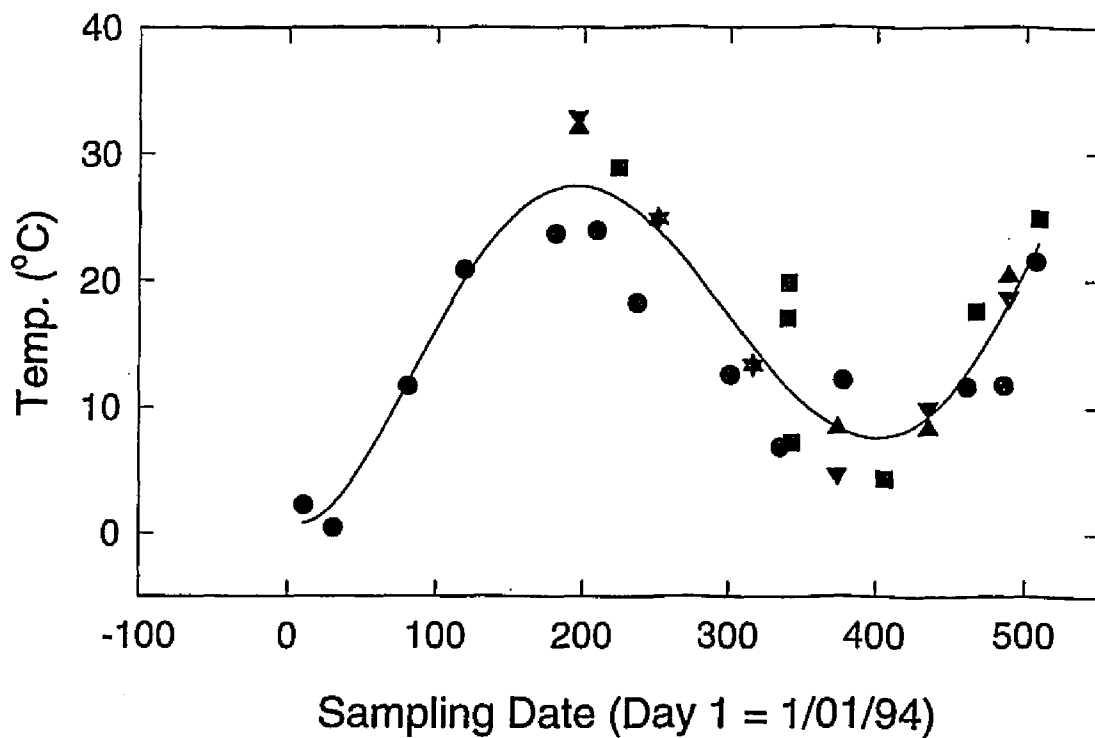


Figure 4.5: Mean Air Temperature During Atmospheric Sampling in the southern Chesapeake Bay region ● Haven Beach, ■ York River, ▼ Hampton, ▲ Elizabeth River

atmosphere as the result of a variety of high temperature combustion processes (Nikolaou *et al.*, 1984), a large fraction of these SOCs are likely initially in the vapor phase and subsequently condense to aerosol and terrestrial surfaces at ambient temperature. This sorbed pool of PAHs will be reemitted to the atmosphere when temperatures increase. The increase in atmospheric concentrations with temperature has been noted previously for PCBs (Panshin and Hites, 1994; Hornbuckle *et al.*, 1994; Hoff *et al.*, 1992). However, due to interannual trends within the data set, the relationship of vapor concentration with temperature is more weakly correlated than that of concentration with time.

PAH particle-associated concentrations were similar at the various sites and exhibited seasonal variability with increased levels occurring during winter months (Figures 2-4). The increase in particulate loadings during colder weather is likely due to regional sources and the temperature dependence of particle-vapor partitioning. Particulate concentrations of PAHs are similar in urban and remote areas of Southern Chesapeake Bay (Figures 2-4). Note that particle-associated concentrations of PAHs are only slightly higher at the industrialized Elizabeth River site compared to the rural Haven Beach and other urban sites. This may indicate that source particles containing PAHs are rapidly dispersed in the atmosphere on a regional basis. However, since background aerosols are expected to compose a larger fraction of the total aerosol particle concentration with increased distance from urban areas (Warneck, 1988), similar aerosol-associated PAH concentrations at all sites is likely due to increased condensation of PAHs to "clean" background aerosols.

Distributions. The distribution of SOCs between gas and aerosol phases depends upon the subcooled liquid vapor pressure, total suspended particulates (TSP), and temperature. Particle-vapor distributions of SOCs are described by:

$$\log K_d = -a \cdot \log P_{\text{sat,SCL}} + c \quad (1)$$

where $K_d = C_p/TSP \cdot C_v$, C_p and C_v are the individual PAH concentrations (pg/m^3) in the particulate and vapor phases, respectively, TSP is the total suspended particulate level (ug/m^3) in the atmosphere, $P_{\text{sat,SCL}}$ is subcooled liquid vapor pressure of the PAH, and a and c are empirical constants (Pankow and Bidleman, 1992). Eq. 1 demonstrates that as $P_{\text{sat,SCL}}$ decreases, the particle-vapor distribution of the compound increases, which is consistent with the PAH distribution patterns noted above.

The $\log K_d$ values were correlated to $\log P_{\text{sat,SCL}}$ of PAHs (Sonnenfeld *et al.* 1983) at the average event temperature (Table 3). Under equilibrium conditions and in the absence of sampling artifacts, the slope a should be 1 (Pankow and Bidleman, 1992) as observed for the non-rural sites. However, regressions of eq 1 indicate that PAH particle-vapor partitioning at the rural Haven Beach site is not at equilibrium (Table 3).

The intercept value of eq 1 is a function of both the specific surface area of the TSP and enthalpies of desorption for the PAHs which are expected to vary little for a particular compound class (Pankow and Bidleman, 1992). Nonetheless, similar c values for PAHs at the urban sites (Table 3) do not imply that aerosol particle

Table 3: Regression Coefficients* for Plots of $\log K_d$ vs $\log P_{sat,SCL}$ (eq 1) for Selected PAHs† in Atmospheric Samples from Southern Chesapeake Bay

Site	n	Slope (a) mean \pm std.	Intercept (c) mean \pm std.	r^2 mean \pm std.
Elizabeth River	5	-1.04 \pm .17	-10.3 \pm 1.3	.90 \pm .06
York River	7	-.966 \pm .137	-10.5 \pm 1.1	.85 \pm .13
Hampton	5	-1.03 \pm .19	-10.9 \pm 1.2	.87 \pm .12
Haven Beach	10	-.649 \pm .209	-7.67 \pm 1.19	.83 \pm .17

* Values are the mean and standard deviation

† Regressions included only phenanthrene, anthracene, fluoranthene, pyrene, and benzo(a)anthracene.

characteristics remain constant throughout the regional atmosphere. Similar intercept values for eq 1 among the urban sites may result from the covariance of both specific surface area and the enthalpy of desorption. That is, it is possible that the enthalpy of desorption for PAHs increases from urban to remote sites due to changing particle characteristics and loss of the readily exchangeable pool of PAHs. Simultaneously, due to changing particle size distributions as air masses are transported from source to remote regions, the specific surface areas of aerosols may also decrease. Indeed, the covariance of these parameters is shown below.

Particle-gas disequilibria in the atmosphere may be attributable to a variety of factors. In particular, artificially shallow slopes and high intercepts for plots of eq 1, as observed for PAHs at Haven Beach (Table 3), may be due to non-exchangeable PAHs on source particles, slow gas-to-particle sorption of SOCs to "clean" aerosols, or large temperature decreases during sampling (Pankow and Bidleman, 1992). Studies have noted that non-exchangeable PAHs on particles may significantly affect measured K_{ps} (Cotham and Bidleman, 1995; Pankow and Bidleman, 1992). Furthermore, low gas phase PAH concentrations at Haven Beach would contribute to slow sorption kinetics of PAHs to background aerosols in the local atmosphere. Decreasing temperatures during sampling at the Haven Beach site may have also contributed to particle-vapor disequilibria as samples were collected over 12 h, whereas sampling ranged from 4-8 h at the other sites. It is unclear which of these factors contributed to PAH particle-vapor disequilibria at Haven Beach.

Nonequilibrium PAH distributions at Haven Beach were observed to be correlated to mean atmospheric temperature (Figure 6). The increased disequilibria of PAHs between the particulate and vapor phases with warmer temperatures is likely due to either nonexchangeable PAHs or slow sorption kinetics. At higher temperatures volatile compounds favor the vapor phase, and therefore, nonexchangeable PAHs would have a larger influence on K_d than at lower temperatures (see Pankow and Bidleman, 1992). Similarly, a high temperatures sorption or condensation of PAHs to background aerosols would be slowed. In contrast, temperature changes for sampling would be highest in the fall and spring whereas disequilibria is highest when mean temperatures are highest (*e.g.* summer). Thus, the observed particle-vapor disequilibria at the rural Haven Beach site is due to slow exchange of PAHs between atmospheric pools and not a sampling artifact.

Particle-vapor distributions are also inversely related with temperature as first demonstrated by Yamaskai *et al.* (1982):

$$\log K_d = m/T + b \quad (2)$$

where m and b are empirical constants that are a function of desorption energetics and particle characteristics, and T is temperature (K). The temperature dependence of particle-vapor distributions for PAHs varies greatly between sites, but very little for individual PAHs at any site (Table 4). In contrast, previously published slope and intercept values for selected PAHs at urban sites were consistent from city to city

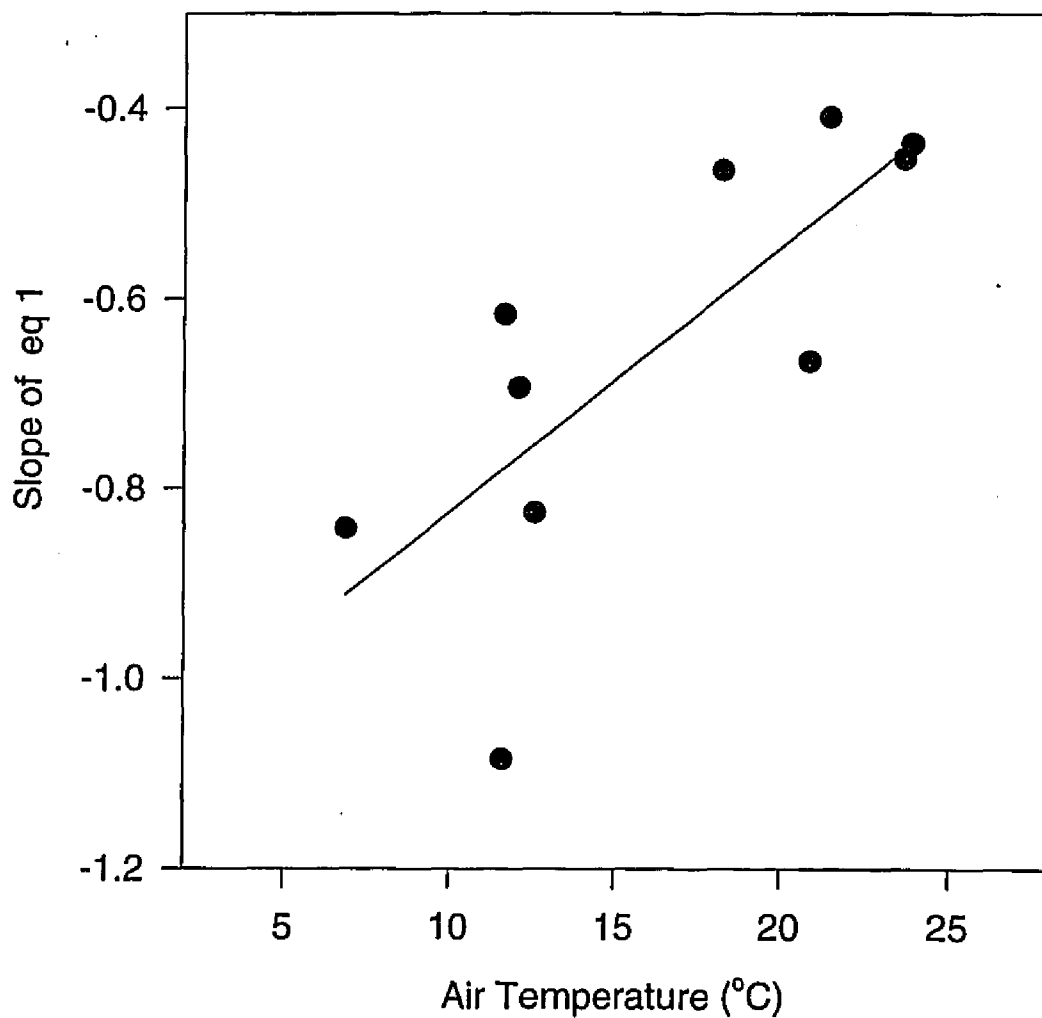


Figure 4.6 : Correlation of PAH Particle-Vapor Partitioning Disequilibria (● Slope of eq 1) at Haven Beach to Air Temperature

Table 4: Regression Coefficients for log K_d versus 1/T plots (eq 2) for selected PAHs* in the Atmosphere of Southern Chesapeake Bay

PAH [†]	<u>Haven Beach Site**</u>			<u>York River Site</u>		
	(n = 10)			(n = 7)		
	m	b	r ²	m	b	r ²
phenanthrene	10090	-38.37	.85	5136	-22.11	.95
anthracene	16080	-58.12	.94	4642	-20.07	.94
fluoranthene	10120	-37.71	.87	4906	-20.49	.95
pyrene	11690	-43.23	.88	4548	-18.96	.90
b(a)a				5335	-20.42	.91
chrysene	9479	-34.47	.85	4366	-17.22	.90
b(b)f	8958	-31.74	.76	6529	-23.65	.92
b(e)p	9021	-31.92	.71	5957	-21.49	.88
avg.	10780	-39.37		5177	-20.55	
std.	2328	8.52		696	1.83	
cv	22%	22%		13%	9%	

PAH [†]	<u>Elizabeth River Site</u>			<u>Hampton Site</u>		
	(n = 5)			(n = 5)		
	m	b	r ²	m	b	r ²
phenanthrene	2282	-11.66	.69	8131	-32.80	1.0
fluoranthene	4721	-19.24	.86	7379	-29.38	.97
pyrene	4349	-17.90	.82	6487	-26.06	1.0
chrysene	5887	-21.84	.94	4828	-19.09	.88
b(b)f	5216	-18.63	.88	8277	-30.01	.97
b(k)f	5498	-19.59	.80			
avg.	4659	-18.14		7020	-27.47	
std.	1174	3.14		1267	4.71	
cv	25%	17%		18%	18%	

* Although regressions are included for compounds in addition to those for which equilibrium distribution was evaluated (Table 3), inclusion of these compounds does not influence the trends in average slope and intercept values.

** Evaluation of K_d at this site indicated nonequilibrium distribution of PAHs between aerosol particles and vapor phase (Table 3).

† Abbreviations for PAHs are as follows: b(a)a, benzo(a)anthracene; b(b)f, benzo(b)fluoranthene; b(e)p, benzo(e)pyrene; b(k)f, benzo(k)fluoranthene.

(Yamasaki et al., 1982; Keller and Bidleman, 1984; Hoff and Chan, 1987; Ligocki and Pankow, 1989), but are comparable to values determined for the Elizabeth River site. The data presented here suggests that there are different particle-vapor distribution processes operating at the rural and urban sites in Southern Chesapeake Bay.

The regression slope of eq 2 is dependent upon the enthalpy of desorption of the PAH (Pankow 1991):

$$m = \frac{H_{desorp}}{2.303 * R} - \frac{T_{amb}}{4.606} \quad (3)$$

where H_{desorp} is the enthalpy of desorption from the surface (kJ/mol), R is the gas constant ($8.314 * 10^{-3}$ kJ/K*mol), and T_{amb} the center of the ambient temperature range (K) over the study period. The intercept of eq 2 depends upon the properties of the individual compound and the specific surface area of the particulate matter (Pankow 1991):

$$b = \log\left(\frac{SA * t}{275 * (MW/T_{amb})^{1/2}}\right) + \frac{1}{4.606} \quad (4)$$

where SA is the specific surface area of the TSP ($\text{cm}^2/\mu\text{g}$), t is the molecular vibration time (s), and MW the molecular weight of the compound of interest. The relatively small variance ($cv \leq 25\%$) in m and b for all PAHs at a particular site

(Table 4) indicates that the properties of the aerosol particulate matter control the spatial variability in the particle-vapor distributions. For example, the different regression values for eq 2 at the various sites may be due to loss of the exchangeable PAHs on the aerosols or to changing particle characteristics as air masses are transported from PAH source regions to remote areas.

Different slopes for PAH particle-vapor distribution as a function of temperature (eq 2) between sites (Table 4) are likely due to the redistribution of PAHs in the aerosol pool resulting in different enthalpies of desorption for the various particle types (*e.g.* pollen versus soot dominated) in the remote and urban atmospheres. Similarly, different intercept values from the various sites are probably due to changes in the specific surface area of the atmospheric particulates. From eqs 3 and 4 enthalpies of desorption for the PAHs and relative surface areas of the aerosol particulates can be calculated. Due to the small spatial variability in air temperatures between sites (Figure 5), the difference in aerosol specific surface areas is a function of the intercept ($SA \propto 10^b$); therefore the specific surface area of the atmospheric particles at the Elizabeth River > York River > Hampton > Haven Beach. Conversely, enthalpies of desorption calculated from eq 3 (using $T_{amb} = 289.9$ K) vary in the opposite manner: Haven Beach (208 kJ/mol) > Hampton (136 kJ/mol) > York River (100 kJ/mol) > Elizabeth River (90.4 kJ/mol). The spatial trends in particle characteristics reflect the gradient from PAH source to remote regions. Although the Hampton and York River sites are reversed as one might expect based on population, the Hampton site was located on the shore of the mainstem bay,

whereas the York River site was located near a petroleum refinery, coal/oil-fired power plant, and major vehicular river crossing and thus may be more influenced by local sources of PAHs.

The greater aerosol SA near the urban sources may be due to the larger volume fraction (and hence number) of fine particles ($< 1 \mu\text{m}$) in the atmosphere, which provide more SA than coarse particles (see Warneck pp 284-287). The lower H_{desorp} in urban source areas means that PAHs are more readily removed from these particles compared to PAH desorption from rural atmospheric aerosol particles. If near urban sources PAHs are sorbed to particulates in a "liquid-like" manner (Pankow and Bidleman, 1992), and in rural air PAHs are reversibly sorbed to the aerosol particle matrix, then the energy required to release PAHs from urban particulate matter would be lower than that for removal of PAHs from rural aerosol particles. Alternatively, the higher H_{desorp} for PAHs from rural air particles may be due to loss of the readily exchangeable PAHs on the particle surface as these aerosols are transported from source to remote regions. PAHs incorporated within particulate matter would be extremely difficult to vaporize and would likely contribute higher enthalpies of desorption compared with those of surface desorption in source regions.

Atmospheric Redistribution of PAHs. It should be noted that the above interpretation of particle-vapor partitioning processes assumes that the exchange of a pollutant occurs only between the atmospheric vapor and particulate phases. However, the fraction of SOCs in the vapor phase may be influenced by distribution to terrestrial surfaces. As noted above, the increase in vapor phase PAHs as

temperatures rise is consistent with the expectation of volatilization from contaminated surfaces. Nevertheless, if horizontal mixing of air masses (and hence aerosol-associated PAHs) occurs faster than deposition of particulates to the Earth's surface (see Lerman p 57.), but slower than exchange of PAHs between the vapor phase and terrestrial surfaces, then the rate of terrestrial surface-vapor exchange will not influence the rate limiting process of aerosol particle-vapor transfer. Indeed, the atmospheric residence time of aerosol particles are on the order of 2-10 days (Lerman, Chap. 7), but hourly variability in atmospheric gases such as carbon dioxide are observed due to local exchange between vegetative surfaces (Warneck, Chap 1).

In Southern Chesapeake Bay it is clear that aerosol particles generally mix laterally faster than the rate of photodegradation of particle-associated PAHs. The ratios of atmospheric particle-associated PAH concentrations for compounds with similar subcooled liquid vapor pressures, but very different photochemical reactivities remain similar between various urban and rural sites (Figure 7). Although there is some evidence of depletion of the most photochemically reactive PAH (benzo(a)pyrene) at the rural Haven Beach site during spring and summer, this simply supports our expectation that the aerosol particles containing PAHs originate near urban areas and may redistribute to the background vapor and aerosol pools during transport, particularly as temperatures increase. Kormacher et al. (1980) found that PAHs sorbed to fly-ash particulates were highly resistant to photodegradation. Thus, depletion of photochemically reactive PAHs on aerosol particulate matter likely occurs as a result of redistribution of these compounds to the vapor phase as temperatures increase, and is promoted by rapid photodegradation in the gas phase.

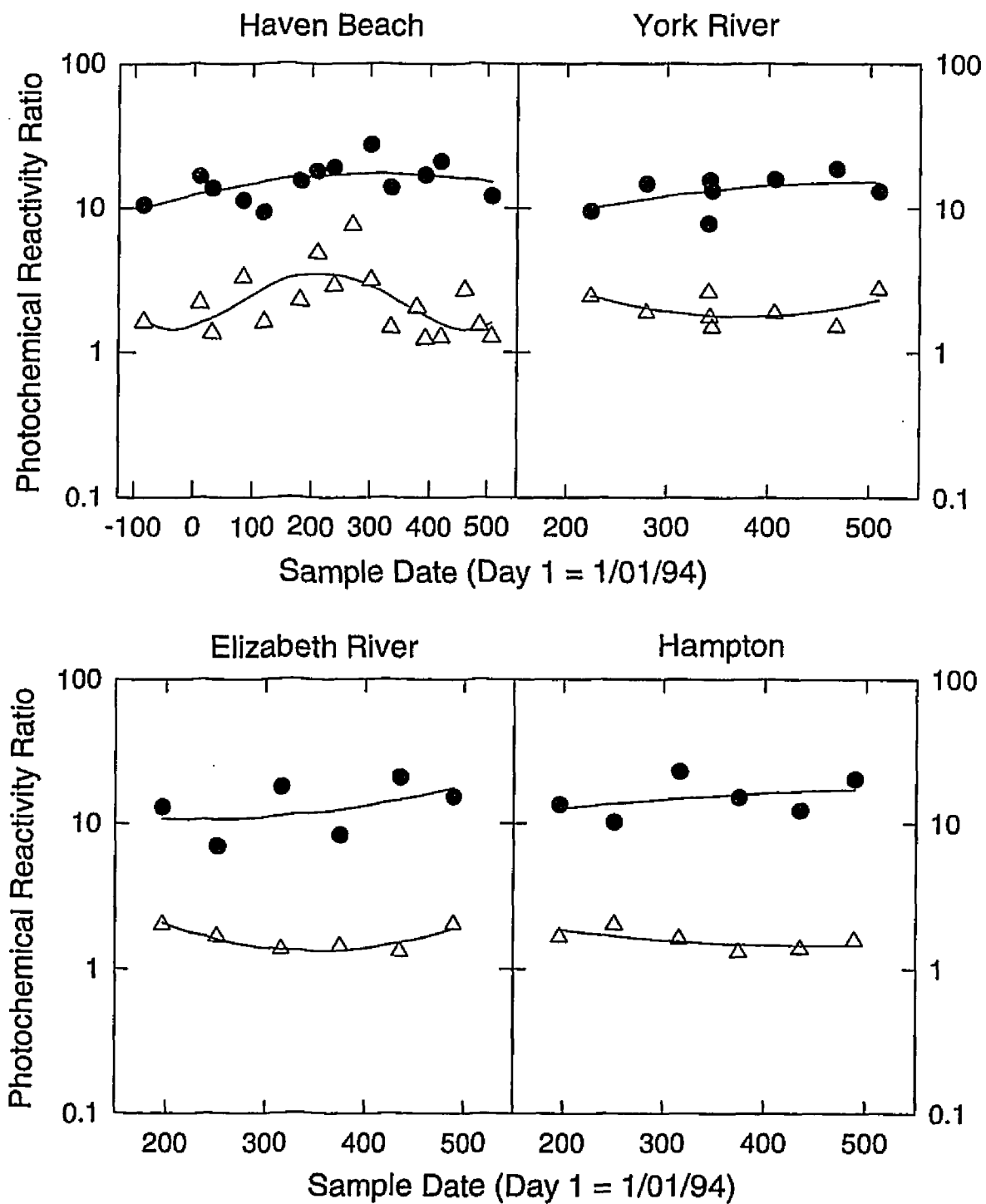


Figure 4.7: Ratios of Particulate Concentrations for PAHs with Similar Liquid Vapor Pressures, but Different Photochemical Reactivities Δ [benzo(e)pyrene]/[benzo(a)pyrene]

● [phenanthrene]/[anthracene]

Finally, large aerosol particles are expected to deposit near urban sources and PAH vapors produced by combustion at elevated temperatures (auto exhaust, industrial activities) would also be expected to condense to surfaces near sources due to a much lower ambient temperature upon emission. Therefore, it is suggested that analogous to the "global distillation" and "cold condensation" theories, atmospheric PAH vapor loadings in Southern Chesapeake Bay are mediated by secondary volatilization from non-atmospheric surfaces especially near source regions during warmer temperatures. This secondary source of PAHs indirectly influences particle-vapor exchange in the atmosphere since the latter process is rate limiting. This is apparent in the observed departure from equilibrium for PAH particle-vapor distributions which increase in summer due to a relatively rapid release of PAHs condensed to terrestrial surfaces compared with the expected slower sorption of these SOCs by the ambient aerosols. PAH aerosol-associated concentrations are mediated by condensation of PAH vapors to background aerosols as air masses are dispersed from source to remote regions.

Conclusions:

Atmospheric vapor concentrations of PAHs varied significantly between sites and increased logarithmically with temperature at the non-rural sites indicating the major source of these compounds to the atmosphere of Southern Chesapeake Bay is volatilization from contaminated surfaces (soil, roads, vegetation). Aerosol-particle

concentrations of PAHs were similar at the various sites and higher during winter months indicating that particulate concentrations are controlled by increase combustion sources, the temperature dependence of particle-vapor partitioning, and the redistribution of PAH vapors to background aerosols as air masses are dispersed from source to remote regions. $\log K_d$ versus $1/T$ regression equations indicate that while particle-vapor distributions are temperature dependent, the process is site specific due to variation in the aerosol particle pool. A gradient from urban to remote sites was observed in both specific surface area of atmospheric particulates and enthalpies of desorption for PAHs. Furthermore, plots of $\log K_d$ vs $\log P_{\text{sat,SCL}}$ imply that PAH gaseous and atmospheric aerosol partitioning is not at equilibrium in rural areas. Therefore, atmospheric particulate and non-atmospheric surface characteristics are important factors controlling the distributions of PAHs between the vapor and surface-associated phases. However, more work needs to be done characterizing particle and non-atmospheric surface types and sorption properties in the remote and urban atmospheres to fully understand the properties that control the distribution of SOCs between vapor and associated phases, total atmospheric loadings, and hence exposure levels of semivolatile organic contaminants.

References

- Atlas, E., R. Foster, and C.S. Giam. 1981. Global Transport of organic pollutants: ambient concentrations in the remote marine atmosphere. *Science*. 211:163-165.
- Baker, J.E., D. Burdige, T.M. Church, G.A. Cutter, R.M. Dickhut, D.L. Leister, J.M. Ondov, and J.R. Scudlark. 1994. Chesapeake Bay Atmospheric Deposition Study: Phase II final report, EPA Chesapeake Bay Program Office, Annapolis, MD.
- Bidleman, T.F., G.E. Patton, M.D. Walla, B.T. Hargrave, W.P. Vass, P. Erickson, B. Fowler, V. Scott and D.J. Gregor. 1989. Toxaphene and other organochlorines in arctic ocean fauna: evidence for atmospheric delivery. *Arctic*. 42:307-313.
- Bidleman, T.F., C.G. Simon, N.F. Burdick, and F. You. 1984. Theoretical plate measurements and collection efficiencies for high-volume air samplers using polyurethane foam. *J. Chromatogr.* 301:448-453.
- Burdick, N.F. and T.F. Bidleman. 1981. Frontal movement of hexachlorobenzene and polychlorinated biphenyl vapors through polyurethane foam. *Anal. Chem.* 53:1926-1929.
- Cotham, W.E. and T.F. Bidleman. 1995. Polycyclic Aromatic Hydrocarbons and Polychlorinated Biphenyls in Air at an Urban and Rural Site near Lake Michigan. *Environ. Sci. Technol.* 29:2782-2789.
- Dickhut, R.M. and K.E. Gustafson. 1995. Atmospheric Inputs of Selected Polycyclic Aromatic Hydrocarbons and Polychlorinated Biphenyls to Southern Chesapeake Bay. *Mar. Pollut. Bull.* 30:385-396.
- Eisenreich, S.J., B.B. Looney, and J.D. Thornton. 1981. Airborne organic contaminants in the Great Lakes ecosystem. *Environ. Sci. Technol.* 15:30-38.
- Foreman, W.T. and T.F. Bidleman. 1990. Semivolatile Organic Compounds in the Ambient Air of Denver, Colorado. *Atmos. Environ.* 24A:2405-2416.
- Gardner, B., C.N. Hewitt, and K.C. Jones. 1995. PAHs in Air Adjacent to Two Inland Water Bodies. *Environ. Sci. Technol.* 29:2405-2413.

- Hoff, R.M., Kar-Wah Chan. 1987. Measurement of Polycyclic Aromatic Hydrocarbons in the Air along the Niagra River. *Environ. Sci. Technol.* 21:556-561.
- Hoff, R.M., D.C.G. Muir, and N.P. Grift. 1992. Annual cycle of polychlorinated biphenyls and organohalogen pesticides in air in southern Ontario. 1. Air concentration data. *Environ. Sci. Technol.* 26:266-275.
- Hornbuckle, K.C., D.R. Achman, and S.J. Eisenreich. 1993. Over-water and over-land polychlorinated biphenyls in Green Bay, Lake Michigan. *Environ. Sci. Technol.* 27:87-96.
- Hornbuckle, K.C., J.D. Jeremiason, C.W. Sweet, and S.J. Eisenreich. 1994. Seasonal Variations in Air-Water Exchange of Polychlorinated Biphenyls in Lake Superior. *Environ. Sci. Technol.* 28:1491-1501.
- Keller, C.D. and T.F. Bidleman. 1984. Collection of airborne polycyclic aromatic hydrocarbons and other organics with a glass fiber filter-polyurethane foam system. *Atm. Environ.* 18:837-845.
- Kormacher, W.A., E.L. Wehry, G. Mamantov, and D.F.S. Natusch. 1980. Resistance to Photochemical Decomposition of Polycyclic Aromatic Hydrocarbon Vapor-Adsorbed on Coal Fly Ash. *Environ. Sci. Technol.* 14:1094-1099.
- Leister, D.L. and J.E. Baker. 1994. Atmospheric Deposition of organic contaminants to the Chesapeake Bay. *Atmos. Environ.* 28:1499-1520.
- Lerman, A. 1979. *Geochemical Processes Water and Sediment Environments*. John Wiley and Sons: New York.
- Ligocki, M.P. and J.F. Pankow. 1989. Measurements of the gas/particle distributions of atmospheric organic compounds. *Environ. Sci. Technol.* 23:75-83.
- McVeety, B.D. and R.A. Hites. 1988. Atmospheric Deposition of Polycyclic Aromatic Hydrocarbons to Water Surfaces: A Mass Balance Approach. *Atmos. Environ.* 22:511-536.
- Nikolaou, K., P. Masclet, and G. Mouvier. 1984. Sources and Chemical Reactivity of Polynuclear Aromatic Hydrocarbons in the Atmosphere-A Critical Review. *Sci. Tot. Environ.* 32:103-132.
- Pankow, J.F. 1991. Common y-Intercept and Single Compound Regressions of Gas-Particle Partitioning Data VS 1/T. *Atmos. Environ.* 25A:2229-2239.

- Pankow, J.F. and T.F. Bidleman. 1992. Interdependence of the slopes and intercepts from log-log correlations of measured gas-particle partitioning and vapor pressure-I. Theory and analysis of available data. *Atmos. Environ.* 26A:1071-1080.
- Panshin, S.Y. and R.A. Hites. 1994. Atmospheric Concentrations of Polychlorinated Biphenyls at Bermuda. *Environ. Sci. Technol.* 28:2001-2007.
- Schreitmuller, J. and K. Ballschmiter. 1995. Air-water Equilibrium of Hexachlorocyclohexanes and Chloromethoxybenzenes in the North and South Atlantic. *Environ. Sci. Technol.* 29:207-215.
- Sonnefeld, W.J., W.H. Zoller, and W.E. May. 1983. Dynamic Coupled-column liquid chromatographic determination of ambient vapor pressures of polynuclear aromatic hydrocarbons. *Anal. Chem.* 55:275-280.
- Warneck, P. 1988. *Chemistry of the Natural Atmosphere*. Academic Press, Inc. San Diego. pp 284-287.
- Yamasaki, H., K. Kuwata, and H. Miyamoto. 1982. Effects of ambient temperature on aspects of airborne polycyclic aromatic hydrocarbons. *Environ. Sci. Technol.* 16:189-194.
- You, F. and T.F. Bidleman. 1984. Influence of volatility on the collection of polycyclic aromatic hydrocarbon vapors with polyurethane foam. *Environ. Sci. Technol.* 18:330-333.

Chapter V: PAH Gase Exchange Fluxes Across the Air-Water Interface of Southern Chesapeake Bay

Abstract

The gas exchange fluxes of polycyclic aromatic hydrocarbons (PAHs) across the air-water interface of southern Chesapeake Bay were calculated using a modified two-film exchange model. Sampling covered the period January 1994 to June 1995 for five sites on the southern Chesapeake Bay ranging from rural to urban and highly industrialized. Simultaneous air and water samples were collected and the atmospheric gas phase and surface water dissolved phase analyzed via GC/MS for 17 PAHs. The instantaneous gas flux was calculated for each compound using Henry's law constants, diffusivities, hydrological and meteorological parameters. The direction and magnitude of gas transfer were found to be controlled by water temperature and vapor concentrations. Fluxes were determined to vary in direction and magnitude both spatially and temporally across the air-water interface of Southern Chesapeake Bay. The range of gas exchange is of the same order as atmospheric wet and dry depositional fluxes to Southern Chesapeake Bay. The results of this study support the hypothesis that gas exchange is a major transport process affecting concentrations and exposure levels of PAHs in southern Chesapeake Bay.

Introduction

Semivolatile organic contaminants (SOCs), *e.g.* polycyclic aromatic hydrocarbons (PAHs), polychlorinated biphenyls (PCBs), and organochlorine pesticides may cycle between air and water with periods of net upward flux during dry weather followed by periods of intense downward flux during rainfall (Mackay *et al.*, 1986; Baker and Eisenreich, 1990). Further, it has been suggested that persistent, semivolatile, hydrophobic pollutants are transferred throughout the world via successive deposition and reemission- a "grasshopper" scenario (Ottar, 1981).

The physical-chemical properties of many trace organic contaminants indicate that SOC's will be long-lived in the environment, cycling between the atmosphere and

water (Mackay *et al.*, 1986) thus increasing their effective residence times in the total environment. The original substances and their transformation products eventually will be deposited to the Earth's surface and may impinge on communities or ecosystems hundreds or even thousands of kilometers removed from the original point of release (Schroeder and Lane, 1988). Thus, the importance of quantifying air-water exchange processes for SOCs is evident.

Air-water transfer processes for chemicals include volatilization and absorption of gases, dry deposition with particles, wet deposition by rain or snow, *i.e.* particle and vapor "washout", spray transfer, and bubble scavenging (Andren, 1983). Gas exchange (volatilization-absorption) is a dominant process governing air-water transfer of chemicals in non-storm conditions via both molecular and turbulent diffusive transfer. Diffusive air-water transfer of gaseous chemicals through stagnant films at the interface is driven by the gradient between equilibrium concentrations at the interface and bulk reservoirs. The rate of diffusive mass transfer is dependent upon windspeed, as it affects surface roughness and film thickness, and the molecular diffusion coefficients of the compound in air and water.

In order to compile a legitimate mass balance and determine exposure levels for SOCs in an aquatic system, it is necessary to consider all of the major air-water exchange processes (Mackay *et al.*, 1986). In the Chesapeake Bay watershed wet and dry depositional fluxes of selected SOCs and trace elements to Chesapeake Bay have been determined (Leister and Baker, 1994; Scudlark *et al.*, 1994; Dickhut and Gustafson, 1995). This research quantitatively measures the volatile-absorptive fluxes

of selected SOCs across the air-water interface at four main sites in lower Chesapeake Bay over the course of a year and a half. Spatial and temporal variability in SOC fugacities in the atmosphere and surface waters, and the influence of interfacial conditions (*i.e.* temperature and windspeed) on air-water gas exchange of SOCs in lower Chesapeake Bay have been evaluated. The diffusive fluxes determined in this study will provide insight into the importance of gaseous exchange at the air-water interface in contributing to loadings of toxicants to aquatic ecosystems such as Chesapeake Bay.

Quantification of Gaseous Exchange Fluxes

Gas Exchange Models. Quantification of the evaporation or absorption rate (volatile transport) of chemicals across the air-water interface relies primarily on the two layer (film) model presented by Liss and Slater (1974). The basic assumption of this model is that the two fluid phases are separated by stagnant layers, a liquid film and a gaseous film, through which transport occurs via molecular diffusion driven by the concentration (or fugacity) gradient of the chemical between the bulk reservoirs. This framework was extended by Mackay and Leinonen (1975), wherein they presented calculations for the transport of low solubility compounds including selected saturated and aromatic hydrocarbons, pesticides, and PCBs expressed in terms of mass transfer coefficients instead of diffusion coefficients and boundary layer thicknesses. Transport by molecular diffusion across two boundary layers has also

been adopted by Doskey and Andren (1981), and Bopp (1983), in separate PCB air-water transfer models, and by Eisenreich *et al.*, (1981), Baker and Eisenreich (1991), Hornbuckle *et al.*, (1992), and McConnell *et al.*, (1993) in modeling organic contaminants in the Great Lakes ecosystem.

The volatile flux (F_{vol}) expression is:

$$F_{vol} = k_{ol}(C_{f,w} - C_{v,a}/K_{aw}) \quad (1)$$

where

$$1/k_{ol} = RT/Hk_a + 1/k_w \quad (2)$$

and

$$K_{aw} = H/RT \quad (3).$$

The overall mass-transfer coefficient or total resistance to mass transfer is k_{ol} ; k_w is the mass transfer coefficient across the stagnant water layer and k_a is the rate coefficient for transfer across the stagnant air layer. $C_{f,w}$ is the freely dissolved water concentration and $C_{v,a}$ is the vapor phase concentration in the atmosphere. K_{aw} is the air-water partition coefficient which defines the equilibrium distribution of the chemical in air and water, H is Henry's law constant, R is the ideal gas constant and T is temperature (K) at the air-water interface.

Correct assessments of Henry's law constants as a function of salinity and temperature are needed to determine the magnitude and direction of flux. Henry's law constants were calculated from sub-cooled liquid vapor pressures (Sonnenfeld et al. 1983, Appendix B, D) and sub-cooled liquid solubilities (May et al 1978, 1983; Appendix A, D) which were corrected for salinity by the Setschenow equation (Rossi and Thomas, 1981; May et al., 1978; Whitehouse, 1985; Schwarz, 1977; Eganhouse and Calder, 1976; Appendix C). For benzo(b)fluoranthene, benzo(k)fluoranthene, benzo(a)pyrene, indeno(1,2,3-cd)pyrene, and benzo(g,h,i)perylene solubility and vapor pressure data are not available; therefore, flux calculations relied on temperature correlations (Appendix D) for Henry law constants measured at several temperatures in freshwater (Th.E.M. ten Hulscher et al., 1992).

Mass transfer coefficients control the rate of passive transport across interfaces and for air-water systems have been related to the Schmidt numbers for a chemical in water (Sc_w) and air (Sc_a), and wind speed at a reference height of 10 meters (U_{10}) by Mackay and Yeun (1983):

$$k_a = 0.001 + 0.0462(U^*)(Sc_a)^{-0.67} \quad (4)$$

$$k_w = 1.0(10)^{-6} + 34.1(10)^{-4}(U^*)(Sc_w)^{-0.5} \quad (5)$$

$$k_w = 1.0(10)^{-6} + 144(10)^{-4}(U^*)^{2.2}(Sc_w)^{-0.5} \quad (6)$$

where equation (5) applies for $U^* > 0.3$, equation (6) applies for $U^* < 0.3$, and $U^* = U_{10}(6.1 + 0.63U_{10})^{0.5}(10)^{-2}$. The air and water mass transfer coefficients (k_a and k_w) are related to the compound specific molecular diffusion coefficients via the Schmidt numbers (Bird *et al.*, 1960):

$$Sc_w = \mu_w / (\rho_w D_{sw}) \quad (7)$$

$$Sc_a = \mu_a / (\rho_a D_{sa}) \quad (8)$$

where D_{sa} and D_{sw} are the molecular diffusivities of a chemical solute in air and water, respectively, and the ρ 's and μ 's are the densities and dynamic viscosities of the bulk phases, respectively.

For calculation of mass transfer coefficients, knowledge of windspeeds, viscosity and density of the bulk phases, as well as molecular diffusivities of the compound of interest at the environmental temperatures and salinities must be known. Consequently, the temperature of each phase (air and water) in the stagnant film layers is required. Surface skin temperatures have been determined to be only some tenths of a degree celsius cooler than the underlying water due to energy losses from long-wave radiation and evaporation (Paulson and Parker, 1972; Hornbuckle *et al.* 1995). Therefore, in this study, surface water temperatures were used for calculating parameters (i.e. density, viscosity, diffusivity, Henry law constants) necessary to determine gaseous fluxes. Molecular diffusivities for PAHs in air and water were

calculated according to the methods of Gustafson and Dickhut (1994a,1994b); bulk phase viscosities and densities were calculated according to the equations of Millero et al. (1976), Riley et al. (1975), Horne (1969), and Weast (1987) using field measured temperatures and salinities.

Sampling Sites. Concentrations were measured for selected PAHs in air and surface waters and gas exchange fluxes determined at four sites in the southern Chesapeake Bay (Figure 1, Table 1) during the period January 1994 through May 1995. The main study site located in the Wolftrap region of the lower Chesapeake Bay is removed from local sources of contamination (land based) and is close to the Haven Beach (Mathews County, VA) Chesapeake Bay Atmospheric Deposition (CBAD) study site (37 26.15'N, 76 15.25'W) where SOC depositional inputs to the Bay were measured (Dickhut and Gustafson, 1995). A second Wolftrap region (Haven Beach) site approximately 1500 m from shore was added for sampling method development due to its accessibility from the Haven Beach CBAD study site where the air sampler was located during water sampling at both Wolftrap sites. The Haven Beach CBAD study site is located approximately 100 m from the shore of the Chesapeake Bay in a high marsh area, as well as >50 m from the nearest road which has limited traffic (gravel, dead-end) and >200 m from the nearest residence. The closest regional sources of contaminants to the site include shipping traffic on the main stem Bay, and a coal/oil fired power plant and refinery located approximately 30 km to the southwest.

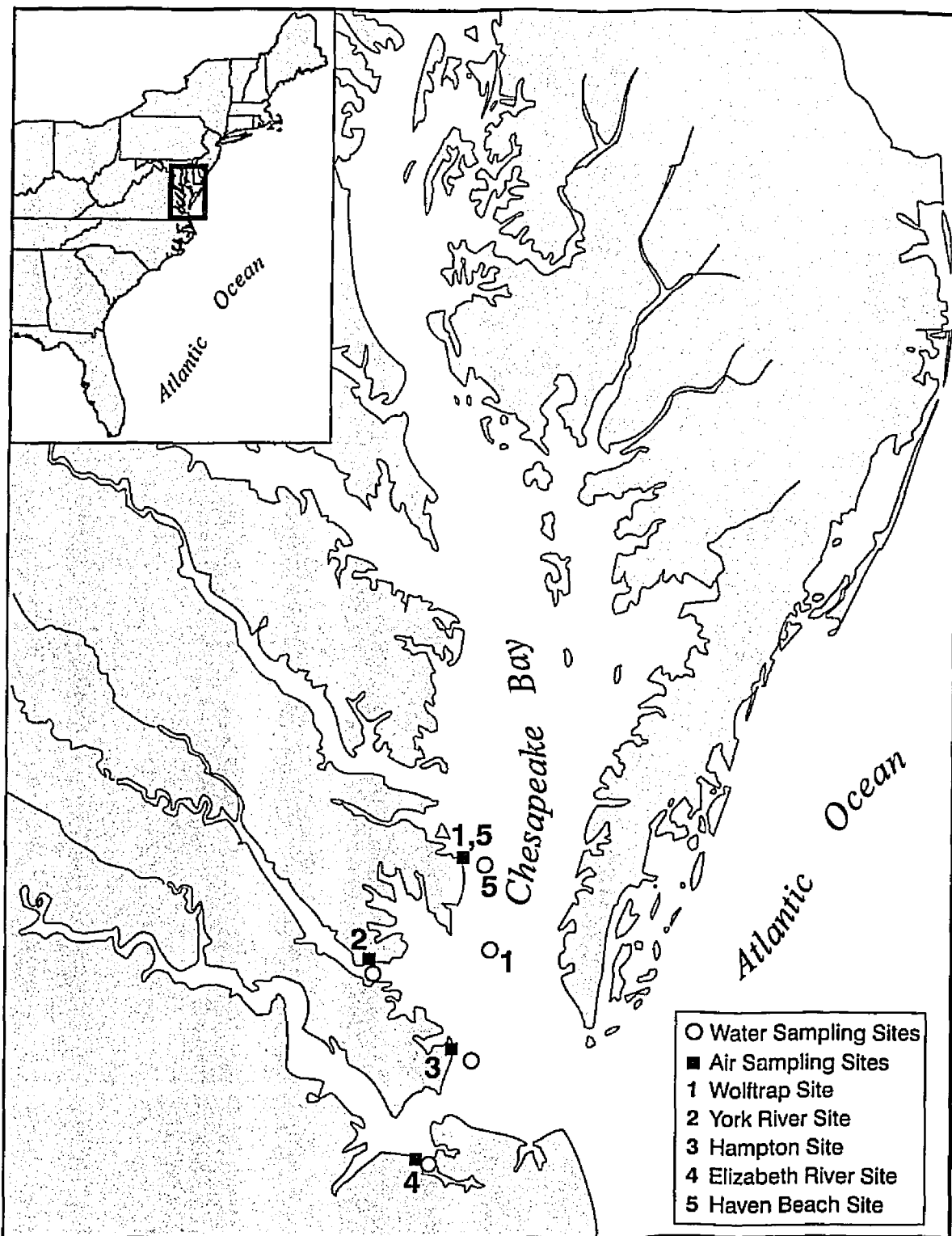


Figure 5.1: Atmospheric and Surface Water Sampling Locations for Determination of PAH Gaseous Exchange Across the Air-Water Interface of Southern Chesapeake Bay.

Table 1: Gas Exchange Sampling Locations for Simultaneously Paired Air and Water Samples

Site	Atmospheric Samples	Surface Water Samples
Elizabeth River	36°53.2 N, 76°21.2 W	36°52.0 N, 76°19.6 W
Hampton	37°4.6 N, 76°16.4 W	37°5.0 N, 76°13.3 W
York River	37°14.75 N, 76°30.0 W	37°14.5 N, 76°29.0 W
Wolftrap	37°26.16 N, 76°15.25 W	37°16.53 N, 76°12.0 W
Haven	37°26.16 N, 76°15.25 W	37°25.7 N, 76°13.1 W

A Hampton roads region study site on Chesapeake Bay was located near Grandview beach. The air sampler was located no more than 10 m from shore of the bay at Grandview fishing pier or Bel Isle Marina. The Hampton site was considered an urban site, lying in the eastern most section of the city of Hampton (pop. 138,000) and within 5 km of the cities of Newport News (pop. 179,000) and Norfolk (pop. 245,000). It was anticipated that this region will be characterized by larger absorptive-volatile fluxes as the surrounding region is heavily populated, and therefore, will contribute largely to atmospheric levels of SOCs.

The Elizabeth River was selected as a study site as it is an intensely industrialized waterway representative of contaminated rivers-estuaries and likely to include surface films in the form of slicks. The Elizabeth River site was located at the mouths of the river's western and southern branches. The air sampler was located on the shore, within an idle area, of the Portsmouth Coast Guard station adjacent to the Elizabeth River. The Elizabeth River sampling site was in close proximity (< 5 km) to Lambert's Point coal terminals, Norfolk Naval Station, and Portsmouth Naval Shipyard; in addition, the site is centrally located within the Hampton Roads Metropolitan area (pop. 1.5 million).

Finally, the York River was chosen as an additional site as part of a joint project (see Liu, 1994) to examine the effect of the sea surface microlayer on gaseous diffusive transfer. The York River study site was located in the center of the river approximately 1 km downstream from the Virginia Institute of Marine Science. The air sampler was located on the windward side (during sampling) at the end of one of

the Institute's research piers, approximately 50 m from shore. The York River site was considered semi-urban but was also located within 5 km of an oil refinery and coal/oil-fired power plant and within 1 km of a major vehicular river crossing.

Sampling Strategy.

Simultaneous paired air and water samples were collected at 4 main sites in Southern Chesapeake Bay during the period January 1994 to June 1995. Sampling was conducted monthly at the Wolftrap site and every other month at the Hampton, York River, and Elizabeth River sites. Air samples were collected using high volume air samplers placed on the shore as close to the water sampling sites as possible (Figure 1). Air sampling times and volumes ranged from 4 to 12 h and 172 to 665 m³, respectively, at flow rates ranging from 0.51 to 0.75 m³/min. (Chapter IV). Water samples were collected at each site from a 1 m depth using a submersible pump. Approximately 1 to 2 sample volumes were passed through the pump system prior to sample collection to equilibrate pump and tubing surfaces with ambient contaminant levels and minimize sorptive losses. Particulate and dissolved fractions were separated in the field by filtration through 142 mm GFFs and sorption of the dissolved fraction to XAD-2 resin in a 30 cm column (Chapter III). Meteorologic and hydrologic data (wind speed, air and water temperatures, and salinities) were obtained both shipboard and from shore stations at the Haven Beach and York River sites, and in close proximity to the Elizabeth River site.

Analytical Procedures.

Analytical procedures used for water and air samples are described in detail elsewhere (Dickhut and Gustafson 1995, Chapters III and IV) and are summarized here (Table 2). Freely dissolved water concentrations were determined by filtration through a pre-ashed 142mm glass fiber filter (GFF 1 μm nominal pore size) with subsequent sorption of the freely dissolved phase to XAD-2 resin. After sample collection, XAD-2 resin samples were sequentially extracted with acetone and hexane (24 h each) in a Soxhlet apparatus. Vapor phase samples were collected using a high volume air sampler; gas concentrations were determined by filtering air through 8x10 in. GFFs and isolating the vapor phase on polyurethane foam plugs. After sampling, polyurethane foam plugs were sequentially extracted for 24 h each in acetone and petroleum ether. All samples were spiked with surrogate deuterated PAHs (d-8 naphthalene, d-10 anthracene, d-12 benzo(a)anthracene, and d-12 benzo(a)pyrene) prior to extraction. The extracts were concentrated, exchanged into hexane with a rotary evaporator, further condensed under nitrogen, and cleaned on a silica column prior to analysis. Samples were analyzed using a Hewlett Packard 5890 gas chromatograph equipped with a 5971A mass selective detector. The samples were corrected for recovery by quantifying the PAHs relative to the closest eluting surrogate standard.

Quality control procedures have also been detailed elsewhere (Chapter III and IV). Both field and laboratory blanks were generally less than 5% of levels found in

Table 2: Analytical Procedures\Quality Control Results

	Water Samples (Dissolved Fraction) (n = 59; including blanks)	Atmospheric Samples (Vapor Fraction) (n = 65; including blanks)
sample collection	submersible pump glass fiber filter (GFF) XAD-2 resin	high volume air sampler GFF/polyurethane foam
matrix preparation	GFF ashed 4h at 450°C XAD-2 Soxhlet extracted w/organic solvents 8 d*	GFF ashed at 450°C PUF Soxhlet extracted w/organic solvents 48 h*
extraction	Soxhlet 24 h each w/acetone, hexane	Soxhlet 24 h each w/acetone, petroleum ether
cleanup	silica gel	silica gel
chromatography	HP 5890/5971A GC/MS selective ion mode 30 m DB-5 column	HP 5890/5971A GC/MS selective ion mode 30 m DB-5 column
recoveries	d-8 naphthalene: 62 ± 11% d-10 anthracene: 86 ± 12% d-12 b[a]a ¹ : 97 ± 8% d-12 b[a]p ² : 86 ± 8%	d-8 naphthalene: 49 ± 13% d-10 anthracene: 89 ± 19% d-12 b[a]a ¹ : 100 ± 21% d-12 b[a]p ² : 87 ± 20%
replicate samples	side by side samples	side by side samples
% rel. difference	avg. 17 PAHs = 5.4%	avg. 17 PAHs = 8.6%
blank values	2 field, 10 lab blanks	6 field, 13 lab blanks
% sample values	avg. 17 PAHs = 1.5%	avg. 17 PAHs = 3.8%
limit of detection	3 pg/l	.30 pg/m ³

* see Dickhut and Gustafson, 1995.

¹ benzo[a]anthracene

² benzo[a]pyrene

samples. Recoveries ranged from $49\% \pm 13$ for naphthalene from PUF samples to $100\% \pm 21$ for benzo(a)anthracene also from PUF samples (Table 2). Sampling artifacts for both XAD-2 and PUF were investigated thoroughly (Chapters III and IV) and were determined not to affect reported fluxes.

Results and Discussion

Instantaneous fluxes were calculated for 46 paired air and water samples (surface water concentrations measured within the duration of, or a few hours of, the collection of an atmospheric sample at the same site) collected in the southern Chesapeake Bay during the period January 1994 to June 1995. Atmospheric vapor and surface water PAH concentrations and distributions have been described in detail elsewhere (Chapters III and IV). Briefly, PAH vapor concentrations increased exponentially with temperature at the non-rural sites. No seasonal trend in PAH vapor concentrations was observed at the rural Wolftrap\Haven Beach site; however vapor concentrations decreased with time. As with vapor concentrations, dissolved water concentrations also decreased with time at the rural Wolftrap site. Nonetheless, there was little temporal variability (ca 30%) in PAH dissolved concentrations and no seasonal trends at all sites.

From analysis of variance, the Elizabeth River site exhibited elevated dissolved water concentrations relative to all other sites, with exception of the lighter molecular weight PAHs (e.g. fluorene, phenanthrene) at the Wolftrap site (Chapter III).

Dissolved PAH concentrations at the York River site were significantly different from concentrations at all other sites except Hampton. The mean dissolved PAH concentrations at the Hampton and Wolftrap sites were significantly different only for the lighter molecular weight PAHs. Additionally, vapor concentrations of PAHs were highest at the Hampton site and lowest at the rural Haven Beach site, varying up to 50-fold between sites during summer (Chapter IV). Hence, a gradient in both atmospheric vapor and surface water dissolved PAH concentrations was observed with contaminant concentrations decreasing from urban to remote areas, except for the lighter PAHs which were elevated in the surface waters of both the Elizabeth River and the mainstem bay Wolftrap site.

Water and air temperatures were measured at each site during sample collection (Figure 2). Large seasonal trends were observed in both air and water temperatures; however, there was little spatial variability in temperature between sites. Short-term temporal variation in measured windspeeds for each site was large; nevertheless, again little spatial variation was observed between sites. Therefore, because spatial variability in hydrologic and meteorologic parameters was low, spatial variation in gas-exchange fluxes should not be due to differences in meteorologic or hydrologic conditions, but rather, due to the differences in air-water concentration gradients of PAH between sites.

Gas exchange behavior of PAHs. Gas exchange behaviors of selected PAHs across the air-water interface of southern Chesapeake Bay during two seasonal extremes (Figure 3) indicate that fluxes of the volatile two-ring PAH naphthalene are

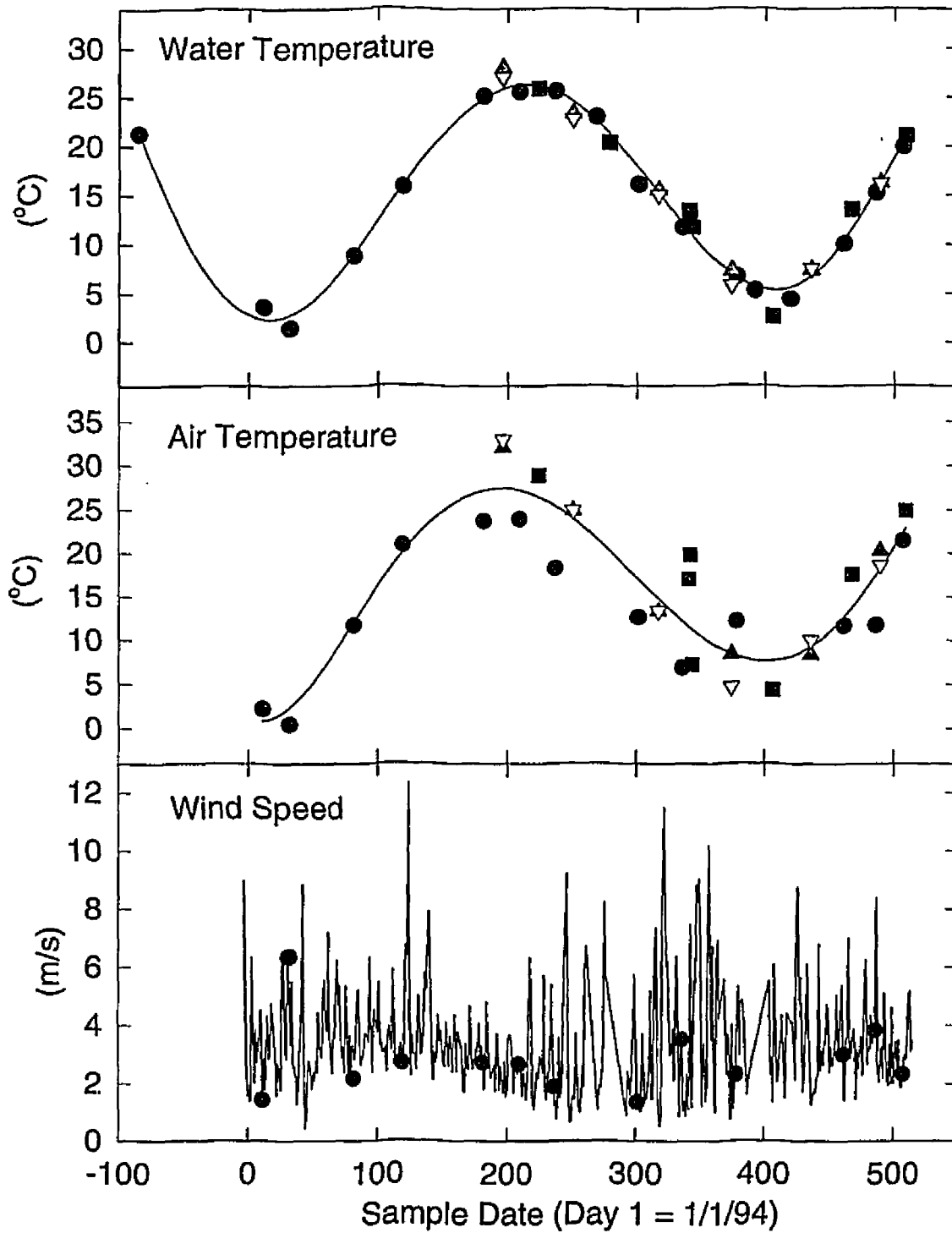


Figure 5.2: Hydrologic and Meteorologic Data for the Southern Chesapeake Bay (10-7-93 to 5-24-95) ● Wolftrap
 ▽ Hampton ■ York River ▲ Elizabeth River

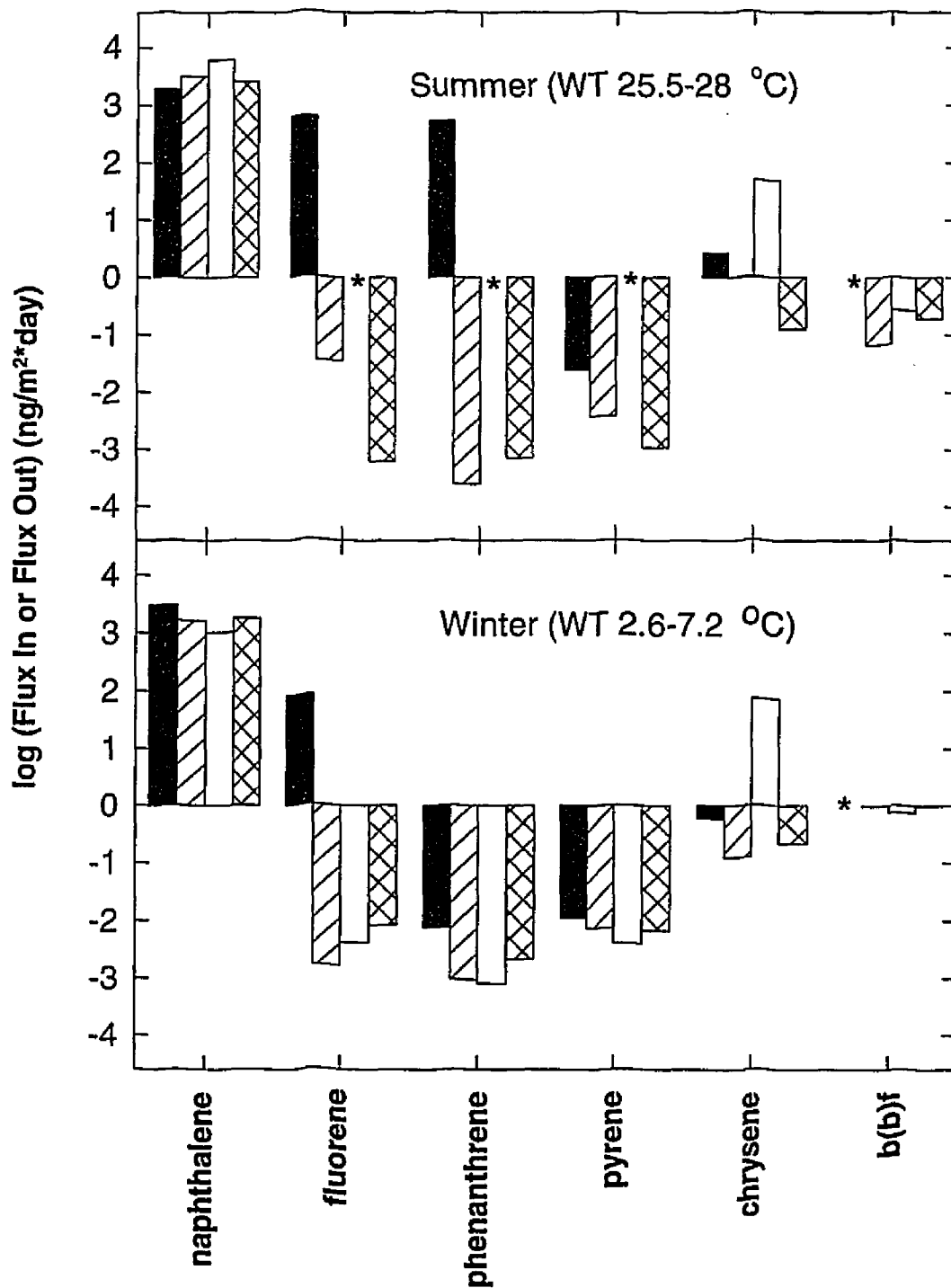


Figure 5.3: Gas Exchange Behaviors of Selected PAHs Across the Air-Water Interface During Two Seasonal Extreme Sampling Periods in the Southern Chesapeake Bay * = not quantifiable

■ Wolftrap Site ▩ Hampton Site ▨ York River Site
 □ Elizabeth River Site; b(b)f = benzo[b]fluoranthene

always out of surface waters to the atmosphere of the bay regardless of site location or sampling date. Volatile de-gassing of naphthalene from surface waters of the bay is due to the large Henry's law constant for this compound (i.e. naphthalene's affinity for the vapor phase relative to being dissolved). In contrast, fluxes of the heavier more non-volatile 5 ring PAH benzo[b]fluoranthene (b[b]f) are always from the atmosphere into surface waters of the bay at all locations and sampling periods due to the compound's very low Henry's law constant or affinity for being dissolved relative to being in the vapor phase. Additionally, the magnitude of flux of b[b]f from the atmosphere into surface waters was substantially greater during summer relative to winter due to a large increase in vapor concentrations (Chapter IV), and hence, air-water concentration gradient with temperature. Also note that the magnitude of gaseous flux decreases as molecular size of the PAH increases. The decrease in flux with molecular size is largely a result of lower molecular diffusion coefficients, and hence, overall mass transfer as the number of PAH aromatic rings increases. Finally, gas exchange behaviors of the 3-4 ring PAHs (such as fluorene, phenanthrene, pyrene) vary widely with large spatial and seasonal variability both in direction and magnitude of flux (Figure 3). The spatial and temporal differences in the gas exchange fluxes of these semivolatile PAHs is due to both the affect of temperature on the air-water partition coefficient, as well as seasonal differences in atmospheric vapor concentrations, and thus, air-water concentration gradients.

Controlling Factors Governing Gaseous Flux. In describing the gas exchange behavior of the 3-4 ring PAHs in southern Chesapeake Bay, the sites can be

typified (based on equilibrium concentration or fugacity ratios) as those sites at which vapor and dissolved concentrations are close to equilibrium (fugacity ratios near 1) and those sites at which vapor and dissolved concentrations are far from equilibrium (fugacity ratios far from 1). Fugacity or equilibrium concentration ratios are the vapor concentrations expressed as a partial pressure (or fugacity) relative to the dissolved concentration corrected by the chemical specific air-water partition coefficient. The sites at which vapor and dissolved concentrations are close to equilibrium are the rural Wolftrap site, with relatively pristine levels of PAH in the vapor and dissolved phases, and the contaminated Elizabeth River site with elevated vapor and dissolved PAH concentrations. In contrast, the York River and Hampton sites are classified as being far from equilibrium, each having relatively low levels of dissolved PAH in water but seasonally elevated atmospheric PAH vapor concentrations.

Gas exchange fluxes at Wolftrap and the Elizabeth River sites, where vapor and dissolved concentrations are close to equilibrium, are governed by temperature most likely as it affects Henry's law constants, and thus, equilibrium fugacity gradients. For example, gas fluxes of phenanthrene at the Wolftrap site strongly mirrored the seasonal trend for water temperatures observed at this site (Figure 4). Furthermore, phenanthrene gas fluxes were lower in magnitude at the equilibrium compared to the nonequilibrium sites (Figures 4, 5) because vapor and dissolved PAH concentrations were close to equilibrium at these sites; thus gaseous flux is due simply to relatively small perturbations in the fugacity gradient with temperature. Similarly,

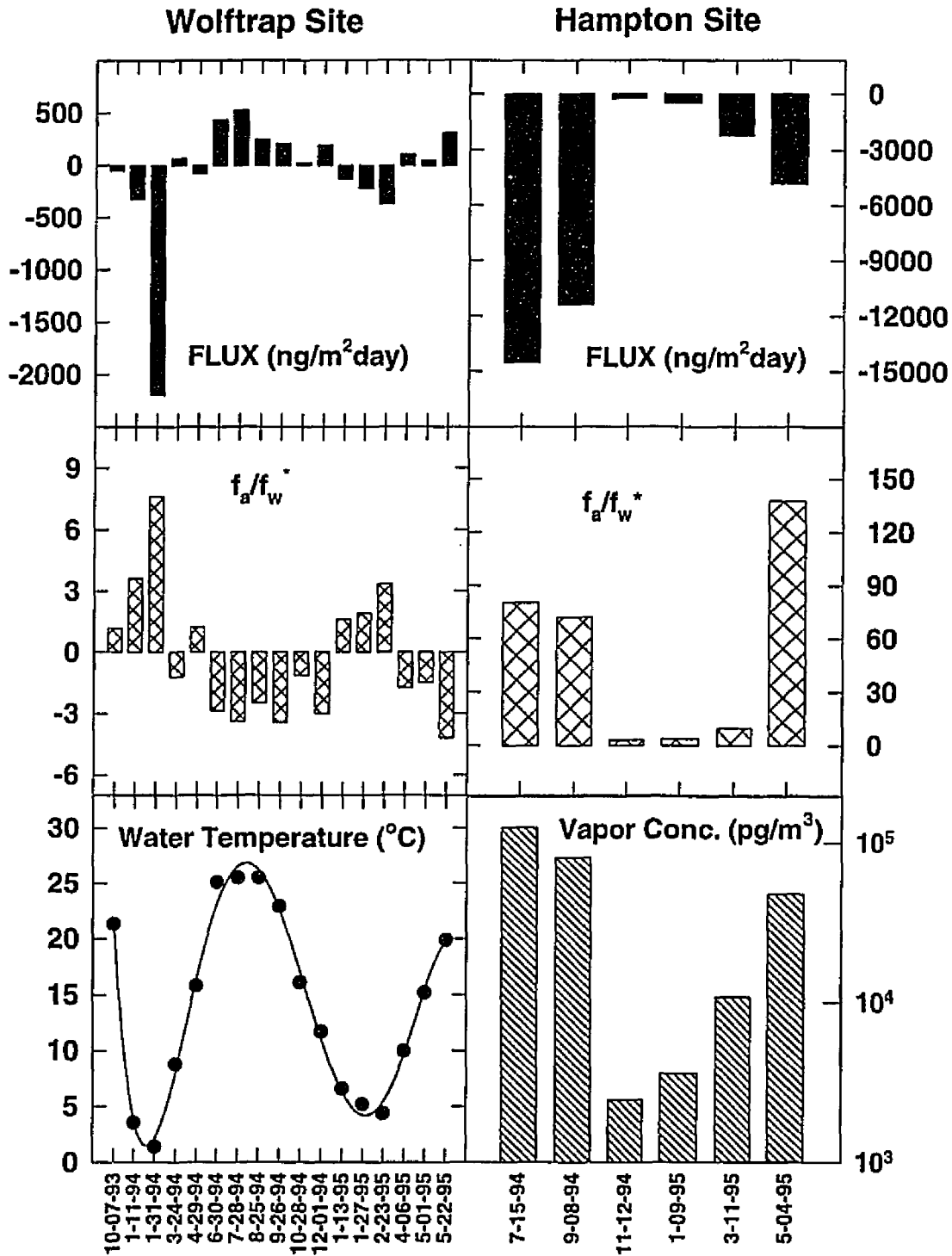


Figure 5.4: Controlling factors (---●--- water temperature and ▨ vapor concentrations) governing gaseous fluxes (■) of phenanthrene at equilibrium vs nonequilibrium sites. Equilibrium sites have air and water concentrations close to equilibria and fugacity ratios (▤) close to 1, nonequilibrium sites have concentrations far from equilibria and fugacity ratios far from 1 (values <1 indicate the inverse ratio).

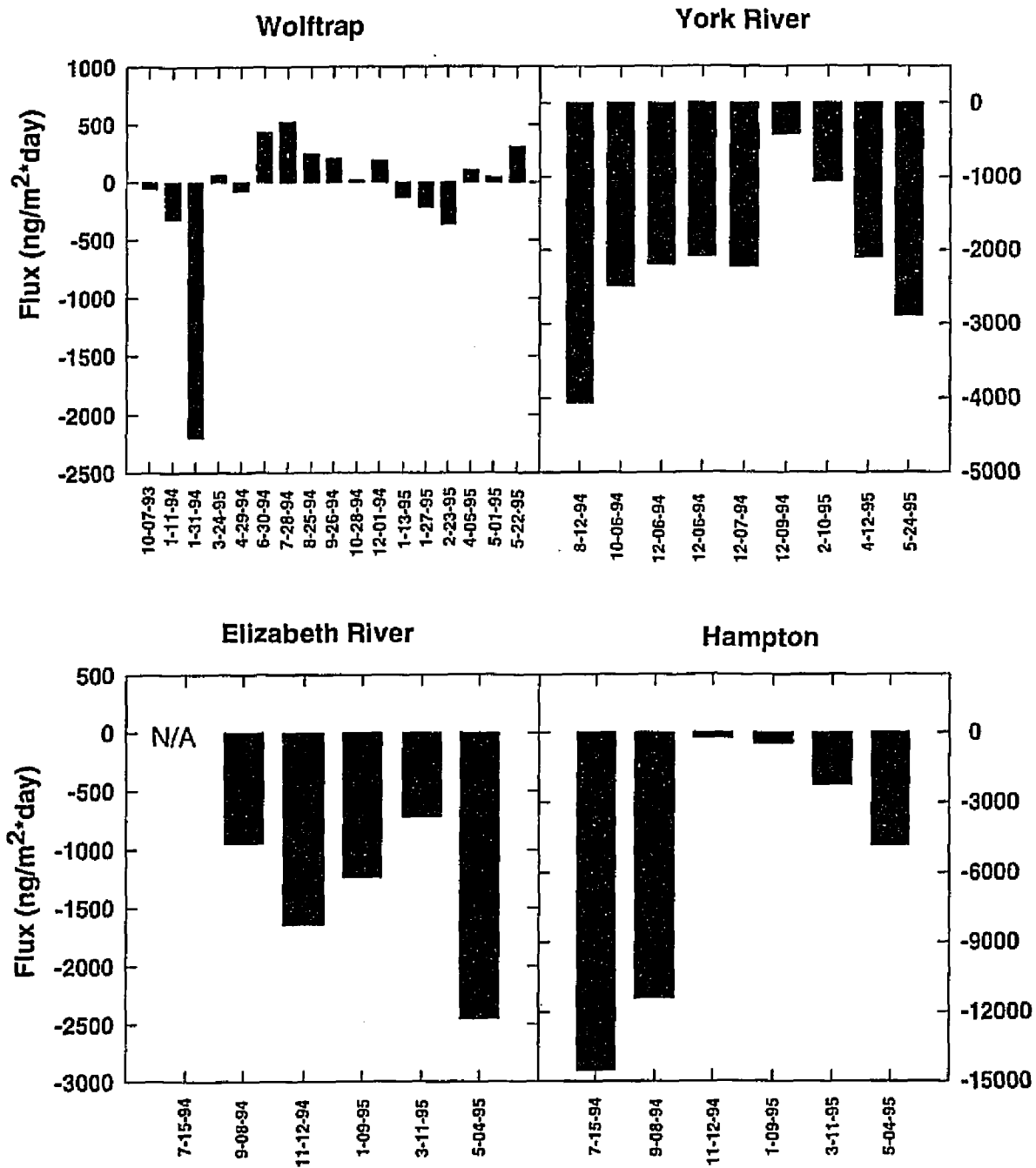


Figure 5-5: Gaseous Fluxes of Phenanthrene Across the Air-water Interface of Southern Chesapeake Bay

gas fluxes of pyrene were lower at the equilibrium sites, and at the Elizabeth River site were variable in both direction and magnitude (Figure 6). As the Elizabeth River site was also close to equilibrium with respect to vapor and dissolved concentrations, small perturbations in concentration levels of either phase likely caused a shift in the equilibrium gradient, and thus, controlled the direction of flux across the air-water interface.

Although the Elizabeth River was generally characterized as an equilibrium site, there were exceptions where PAH vapor and dissolved concentrations were far from equilibrium. Gas exchange fluxes of chrysene and fluoranthene in the Elizabeth River were controlled by dissolved water concentrations which dominated the equilibrium gradient term. Furthermore, the dissolved concentrations of chrysene increased throughout the study, a trend which is reflected in the gas exchange fluxes (Figure 7).

Fluxes at the York River and Hampton sites where concentrations are far from equilibrium are controlled by the vapor concentration which dominates the concentration gradient term. Gas exchange fluxes of the 3-4 ring PAHs at these sites were controlled by the vapor phase which showed a strong seasonal trend in concentrations (Chapter IV) and thus, drove the equilibrium gradient and flux, especially during summer. Note that the direction of exchange for PAHs was from the air into the water at these sites (Figures 4-6) reflecting the dominance of vapor concentrations in determining the gradient and flux.

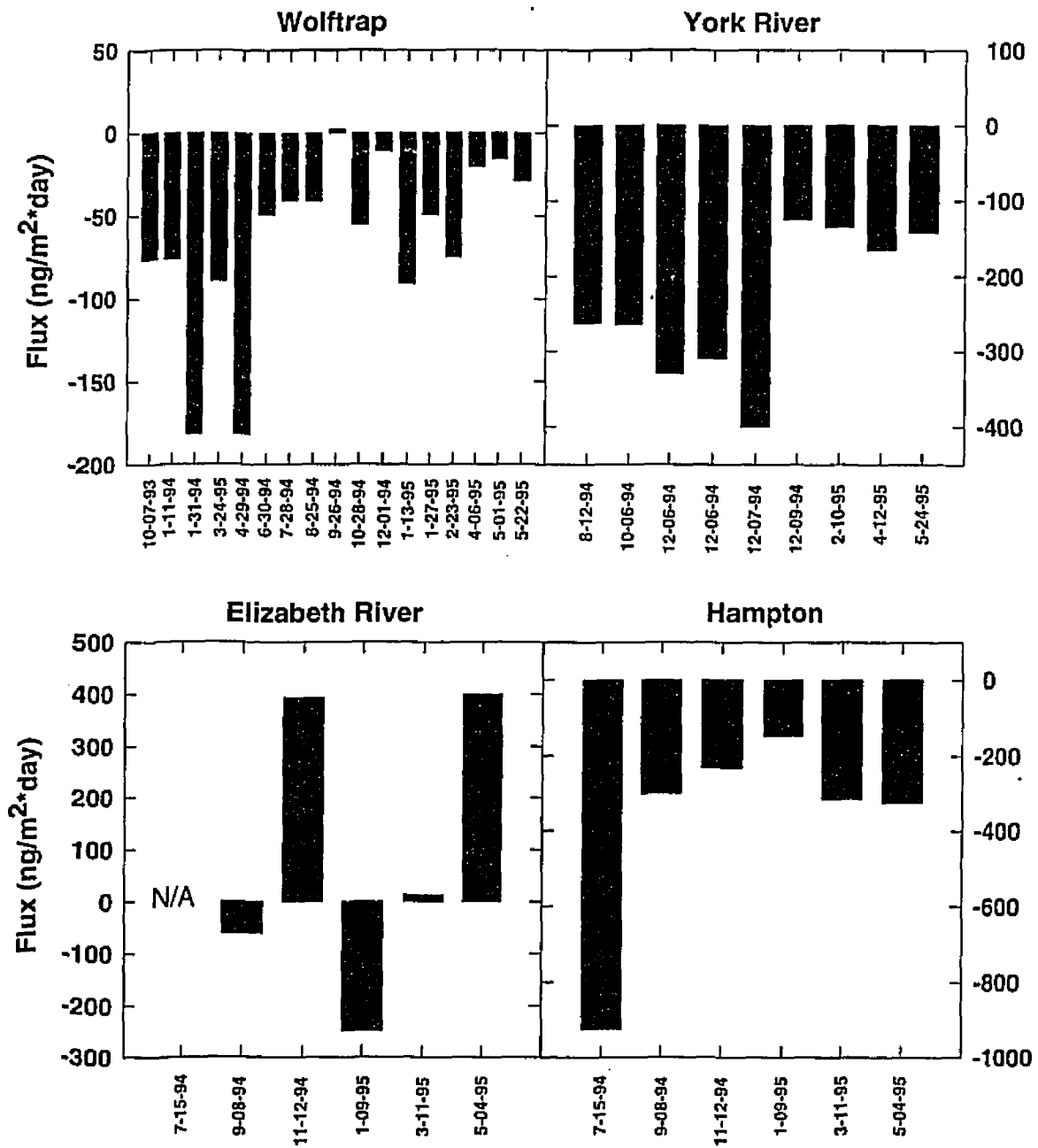


Figure 5.6: Gaseous Exchange of Pyrene Across the Air-Water Interface of Southern Chesapeake Bay

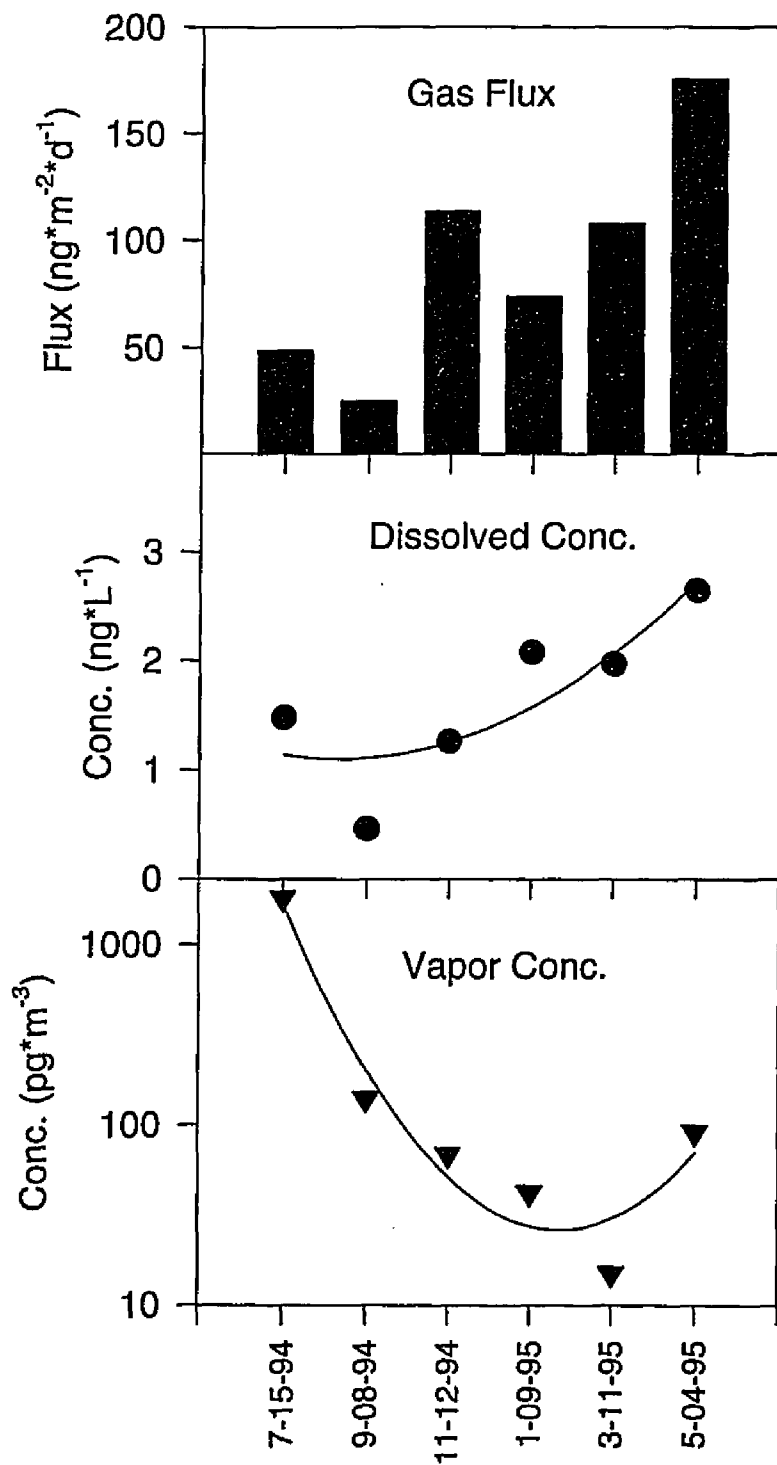


Figure 5.7: Gaseous Exchange of Chrysene Across the Air-water Interface of the Elizabeth River and the Relation to Dissolved Water Concentrations.

Sensitivity Analysis. A sensitivity analysis was performed to examine the effects of changes in windspeed and temperature during the daily sampling period on the reported daily integrated (instantaneous) fluxes. From eqs. 5 and 6, mass transfer coefficients are not linearly related to wind speed; therefore, averaging windspeeds underestimates the gaseous flux. The magnitude of flux increased from 13 % for pyrene to 37 % for naphthalene when fluxes were integrated using wind speed data measured every 15 minutes relative to fluxes determined using daily averaged wind speeds (Table 3). Additionally, water temperatures may change a few degrees on a diurnal or tidal scale as indicated from York River monitoring data (VIMS, 1996). The effect on gas exchange flux of an increase or decrease in water temperature from the daily average temperature during sampling, was also assessed. The change in the magnitude of flux ranged from ± 4 % for naphthalene and ± 30 % for pyrene for a 2 °C change in interface temperature (Table 3). Moreover, the magnitude of flux is such that if vapor concentrations are not replenished on timescales less than a day, then atmospheric gas concentrations will change due to air-water exchange. The magnitude of fluxes reported herein have been calculated using daily averaged wind speeds, vapor concentrations determined over 4 to 15 h, and water temperatures averaged over the sampling period (2 to 12 h); thus, the determined gas exchange fluxes are a best estimate with a variability of up to ± 37 % imposed by the various environmental variables (Table 3).

Integrated Net Annual Fluxes. Net annual gas exchange fluxes of PAHs across the air-water interface of the southern Chesapeake Bay were calculated from

Table 3: Sensitivity Analysis¹- Windspeed and Temperature Effects on Integrated Daily Fluxes for Selected PAHs at the Wolftrap site in Southern Chesapeake Bay.

PAH	Wind Speed ²	-2 °C ΔT [†]	+2 °C ΔT [†]
naphthalene	+37 ± 17	-4 ± 1	+4 ± 1
acenaphthylene	+27 ± 13	-5 ± 2	+9 ± 5
fluorene	+27 ± 10	-12 ± 6	+11 ± 5
phenanthrene	+20 ± 4	-28 ± 10	+22 ± 5
pyrene	+13 ± 3	+29 ± 26	-31 ± 26

¹ reported values are % change ± standard deviation (n=3) of integrated daily fluxes relative to those calculated from average water temperatures during sampling and daily averaged windspeeds (reported herein).

² % change in daily fluxes integrated using windspeeds for 15 minute intervals relative to fluxes determined using daily averaged wind speeds.

[†] % change in fluxes due to a change in interface (water) temperature over the integrative period (1 day) relative to fluxes determined using the average temperature during sampling.

the instantaneous fluxes. Starting with the first sample period, the average daily flux for two consecutive sampling periods was multiplied by the number of days between sampling periods. The integrated fluxes calculated in this manner were summed, divided by the number of days between the first and last sampling period, and multiplied by 365 days to yield a net annual flux ($\mu\text{g}\cdot\text{m}^{-2}\cdot\text{y}$) for each site (Table 4). At all sites, the annual gas exchange flux of naphthalene was out (i.e. volatilization) of the surface water. In contrast, the annual fluxes of 5-6 ring PAHs was into (i.e. absorption) the lower Chesapeake Bay region. The 3-4 ring PAHs exhibited both net absorption and volatilization at the various sites, with the exception of phenanthrene, which was uniformly exchanged into the surface waters of the lower bay. Slow photodegradation of phenanthrene likely contributes to these large absorptive fluxes by keeping the air-water fugacity gradient relatively large.

Overall, gas exchange of most PAHs was lowest at the Wolftrap site reflective of the generally lower atmospheric concentrations of these contaminants at this site (Chapter IV), and higher at the urban/industrialized sites (Table 4). Moreover, gas fluxes tended to be in both directions at sites where the vapor and dissolved concentrations were near equilibrium (i.e. Wolftrap and Elizabeth River), whereas absorption of PAHs dominated at the nonequilibrium sites (i.e. Hampton and York River) where atmospheric fugacities greatly exceeded surface water fugacities (Figure 4). For areas in which vapor and dissolved concentrations are close to equilibrium, fluxes occur in both directions across the air-water interface throughout the year as a function of temperature.

Table 4: Net Annual Gas Exchange (Volatilization)[†] Fluxes ($\mu\text{g}\cdot\text{m}^{-2}\cdot\text{y}^{-1}$) of Selected PAHs Across the Air-water Interface of Southern Chesapeake Bay (1994-1995)

PAH	Site			
	Wolftrap	York River	Elizabeth River	Hampton
naphthalene	1170	820	1110	1330
acenaphthylene	1.50	-4.99	-13.5	3.45
acenaphthene	21.9	-44.6	182	-292
fluorene	80.6	-144	-63.5	-292
phenanthrene	-29.2	-735	-480	-1720
anthracene	n.q.	-25.2	4.83	-76.3
fluoranthene	-22.0	-173	297	-245
pyrene	-25.3	-72.9	29.0	-116
b(a)a	n.q.	-1.07	5.37	n.q.
chrysene	-.272	-1.45	31.4	-2.28
b(b)f	-.246	-1.53	-.755	-1.33
b(a)p	N.D.	N.D.	-1.18	N.D.
b(ghi)p	N.D.	N.D.	-.881	N.D.

N.D. Not determined

[†] Positive flux indicates volatilization; negative flux depicts absorption.

The integrated annual gas exchange fluxes for selected PAHs at the rural Haven Beach\Wolftrap site have been compared to wet and dry atmospheric depositional fluxes measured at the same site (Figure 8). For volatile PAHs such as fluorene, gas exchange dominates as an air-water transfer process. Gas exchange fluxes into the bay are of the same order as total wet and dry atmospheric depositional fluxes for the semivolatile PAHs such as phenanthrene, fluoranthene, and pyrene. However, particle-associated (i.e. dry deposition and particle washout) processes dominate net fluxes for the least volatile PAHs such as chrysene and benzo[b]fluoranthene. Nonetheless, it is important to note that although net annual gas exchange fluxes may be low, exposure levels of organisms residing near the interface will be influenced by the larger seasonal instantaneous fluxes (e.g. Figures 4-6).

Conclusions

Spatial variations in PAH gas exchange fluxes across the air-water interface are significant, and are due to differences in fugacity gradients between sites. Temporal variations in gas exchange fluxes are due to both the seasonal change in water temperature for sites at which vapor and dissolved concentrations are close to equilibrium, and seasonal changes in vapor concentrations for the sites at which concentrations are far from equilibrium. Large net fluxes occur as a result of large fugacity gradients, not necessarily high concentrations of SOCs in air or water. Net

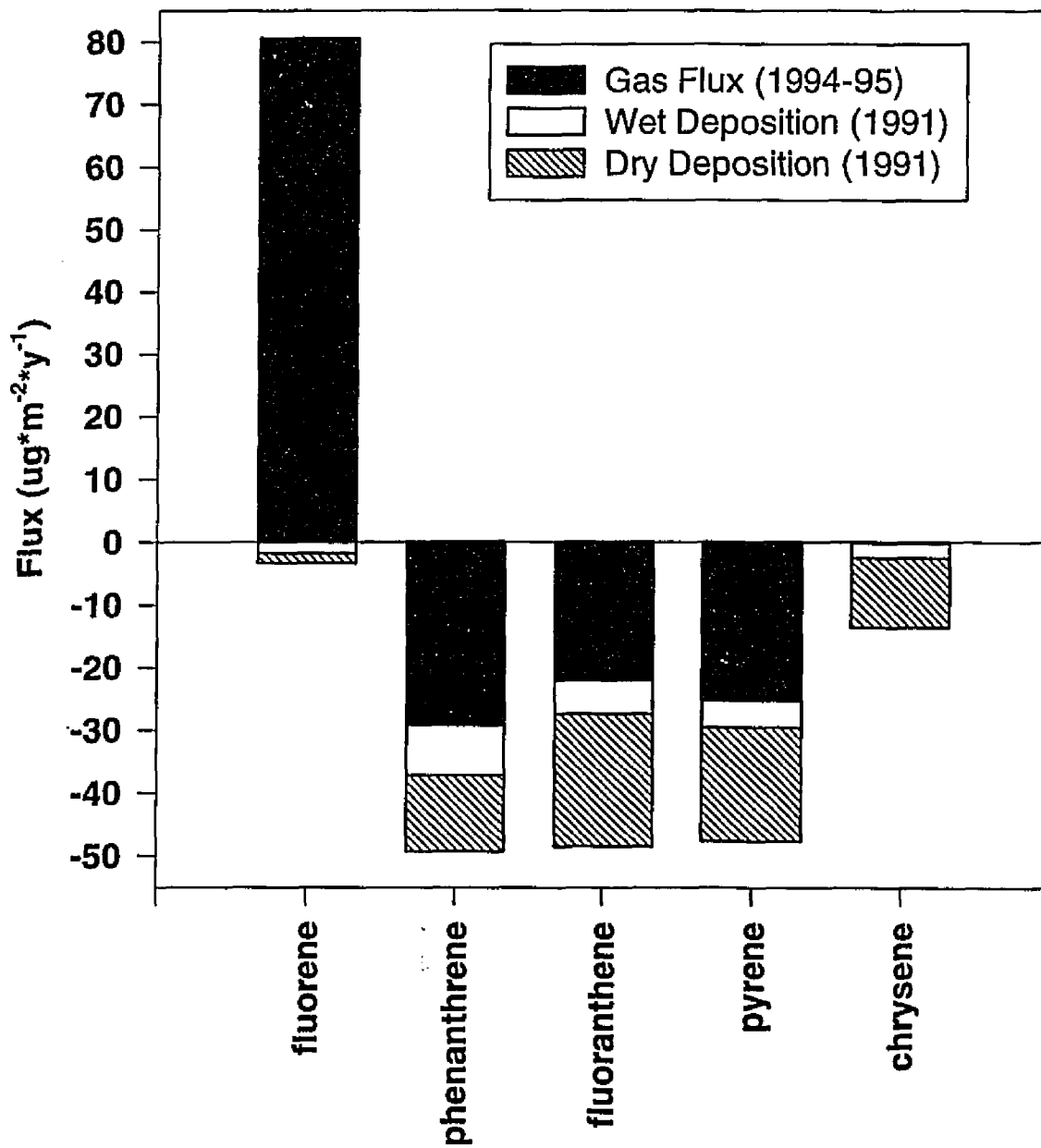


Figure 5.8: Comparison of Net Annual Gaseous Exchange and Atmospheric Wet and Dry Depositional Fluxes as Transfer Vectors for PAHs Across the Air-water Interface of Southern Chesapeake Bay

annual gas exchange fluxes across the air-water interface of Southern Chesapeake Bay are of the same order of magnitude as total wet and dry atmospheric depositional fluxes to the bay. The results support the hypothesis that gas exchange is an important process controlling the transfer and transport of PAHs across the air-water interface of southern Chesapeake Bay. In order to better assess the short term variability in gaseous exchange fluxes for trace organic contaminants due to changing environmental parameters such as wind speed and water temperature, more work needs to be done improving air sampling analytical detection limits to allow short-term resolution (< 2 h) of vapor concentrations, and hence fluxes.

References

- Achman, D.R., K.C. Hornbuckle, and S.J. Eisenreich. 1993. Volatilization of Polychlorinated Biphenyls from Green Bay, Lake Michigan. *Environ. Sci. Technol.* 27:75-87.
- Andren, A.W. 1983. Processes determining the flux of PCBs across air/water interfaces. Chapter 8 in Mackay, D., S. Patterson, S.J. Eisenreich and M.S. Simmons (eds), *Physical behavior of PCBs in the Great Lakes*, Ann Arbor Science, 127-140.
- Baker, J.E. and S.J. Eisenreich. 1990. Concentrations and fluxes of polycyclic aromatic hydrocarbons and polychlorinated biphenyls across the air-water interface of Lake Superior. *Environ. Sci. Technol.* 24:342-352.
- Baker, J.E. and S.J. Eisenreich. 1989. PCBs and PAHs as tracers of particulate dynamics in large lakes. *J. Great Lakes Res.* 15(1):84-103.
- Bidleman, T.F., C.G. Simon, N.F. Burdick, and F. You. 1984. Theoretical plate measurements and collection efficiencies for high-volume air samplers using polyurethane foam. *J. Chromatogr.* 301:448-453.

- Bird, R.B., W.E. Stewart and E.N. Lightfoot. 1960. Transport phenomena, John Wiley and Sons, New York, p. 512.
- Black, J.J., T.F. Hart, Jr., P.J. Black. 1982. A novel integrative technique for locating and monitoring polynuclear aromatic hydrocarbon discharges to the aquatic environment. *Environ. Sci. Technol.* 16:247-250.
- Bopp, R.F. 1983. Revised parameters for modeling the transport of PCB components across an air water interface. *J Geophysical Res.* 88:2521-2529.
- Burdick, N.F. and T.F. Bidleman. 1981. Frontal movement of hexachlorobenzene and polychlorinated biphenyl vapors through polyurethane foam. *Anal. Chem.* 53:1926-1929.
- Capel, P.D., and S.J. Eisenreich. 1985. PCBs in Lake Superior, 1978-1980. *J. Great Lakes Res.* 11(4):447-461.
- Cotham, W.E. and T.F. Bidleman. 1992. Laboratory investigations of the partitioning of organochlorine compounds between the gas phase and atmospheric aerosols on glass fiber filters. *Environ. Sci. Technol.* 26:469-478.
- Daignault, S.A., D.K. Noot, D.T. Williams, and P.M. Huck. 1988. A review of the use of XAD resins to concentrate organic compounds in water. *Water Resour.* 22:803-813.
- Dickhut, R.M., K.E. Gustafson. 1995. Atmospheric inputs of selected polycyclic aromatic hydrocarbons and polychlorinated biphenyls to southern Chesapeake Bay. *Mar. Pollut. Bull.* 30:385-396.
- Doskey, P.V. and A.W. Andren. 1981. Modeling the flux of atmospheric polychlorinated biphenyls across the air/water interface. *Environ. Sci. Technol.* 15:705-711.
- Eadie, B.J. and J.A. Robbins. 1987. In-Sources and fates of aquatic pollutants. Hites, R.A. and S.J. Eisenreich, Eds., *Advances in Chemistry Series 216*. American Chemical Society. Washington, DC. 319-364.
- Eisenreich, S.J., B.B. Looney, and J.D. Thornton. 1981. Airborne organic contaminants in the Great Lakes ecosystem. *Environ. Sci. Technol.* 15:30-38.
- Friesen, K.J., W.L. Fairchild, M.D. Loewen, S.G. Lawrence, M.H. Holoka, and D.C.G. Muir. 1993. Evidence for particle-mediated transport of 2,3,7,8-Tetrachlorodibenzofuran during gas sparging on natural water. *Environ. Tox. and Chem.* 12:2037-2044.

- Gallo, L.J. 1990. Atmospheric input of PAH to the sea surface microlayer. Ph.D. dissertation- The College of William and Mary- Virginia Institute of Marine Science.
- Hornbuckle, K.C., D.R. Achman, S.J. Eisenreich. 1993. Over-water and over-land polychlorinated biphenyls in Green Bay, Lake Michigan. *Environ. Sci. Technol.* 27:87-96.
- Hornbuckle, K.C., C.W. Sweet, R.F. Pearson, D.L. Swackhamer, and S.J. Eisenreich. 1995. Assessing annual water-air fluxes of polychlorinated biphenyls in Lake Michigan. *Environ. Sci. Technol.* 29:869-877.
- Huckins, J.N., M.W. Tubergen, and G.K. Manuweera. 1990. Semipermeable membrane devices containing model lipid: A new approach to monitoring the bioavailability of lipophilic contaminants and estimating their bioconcentration potential. *Chemosphere.* 20:533-552.
- Hunter, K.A. and P.S. Liss. 1981. Organic sea surface films. In *Marine Organic Chemistry*, Duursma, E.K. and R. Dawson, ed., Elsevier: New York, Chap. 9.
- Keller, C.D. and T.F. Bidleman. 1984. Collection of airborne polycyclic aromatic hydrocarbons and other organics with a glass fiber filter-polyurethane foam system. *Atm. Environ.* 18:837-845
- Landrum, P.F., S.R. Nihart, B.J. Eadie, and W.S. Gardner. 1984. *Environ. Sci. Technol.* 18:187-192.
- Leister, D.L. and J.E. Baker. 1994. Atmospheric Deposition of Organic Contaminants to the Chesapeake Bay. *Atmos Environ.* 28:1499-1520.
- Lebo, J.A., J.L. Zajicek, J.N. Huckins, J.D. Petty, and P.H. Peterman. 1992. Use of semipermeable membrane devices for in situ monitoring of polycyclic aromatic hydrocarbons in aquatic environments. *Chemosphere.* 25:697-718.
- Liss, P.S. and P.G. Slater. 1974. Flux of gases across the air-sea interface. *Nature* 247:181-184.
- Liu, K. 1994. Ph.D. Prospectus submitted to the faculty of The College of William and Mary, School of Marine Science, Gloucester Pt., VA.
- Mackay, D. 1982. Effects of surface films on air-water exchange rates. *J. Great Lakes Res.* 8:299-306.
- Mackay, D. 1979. Finding fugacity feasible. *Environ. Sci. Technol.* 13:1218-1223.

- Mackay, D. and P.J. Leinonen. 1975. Rate of evaporation of low-solubility contaminants from water bodies to atmosphere. *Environ. Sci. Technol.* 9:1178.
- Mackay, D., S. Paterson and W.H. Schroeder. 1986. Model describing the rates of transfer processes of organic chemicals between the atmosphere and water. *Environ. Sci. Technol.* 20:810-816.
- Mackay, D. and A.T.K. Yeun. 1983. Mass transfer coefficient correlations for volatilization of organic solutes from water. *Environ. Sci. Technol.* 17: 211-217.
- May, W.E., S.P. Wasik, M.M. Miller, Y.B. Tewari, J.M. Brown-Thomas, and R.N. Goldberg. 1983. Solution thermodynamics of some slightly soluble hydrocarbons in water. *J. Chem. Eng. Data* 28:197-200.
- McConnell, L.L., W.E. Cotham, and T.F. Bidleman. 1993. Gas exchange of hexachlorocyclohexane in the Great Lakes. *Environ. Sci. Technol.* 27: 1304-1311.
- McDow, S.R. and J.J. Huntzicker. 1990. Vapor adsorption artifact in the sampling of organic aerosol: face velocity effects. *Atmos. Environ.* 24A, 2653-2671.
- Murray, M.W. and A.W. Andren. 1991. Preliminary evaluation of the potential of gas purging for investigating the air-water transfer of PCBs. In *Organic Substances and Sediments in Water: Volume 2, Processes and Analytical*. CRC Press: Boca Raton, FL. pp 3-13.
- Norkrans, B. 1980. Surface microlayers in aquatic environments. In *Advances in Microbial Ecology Volume 4*; Alexander, A. ed. Plenum Press: New York. pp 51-85.
- Ottar, B. 1981. The transfer of airborne pollutants to the arctic region. *Atmos. Environ.* 15: 1439-1445.
- Paulson, C.A. and T.W. Parker. 1972. *J. Geophys. Res.* 77. 491-495.
- Prest, H.F., W.M. Jarman, S.A. Burns, T. Weismuller, M. Martin, and J.N. Huckins. 1992. Passive water sampling via semipermeable membrane devices (SPMDS) in concert with bivalves in the Sacramento/San Joaquin river delta. *Chemosphere.* 25:1811-1823.
- Schroeder, W.H. and D.A. Lane. 1988. The fate of toxic airborne pollutants. *Environ. Sci. Technol.* 22:240-246.

- Scudlark, J.R., K.M. Conko, and T.M. Church. 1994. Atmospheric Wet Deposition of Trace Elements to Chesapeake Bay: CBAD Study Year 1 Results. *Atmos. Environ.* 28:1487-1498.
- Sodergren, A. 1987. Solvent-filled dialysis membranes simulate uptake of pollutants by aquatic organisms. *Environ. Sci. Technol.* 21:855-859.
- Sonnefeld, W.J., W.H. Zoller, and W.E. May. 1983. Dynamic coupled-column liquid chromatographic determination of ambient vapor pressures of polynuclear aromatic hydrocarbons. *Anal. Chem.* 55:275-280.
- Sproule, J.W., W.Y. Shiu, D. Mackay, W.H. Schroeder, R.W. Russell, and F.A.P.C. Gobas. 1991. Direct in situ sensing of the fugacity of hydrophobic chemicals in natural waters. *Environ. Toxicol. Chem.* 10:9-20.
- Ten Hulscher, Th.E.M., L.E. Van Der Velde, and W.A. Bruggeman. 1992. Temperature dependence of Henry's Law Constants for Selected Chlorobenzenes, Polychlorinated Biphenyls and Polycyclic Aromatic Hydrocarbons. *Environ. Tox. Chem.* 11:1595-1603.
- Yin, C. and J.P. Hassett. 1986. Gas-partitioning approach for laboratory and field studies of mirex fugacity in water. *Environ. Sci. Technol.* 20:1213-1217.
- Yin, C. and J.P. Hassett. 1989. Fugacity and Phase Distribution of Mirex in Oswego River and Lake Ontario waters. *Chemosphere.* 19:1289-1296.
- You, F. and T.F. Bidleman. 1984. Influence of volatility on the collection of polycyclic aromatic hydrocarbon vapors with polyurethane foam. *Environ. Sci. Technol.* 18:330-333.

Chapter VI: Summary

Atmospheric input of contaminants have been noted as a prominent source of pollutants to various ecosystems (McVeety and Hites, 1988; Eisenreich et al., 1981; Schreitmuller and Ballschmiter, 1995; Bidleman et al., 1989, Atlas et al., 1981). The physical characteristics of the Chesapeake Bay, a large surface area to mean water volume ratio and 75 to 100 cm of precipitation annually, make the atmosphere likely to be a significant source of contaminants to this large estuary (Leister and Baker, 1994) which is an important habitat for many fisheries. Municipal and industrial point sources of contaminants are scattered along the shores of the Chesapeake Bay and its tributaries; however, urban and industrial centers are concentrated along the northwest and southern shores. Emissions into the urban atmosphere and the subsequent transport and deposition of contaminants as air masses move across the Chesapeake Bay may significantly impact pollutant levels in the bay and its fisheries. Assessment of water and air quality, implementation of environmental legislation, and risk management require an understanding and quantification of all the major air-water transfer processes for contaminants such that net fluxes of pollutants to and from aquatic systems and exposure levels can be accurately modeled.

Air-water transfer processes for semivolatile organic contaminants (SOCs) include volatilization and absorption of gases, dry deposition with particles, wet deposition by rain or snow, (i.e. particle and vapor "washout"), spray transfer and bubble scavenging (Andren, 1983). Thus, quantitative assessments of air-water exchange processes must consider chemical speciation in both the atmosphere and

water column. The distribution of a contaminant between vapor and aerosol particles, and, water and suspended particulates, determines the amount of chemical available for air-water transfer through a particular vector.

In the Chesapeake Bay watershed, researchers have determined the wet and dry depositional fluxes of selected SOCs and trace elements to Chesapeake Bay (see refs. Chap. V). In this study, the gaseous fluxes of polycyclic aromatic hydrocarbons (PAHs) across the air-water interface of Southern Chesapeake Bay have been determined for the period 1994-1995. In addition to the measurement of gaseous contaminant fluxes in this study, the investigation of the distributions of PAHs between the vapor and aerosol phases in the atmosphere, and, between the freely dissolved and suspended particulate phases in the water column provides insight into transport and distribution processes for contaminants in estuarine systems such as Chesapeake Bay.

In natural waters, only the freely dissolved fraction of a contaminant is related to chemical potential and contributes to diffusive fluxes. Freely dissolved PAH concentrations have been measured in Chesapeake Bay surface waters via three methods: air sparging, semipermeable membrane devices (SPMDs), and filtration through glass fiber filters with subsequent sorption of the freely dissolved contaminant fraction to Amberlite^R XAD-2 resin. Dissolved concentrations measured by air sparging and SPMDs were significantly different from those measured by filtration/XAD-2. Evidence of particle-mediated transport of PAHs was observed in gas sparging experiments. Uptake of contaminants into SPMDs appears to be

kinetically limited under environmental conditions. Sampling artifacts for filtration/XAD-2 were determined not to affect measured dissolved concentrations for PAHs. Therefore, dissolved concentrations in this study were determined using filtration/XAD-2.

Measured PAH concentrations in Southern Chesapeake Bay surface waters were higher than those reported by Ko and Baker (1995) for the northern bay. Concentrations of larger molecular weight PAHs in the southern bay were significantly higher in the Elizabeth and York Rivers than in the mainstem bay sites. Distributions of PAHs between the particulate and dissolved phases (log distribution coefficient) were linearly related to their log K_{ow} s with an average slope ($m = .92 \pm .14$); thereby obeying equilibrium partitioning theory. Furthermore, PAHs in the dissolved and particulate phases were observed to be at equilibrium for all sites and sampling periods.

Atmospheric concentrations of PAHs in the southern Chesapeake Bay region were measured during the period 1994-1995 and were comparable to values reported elsewhere for similar urban and rural sites (Leister and Baker, 1994; Keller and Bidleman, 1984; Hoff and Chan, 1987; Gardner et al., 1995; Foreman and Bidleman, 1990). Vapor concentrations of PAHs in air varied significantly between sites and increased logarithmically with temperature at the non-rural sites indicating the major source of these compounds to the atmosphere of Southern Chesapeake Bay is secondary volatilization from contaminated surfaces (soils, roads, vegetation). Aerosol-particle concentrations of PAHs were similar at the various sites and were

higher during winter months indicating that particulate concentrations are controlled by increased combustion sources, the temperature dependence of vapor-particle partitioning, and "cold condensation" of PAH vapors to background aerosols as air plumes are dispersed from source to remote regions.

The temperature dependence of particle-vapor distributions for individual PAHs varies between urban and rural areas in the Chesapeake Bay region. A gradient from urban to remote sites was observed for both specific surface area of particulates and enthalpies of desorption of PAHs. More work needs to be done in the area of characterizing particle-vapor distributions to fully understand the factors which result in differences in the particle-vapor distributions, and hence exposure levels of SOCs in rural and urban air. Additionally, the proposed tight coupling of atmospheric concentrations via secondary volatilization from contaminated terrestrial surfaces in urban and industrial areas, and the cold condensation of PAH vapors to background aerosols supports the global distillation and cold condensation theories of global atmospheric transport of SOCs. Moreover, due to cold condensation and secondary volatilization of PAHs in the southern Chesapeake Bay region, it is likely that during warmer weather (i.e. summer) that atmospheric PAH loadings and exposure levels may be an order of magnitude higher than emission levels during this period. Therefore, it is evident that investigation of the sorption properties of both aerosol and terrestrial surfaces merits further research such that ecosystem and human health risk can be accurately assessed.

Instantaneous gas exchange fluxes for PAHs across the air-water interface of Southern Chesapeake Bay were calculated from simultaneously collected air and water samples during the period January 1994 through the end of May 1995. Gas exchange behaviors of PAHs can be grouped into three categories: net exchange fluxes of high Henry's law constant compounds (i.e. naphthalene) are always out of the bay at all locations and seasons, net gas fluxes of very low Henry's law constant compounds (i.e. benzo(b)fluoranthene) are always into the bay at all locations and seasons, and net gas fluxes of mid-range Henry's law compounds (i.e. three and four ring PAHs) are variable in both magnitude and direction and are dependent upon several controlling factors.

In describing the gas exchange behavior of three and four ring PAHs in southern Chesapeake Bay, the sites can be classified (based on equilibrium concentration or fugacity ratios) as those sites at which vapor and dissolved concentrations are far from equilibrium, and those sites at which vapor and dissolved concentrations are close to equilibrium. Fluxes at the sites where vapor and dissolved concentrations are close to equilibrium are governed by water temperature, most likely as it affects Henry's law constants, to determine air-water partition coefficients and hence concentration gradients. For example, fluxes for PAHs in the rural mainstem bay strongly mirror the seasonal trend for water temperatures observed for this region.

For sites at which vapor and dissolved concentrations are far from equilibrium, fluxes are controlled by the phase which dominates the concentration gradient; most

likely due to the influence of local sources. In the Southern Chesapeake Bay, the secondary volatilization of PAHs from contaminated surfaces during summer with increased temperatures, and the dissolution of PAHs from petroleum contamination in the Elizabeth River serve as local sources that influence concentration gradients and gas exchange of PAHs.

Spatial variations in gas exchange fluxes in Southern Chesapeake Bay were significant and resulted from differences in air-water fugacity gradients between sites. However, temporal variation in gas exchange fluxes are due to seasonal changes in water temperatures, vapor concentrations, and variations in windspeeds.

The sampling interval and integration resolution also impacts net gaseous exchange fluxes determined using the two-film model. Mass transfer coefficients which govern the rate of transfer across the air-water interface increase nonlinearly with windspeed. Therefore, averaging windspeeds results in an under-estimation of gaseous exchange. Henry's law constants which determine the air-water fugacity gradient increase logarithmically with temperature; hence, averaging water temperatures of the interface over a diurnal or tidal cycle may also significantly alter gaseous exchange.

From a sensitivity analysis, integrating fluxes using daily averaged windspeeds resulted in 37, 20, and 13% reductions of the gaseous fluxes calculated for naphthalene, phenanthrene, and pyrene, respectively, relative to fluxes integrated for windspeeds collected every 15 minutes. In addition, a 2 °C change in water temperature at the interface on a diurnal or tidal cycle could change gaseous exchange

for naphthalene, phenanthrene, and pyrene on the order of 4, 25, and 30%, respectively. Vapor concentrations for determining fluxes were collected over periods ranging from 4 to 15 h; furthermore, the magnitude of flux is very large compared to atmospheric vapor loadings. Hence, integrating fluxes over periods shorter than the duration of atmospheric sampling may not be appropriate. Nevertheless, from both error propagation and sensitivity analysis, the variability imposed on the gaseous fluxes determined in this study should be less than 40% for all compounds quantified.

Integrated annual gas exchange fluxes for selected PAHs at the rural Haven Beach/Wolftrap site have been compared to wet and dry depositional fluxes measured at the same site. For volatile PAHs such as fluorene, gas exchange dominates as an air-water transfer process. Gas exchange fluxes are of the same order of magnitude as total wet and dry atmospheric depositional fluxes for the semivolatile PAHs such as phenanthrene, fluoranthene, and pyrene. Particle associated processes (dry deposition and particle washout) dominate net annual air-water fluxes for the least volatile PAHs such as chrysene and benzo[b]fluoranthene.

For sites in Southern Chesapeake Bay at which vapor and dissolved concentrations are close to equilibrium and fluxes occur in both directions (i.e. absorption and volatilization) dependent upon temperature. Nonetheless, it is important to note that although net annual fluxes may be low, exposure levels of organisms on both sides of the air-water interface will be influenced by the larger instantaneous fluxes. Furthermore, gas exchange fluxes determined at Haven Beach support the global distillation or grasshopper theory of contaminant transport

operating on a seasonal time scale due to change in a compound's physical properties with temperature. This scenario is also evident on shorter time scales if one considers other air-water transport processes. Atmospheric vapor and particle washout provide an episodic input of contaminants to the southern Chesapeake Bay during storm events; whereas, any net volatile flux provides an efflux mechanism for a contaminant from the bay. Therefore, at locations or periods where/when the fugacity gradient of a contaminant at the interface supports volatile flux, the grasshopper or global distillation scenario will be important on the duration between storm events.

Finally, the effect of the surface microlayer on gaseous flux has been considered. Measured physical-chemical properties are similar to properties of subsurface water; whereas, the microlayer exhibited an enrichment in dissolved PAHs (Liu, personal communication). Therefore, because of these confounding factors, assessment of the effect of the surface microlayer on gaseous exchange may be questionable at best. It is likely that the microlayer is not an inert layer of added resistance as suggested by Mackay (1982). Rather, due to the deposition of atmospheric particles which are enriched in PAHs relative to estuarine particles, dissolved PAH concentrations in the microlayer may not be in equilibrium with the particle pools. Regardless, hydrologic and meteorologic conditions necessary for the formation of a significant microlayer do not exist for the majority of time in Southern Chesapeake Bay. Therefore, it is anticipated that the microlayer will have little effect on net annual gas exchange fluxes.

The concentrations, distributions, and fluxes of PAHs in the southern Chesapeake Bay region which have been determined in this study illustrate the importance of considering all the major fate and transport processes of a contaminant in the environment before assessing air and water quality, human health and ecosystem risk, and, implementing environmental legislation. Moreover, the processes of cold condensation and secondary volatilization suggest that the actual atmospheric loadings and exposure levels of atmospheric PAHs may be an order of magnitude higher than actual emission levels during periods of warmer temperatures (i.e., summer). Hence, the characterization of sorption and desorption properties for PAHs in both the rural and urban environments to/from aerosol and terrestrial surfaces, merits further research such that risks can be accurately assessed.

References

- Andren, A.W. 1983. Processes determining the flux of PCBs across air/water interfaces. Chapter 8 in Mackay, D., S. Patterson, S.J. Eisenreich, and M.S. Simmons (eds.), *Physical Behavior of PCBs in the Great Lakes*, Ann Arbor Science, 127-140.
- Atlas, E., R. Foster, and C.S. Giam. 1981. Global Transport of Organic Pollutants: Ambient Concentrations in the Remote Marine Atmosphere. *Science*, 211:163-165.
- Baker, J.E., D. Burdige, T.M. Church, G. Cutter, R.M. Dickhut, D.L. Leister, J.M. Ondov, and J.R. Scudlark. 1994. *Chesapeake Bay Atmospheric Deposition Study: Phase II Final Report*. EPA Chesapeake Bay Program Office.

- Bidleman, T.F., G.E. Patton, M.D. Walla, B.T. Hargrave, W.P. Vass, P. Erickson, B. Fowler, V. Scott, and D.J. Gregor. 1989. Toxaphene and other organochlorines in arctic ocean fauna: evidence for atmospheric delivery. *Artic.* 42:307-313.
- Eisenreich, S.J., B.B. Looney, and J.D. Thornton. 1981. Airborne organic contaminants in the Great Lakes ecosystem. *Environ. Sci. Technol.* 15:30-38.
- Foreman, W.T. and T.F. Bidleman. 1990. Semivolatile Organic Compounds in the Ambient Air of Denver, Colorado. *Atmos. Environ.* 24A:2405-2416.
- Gardner, B., C.N. Hewitt, and K.C. Jones. 1995. PAHs in Air Adjacent to Two Inland Water Bodies. *Environ. Sci. Technol.* 29:2405-2413.
- Hoff, R.M., and K.W. Chan. 1987. Measurement of Polycyclic Aromatic Hydrocarbons in Air Along the Niagra River. *Environ. Sci. Technol.* 21:556-561.
- Keller, C.D. and T.F. Bidleman. 1984. Collection of airborne polycyclic aromatic hydrocarbons and other organics with a glass fiber filter-polyurethane foam system. *Atm. Environ.* 18:837-845.
- Ko, F. and J.E. Baker. 1995. Partitioning of hydrophobic organic contaminants to resuspended sediments and plankton in the mesohaline Chesapeake Bay. *Mar. Chem.* 49:171-188.
- Leister, D.L. and J.E. Baker. 1994. Atmospheric Deposition of Organic Contaminants to the Chesapeake Bay. *Atmos Environ.* 28:1499-1520.
- Liu, K. Personal Communication. 1995.
- MacKay, D. 1982. Effects of Surface Films on Air-water Exchange Rates. *J. Great Lakes Res.* 8:299-306.
- McVeety, B.D. and R.A. Hites. 1988. Atmospheric Deposition of Polycyclic Aromatic Hydrocarbons to Water Surfaces: A Mass Balance Approach. *Atmos. Environ.* 22:511-536.
- Schreitmuller, J. and K. Ballschmiter. 1995. Air-water Equilibrium of Hexachlorocyclohexanes and Chloromethoxybenzenes in the North and South Atlantic. *Environ. Sci. Technol.* 29:207-215.

Appendix A: Measurement of Acenaphthylene Aqueous Solubility

Acenaphthylene aqueous solubilities were determined at 10, 15, 25, and 40 °C in Milli-Q purified water using a generator column method (Dickhut *et al.*, 1986). At each temperature 5 replicate measurements were made by collecting \approx 10 ml of water at 1 ml/min into a 22 ml vial containing \approx 10 ml of methanol. All measurements were made on a mass basis. The vials were capped and stored in the refrigerator at 4°C until the study was completed (< 12 hrs.) upon which time acenaphthylene concentrations were determined by UV absorbance at 320 nm using a standard curve with acenaphthylene standards also made in 50:50 methanol:water.

Acenaphthylene solubility in water:

40°C	27.966 \pm 0.237 mg/l
25°C	16.355 \pm 0.103 mg/l
15°C	11.401 \pm 0.055 mg/l
10°C	9.476 \pm 0.020 mg/l

Measured acenaphthylene concentrations were converted to mole fraction solubilities and a relationship determined as a function of the natural log of mole fraction solubility versus temperature:

$$X = (7.826 * e^{0.03609T}) * 10^{-7} \quad r^2 = 1.00$$

where X is the mole fraction solubility and T is temperature °C.

Reference:

Dickhut, R.M., A.W. Andren, and D.E. Armstrong. 1986. Aqueous Solubilities of Six Polychlorinated Biphenyl Congeners at Four Temperatures. *Environ. Sci. Technol.* 20:807-810.

Appendix B: Estimation of Subcooled-Liquid Vapor Pressures of Chrysene as a Function of Temperature

To estimate the vapor pressure of chrysene, subcooled-liquid vapor pressures of other PAHs were correlated to their subcooled-liquid solubilities and the resulting correlation was applied using the subcooled liquid solubility of chrysene.

Log P_{sc1} (vapor pressure-subcooled liquid) was plotted versus the log X_{sc1} (mole fraction solubility-subcooled liquid, in water) for naphthalene, acenaphthylene, acenaphthene, fluorene, phenanthrene, anthracene, fluoranthene, pyrene, benzo(a)anthracene. Linear relationships were established as a function of temperature ($n=6$) with r^2 ranging from .89 to .99. Log X_{sc1} values for chrysene were used to predict chrysene's subcooled liquid vapor pressure at these temperatures (5 °C to 30 °C).

The natural log of chrysene's vapor pressure was plotted versus inverse temperature ($1/T$, °K) resulting in the following predictive equation for chrysene P_{sc1} as a function of temperature:

$$P_{sc1} = e^{((-7086.28/T) + 8.7188)} ; r^2 = .99$$

where P_{sc1} is in atm and T (K).

Appendix C: Setschenow Constants and Correlations for PAHs

<u>PAH</u>		<u>Study Cited</u>		
naphthalene		0.213 ^{2*}		0.62 ⁴ 0.3031 ⁵
acenaphthene	0.238 ^{1*}			
fluorene		0.267 ^{2*}		
phenanthrene		0.275 ²	0.278 ^{3*}	0.24 ⁴ 0.3871 ⁵
anthracene		0.238 ²	0.274 ^{3*}	0.44 ⁴
fluoranthene		0.339 ^{2*}		
pyrene	0.319 ^{1*}	0.286 ²		0.74 ⁴
chrysene		0.336 ^{2*}		
benzo(a)anthracene		0.354 ^{2*}	n/a ³	
benzo(a)pyrene			0.1678 ³	
benzo(e)pyrene				0.98 ⁴

Predictive Correlation

$K_s = 1.419 \cdot 10^{-3} \cdot MW + .0286$ ($r^2 = .95$); where MW is the molecular weight of the PAH

- ¹ Rossi, S.J. and W.H. Thomas, 1981. Solubility Behavior of Three Aromatic Hydrocarbons in Distilled Water and Natural Seawater. *Environ. Sci. Technol.* 15:715-716.
- ² May, W.E., S.P. Wasik, and D.H. Freeman. 1978. Determination of the solubility behavior of some polycyclic aromatic hydrocarbons in water. *Anal. Chem.* 50:997-1000.
- ³ Whitehouse, B.G. 1985. Observation of abnormal solubility behavior of aromatic hydrocarbons in seawater. *Mar. Chem.* 17:277-284.
- ⁴ Schwartz, F.P. 1977. Determination of temperature dependence of solubilities of polycyclic aromatic hydrocarbons in aqueous solutions by a fluorescence method. *J. Chem. Eng. Data.* 22:273-276.
- ⁵ Eganhouse, R.P. and J.A. Calder. 1976. The solubility of medium molecular weight aromatic hydrocarbons and the effects of hydrocarbon co-solutes and salinity. *Geochim. Cosmochim. Acta.* 40:555-561.

* selected values used in correlation

**Appendix D: Solubility, Vapor Pressure, and Henry Law Constant Correlations†
as a Function of Temperature for Selected PAHs**

compound	property	predictive equation
naphthalene	sol.	$(1.8 * e^{0.038*T}) * 10^{-6}$
	vap.	$(9.869 * 10^{-6}) * e^{(2.303*((-3960)/(T+273.15))+14.3)}$
	vap.	$(1.316 * 10^{-3}) * e^{(2.303*(10.1-(2908/(236.5+T))))}$
acenaphthene	sol.	$(1.33 * e^{0.048*T}) * 10^{-7}$
	vap.	$(9.869 * 10^{-6}) * e^{(2.303*((-4535)/(T+273.15)) + 14.7)}$
acenaphthylene	sol.	$(7.826 * e^{0.03609*T}) * 10^{-7}$
	vap.	$(9.869 * 10^{-6}) * e^{(2.303*((-3822)/(T+273.15)) + 12.8)}$
fluorene	sol.	$(5.3 * e^{0.051*T}) * 10^{-8}$
	vap.	$(9.869 * 10^{-6}) * e^{(2.303*((-4616)/(T + 273.15)) + 14.4)}$
	vap.	$(1.316 * 10^{-3}) * e^{(2.303*(11.6 - (4269/(262.7 + T))))}$
phenanthrene	sol.	$(2.86 * e^{0.054*T}) * 10^{-8}$
	vap.	$(9.869 * 10^{-6}) * e^{(2.303*((-4963)/(T + 273.15)) + 14.9)}$
anthracene	sol.	$(9.14 * e^{0.067*T}) * 10^{-10}$
	vap.	$(9.869 * 10^{-6}) * e^{(2.303*((-4792)/(T + 273.15)) + 13.0)}$
fluoranthene	sol.	$(71.7 - 1.7*T + 0.248*T^2) * 10^{-10}$
	vap.	$(9.869 * 10^{-6}) * e^{(2.303*((-4416)/(T + 273.15)) + 11.9)}$
	H	$10^{((-2980.65/T) + 9.9509)}$ T is K, H Pa*m ³ /mol
pyrene	sol.	$(296 - 23.9*T + 0.586*T^2) * 10^{-10}$
	vap.	$(9.869 * 10^{-6}) * e^{(2.303*((-4761)/(T + 273.15)) + 12.7)}$
chrysene	sol.	$(53.9 - 1.01*T + 0.183*T^2) * 10^{-12}$
	vap.	no data available
	P _{SCL,est}	$\exp((-7086.28/T)+8.7188)$
benzo(a)anthracene	sol.	$(44.5 - 3.05*T + 0.164*T^2) * 10^{-11}$
	vap.	$(9.869 * 10^{-6}) * e^{(2.303*((-4247)/(T + 273.15)) + 9.68)}$

benzo(b)fluoranthene	sol.	no data available
	vap.	no data available
	H	$10^{((-2366.83/T) + 6.7613)}$ T is K, H Pa*m ³ /mol
benzo(k)fluoranthene	sol.	no data available
	vap.	no data available
	H	$10^{((-2541.38/T) + 7.2974)}$ T is K, H Pa*m ³ /mol
benzo(e)pyrene	sol.	$(184 + 2.68*T + 0.244*T^2) * 10^{-12}$
	vap.	no data available
benzo(a)pyrene	sol.	$(60.9 - 3.84*T + 0.24*T^2) * 10^{-12}$
	vap.	no data available
	H	$10^{((-2050.99/T) + 5.5444)}$ T is K, H Pa*m ³ /mol
indeno(1,2,3-cd)pyrene	sol.	no data available
	vap.	no data available
	H	$10^{((-1580.47/T) + 3.8497)}$ T is K, H Pa*m ³ /mol
benzo(g,h,i)perylene	sol.	no data available
	vap.	no data available
	H	$10^{((-1383.93/T) + 3.1672)}$ T is K, H Pa*m ³ /mol
dibenzo(a,h)anthracene	sol.	no data available
	vap.	no data available

Units of measurement are: Temperature, °C; Solubility, mole fraction; and Vapor Pressure, atm, unless otherwise specified.

References:

This study (see Appendices A and B).

May, W.E., S.P. Wasik and D.H. Freeman. 1978. Determination of the Solubility Behavior of Some Polycyclic Aromatic Hydrocarbons in Water. *Anal. Chem.* 50:997-1000.

May, W.E. S.P. Wasik, M.M. Miller, Y.B. Tewari, J.M. Brown-Thomas, R.N. Goldberg. 1983. Solution thermodynamics of some slightly soluble hydrocarbons in water. *J. Chem. Eng. Data.* 28:197-200.

- Sonnefeld, W.J., W.H. Zoller, and W.E. May. 1983. Dynamic coupled-column liquid chromatographic determination of ambient vapor pressures of polynuclear aromatic hydrocarbons. *Anal. Chem.* 55:275:280.
- Ten Hulscher, Th.E.M., L.E. Van Der Velde, and W.A. Bruggeman. 1992. Temperature dependence of henry's law constants for selected chlorobenzenes, polychlorinated biphenyls, and polycyclic aromatic hydrocarbons. *Environ. Tox. Chem.* 11:1595-1603.

Appendix E: Auxiliary Atmospheric Data

TABLE E-1: PAH Atmospheric Vapor Concentrations measured at Haven Beach, Mathews Co., VA. for paired Wolfrap water samples

Haven Beach Site

PAH Atmospheric Vapor Concentrations (pg/m³)

PAH	10-07-93	01-11-94	01-31-94	03-24-94	04-29-94	06-30-94	07-28-94	08-25-94	09-26-94
naphthalene	350.31	2886.31	15723.03	1542.75	105.58	136.79	428.82	154.69	676.71
acenaphthylene	n.d.	1578.70	2245.85	28.57	n.d.	10.48	77.41	10.26	44.25
acenaphthene	221.07	657.18	1554.36	170.77	71.40	116.11	335.78	142.20	141.30
fluorene	2398.91	2446.07	3052.15	663.91	482.43	255.82	729.39	224.33	782.74
phenanthrene	5617.75	3759.03	6900.56	1729.54	3395.83	2748.83	4784.67	1291.99	1076.28
anthracene	n.d.	n.d.	292.84	n.d.	n.d.	69.31	83.91	21.54	n.q.
fluoranthene	651.16	588.62	599.50	354.95	535.75	430.20	577.14	167.59	97.98
pyrene	942.49	449.17	396.30	339.36	967.82	650.56	902.11	308.32	160.98
benzo(a)anthracene	n.d.	10.64	n.d.	n.d.	n.d.	n.d.	n.d.	n.d.	n.q.
chrysene	74.04	n.d.	22.90	22.77	32.85	27.90	33.76	13.27	7.87
benzo(b)fluoranthene	17.18	4.24	1.20	2.20	2.13	n.d.	13.64	3.23	2.49
benzo(k)fluoranthene	n.d.	n.d.	1.0	1.16	n.d.	n.d.	n.d.	n.d.	n.d.
benzo(e)pyrene	40.57	2.46	n.d.	1.34	1.53	n.d.	9.97	7.37	1.41
benzo(a)pyrene	n.d.	n.d.	n.d.	.61	n.d.	n.d.	6.36	1.38	n.q.
indeno(1,2,3-cd)pyrene	n.d.	n.d.	n.d.	n.d.	n.d.	n.d.	n.d.	n.d.	n.d.
dibenzo(a,h)anthracene	n.d.	n.d.	n.d.	n.d.	n.d.	n.d.	n.d.	.60	n.d.
benzo(g,h,i)perylene	10.20	n.d.	n.d.	n.d.	n.d.	n.d.	32.31	19.80	n.d.

PAH	10-28-94	12-01-94	01-13-95	01-27-95	02-23-95	04-06-95	05-01-95	05-22-95
naphthalene	347.86	438.03	244.91	5026.16	2371.32	2194.65	229.85	69.33
acenaphthylene	50.41	8.05	25.15	465.09	186.96	64.57	n.d.	6.20
acenaphthene	105.31	38.83	187.92	546.03	733.90	553.03	138.32	102.34
fluorene	942.47	961.19	1277.53	1919.33	1813.15	1038.75	487.27	390.60
phenanthrene	1936.58	523.98	2329.37	2199.90	1843.46	901.10	516.14	1083.27
anthracene	n.d.	n.d.	n.d.	n.d.	n.d.	n.d.	n.d.	36.96
fluoranthene	433.65	114.18	359.29	323.17	507.26	190.40	116.97	412.89
pyrene	519.49	62.88	417.78	169.11	198.26	100.65	82.25	307.88
benzo(a)anthracene	13.20	6.56	3.30	n.d.	n.d.	n.d.	n.d.	n.d.
chrysene	110.02	28.86	34.48	7.15	16.89	16.44	8.91	19.96
benzo(b)fluoranthene	9.05	9.47	3.36	n.d.	.93	1.70	1.45	1.40
benzo(k)fluoranthene	4.62	7.91	2.81	n.d.	n.d.	.62	.80	n.d.
benzo(e)pyrene	5.37	6.18	2.58	n.d.	.58	1.02	.93	.75
benzo(a)pyrene	n.d.	n.d.	n.d.	n.d.	n.d.	n.d.	n.d.	n.d.
indeno(1,2,3-cd)pyrene	n.d.	n.d.	n.d.	n.d.	n.d.	n.d.	n.d.	n.d.
dibenzo(a,h)anthracene	n.d.	n.d.	n.d.	n.d.	n.d.	n.d.	n.d.	n.d.
benzo(g,h,i)perylene	5.62	n.d.	1.84	n.d.	n.d.	.80	n.d.	n.d.

TABLE E-2: PAH Atmospheric Vapor Concentrations measured at the York River Site, VIMS oyster pier, Gloucester Pt., VA. for paired York River water samples

York River Site

PAH Atmospheric Vapor Concentrations (pg/m³)

PAH	08-12-94	10-06-94	12-06-94	12-07-94	12-09-94	02-10-95	04-12-95	05-24-95
naphthalene	692.69	6871.14	1446.23	1235.37	1680.76	3734.84	427.39	3405.77
acenaphthylene	268.26	2634.84	410.45	428.04	1041.88	299.01	121.69	335.84
acenaphthene	4565.78	5628.54	3021.87	4696.49	2289.27	6426.86	4720.40	12804.33
fluorene	4764.90	9638.81	15377.24	9000.11	3885.72	5714.64	6557.20	16420.99
phenanthrene	65243.00	21219.87	28183.18	21384.75	5782.73	5925.09	16133.94	31113.35
anthracene	3234.85	1153.42	2424.90	932.55	317.48	151.80	267.26	595.91
fluoranthene	8056.13	3992.61	5338.88	5795.52	1438.16	1488.32	2189.64	5019.09
pyrene	3067.21	1826.02	2631.84	2350.18	978.73	506.78	785.96	1467.32
benzo(a)anthracene	48.36	30.14	182.93	38.96	12.89	n.d.	8.00	18.34
chrysene	157.35	75.03	364.72	177.40	71.57	47.42	64.50	97.85
benzo(b)fluoranthene	67.52	15.15	63.36	12.07	4.42	3.63	7.76	6.97
benzo(k)fluoranthene	n.d.	n.d.	71.35	n.d.	n.d.	n.d.	4.86	3.29
benzo(e)pyrene	25.21	19.83	47.96	7.89	2.74	1.41	5.06	4.34
benzo(a)pyrene	8.68	11.30	14.57	3.04	n.d.	n.d.	2.88	n.d.
indeno(1,2,3-cd)pyrene	4.94	n.d.	n.d.	n.d.	n.d.	n.d.	4.85	n.d.
dibenzo(a,h)anthracene	n.d.	n.d.	2.81	n.d.	n.d.	n.d.	.95	n.d.
benzo(g,h,i)perylene	5.00	n.d.	6.44	12.11	1.39	1.10	5.27	n.d.

TABLE E-3: PAH Atmospheric Vapor concentrations measured at Haven Beach, Mathews Co., VA. for paired water samples taken in Chesapeake Bay at Haven Beach Site

Haven Beach Site

PAH Atmospheric Vapor Concentrations (pg/m³)

PAH	05-10-94	05-22-94	06-26-94	06-28-94	06-29-94	11-05-94	11-08-94
naphthalene	577.79	828.90	147.17	589.01	235.25	697.54	888.19
acenaphthylene	132.93	22.27	66.88	125.17	102.08	70.94	191.85
acenaphthene	124.12	253.84	192.50	244.60	233.00	394.57	358.79
fluorene	731.33	671.62	439.96	725.87	376.65	799.66	1007.10
phenanthrene	1914.11	1718.83	3711.71	4227.41	3688.97	2300.57	2518.09
anthracene	n.d.	n.d.	n.d.	n.d.	54.50	123.35	n.d.
fluoranthene	353.22	305.98	416.55	630.83	492.20	432.38	363.83
pyrene	451.54	277.54	512.98	984.84	556.21	419.17	411.92
benzo(a)anthracene	n.d.	n.d.	n.d.	n.d.	n.d.	9.69	9.07
chrysene	25.69	12.80	42.71	41.60	39.90	56.78	74.57
benzo(b)fluoranthene	4.36	1.34	3.32	n.d.	5.30	11.95	13.01
benzo(k)fluoranthene	n.d.	.62	n.d.	n.d.	1.47	n.d.	n.d.
benzo(e)pyrene	1.89	1.01	6.76	n.d.	4.56	106.62	13.53
benzo(a)pyrene	n.d.	n.d.	1.16	n.d.	1.53	4.66	3.64
indeno(1,2,3-cd)pyrene	n.d.	n.d.	n.d.	n.d.	n.d.	n.d.	n.d.
dibenzo(a,h)anthracene	n.d.	n.d.	n.d.	n.d.	3.40	n.d.	n.d.
benzo(g,h,i)perylene	n.d.	n.d.	3.02	n.d.	8.58	15.00	14.17

TABLE E-4: PAH Atmospheric Vapor Concentrations measured at the Elizabeth River, Portsmouth Coast Guard Station, Portsmouth, VA. for paired Elizabeth River water samples

Elizabeth River Site

PAH Atmospheric Vapor Concentrations (pg/m³)

PAH	07-15-94	09-08-94	11-12-94	01-09-95	03-11-95	05-04-95
naphthalene	434.05	1462.30	3631.25	8945.10	3389.92	5587.28
acenaphthylene	n.q.	118.05	419.00	6254.54	411.18	1168.81
acenaphthene	n.q.	3542.53	5867.98	4318.33	1738.77	13663.95
fluorene	n.q.	5056.24	8333.31	5741.74	2788.34	11204.46
phenanthrene	n.q.	17823.32	12894.94	11515.13	6013.35	25225.86
anthracene	n.q.	869.63	281.96	750.63	124.01	1042.99
fluoranthene	n.q.	4576.92	1794.26	1607.14	677.71	3901.73
pyrene	n.q.	2524.15	1209.90	1629.53	500.74	2018.29
benzo(a)anthracene	284.27	29.25	10.96	12.94	n.d.	35.48
chrysene	1812.49	141.08	68.78	42.42	15.07	91.78
benzo(b)fluoranthene	10.79	19.43	5.90	6.92	1.77	10.47
benzo(k)fluoranthene	n.d.	17.81	2.90	4.53	1.74	6.60
benzo(e)pyrene	n.d.	15.73	5.63	5.76	n.d.	5.67
benzo(a)pyrene	66.95	9.05	n.d.	3.71	n.d.	4.17
indeno(1,2,3-cd)pyrene	6.84	n.d.	n.d.	4.72	n.d.	6.62
dibenzo(a,h)anthracene	n.d.	n.d.	n.d.	n.d.	n.d.	9.77
benzo(g,h,i)perylene	10.77	n.d.	7.57	8.93	n.d.	10.07

TABLE E-5: PAH Atmospheric Vapor concentrations measured at the Hampton site, Grandview Pier and Dandy Point, Hampton, VA. for paired water samples taken in Chesapeake Bay at the Hampton Site

Hampton Site

PAH Atmospheric Vapor Concentrations (pg/m³)

PAH	07-15-94	09-09-94	11-12-94	01-09-95	03-11-95	05-04-95
naphthalene	1994.84	2239.18	536.38	1153.47	6779.01	6501.86
acenaphthylene	207.20	504.60	17.53	715.02	550.80	281.47
acenaphthene	15615.14	35837.59	328.27	1571.08	12314.70	40088.44
fluorene	29218.03	24670.86	1738.09	2417.97	4256.63	40581.78
phenanthrene	124573.46	80242.93	2456.33	3598.42	10770.95	47281.54
anthracene	6939.02	2526.69	n.d.	197.56	n.d.	1289.49
fluoranthene	12854.70	4080.84	800.69	834.53	2301.69	8750.36
pyrene	5559.62	1678.95	1131.33	567.93	952.30	2078.87
benzo(a)anthracene	24.99	10.37	n.d.	7.48	n.d.	17.37
chrysene	144.95	49.05	49.90	41.53	198.41	110.93
benzo(b)fluoranthene	16.31	16.60	2.50	2.33	14.39	14.90
benzo(k)fluoranthene	n.d.	n.d.	1.58	n.d.	n.d.	7.77
benzo(e)pyrene	15.56	6.76	1.65	1.45	24.06	10.49
benzo(a)pyrene	1.55	n.d.	n.d.	n.d.	n.d.	4.69
indeno(1,2,3-cd)pyrene	n.d.	n.d.	n.d.	n.d.	n.d.	8.55
dibenzo(a,h)anthracene	n.d.	n.d.	n.d.	n.d.	n.d.	n.d.
benzo(g,h,i)perylene	n.d.	n.d.	1.23	.72	4.96	9.16

TABLE E-6: PAH Atmospheric particulate concentrations measured at Haven Beach, Mathews Co., VA. for paired Wolfrap water samples

Haven Beach Site

PAH Atmospheric Particulate Concentrations (pg/m³)

PAH	10-07-93	01-11-94	01-31-94	03-24-94	04-29-94	06-30-94	07-28-94	08-25-94	09-26-94
naphthalene	768.696	N.Q.	81.959	N.Q.	N.Q.	N.Q.	N.Q.	50.040	N.Q.
acenaphthylene	3.543	3.601	5.721	3.661	2.173	.940	.812	.873	1.099
acenaphthene	5.261	5.479	7.132	n.d.	2.689	3.665	1.390	1.823	1.859
fluorene	7.279	8.361	8.990	6.807	3.358	2.520	2.436	2.281	9.816
phenanthrene	32.437	108.962	154.465	50.010	28.969	16.787	17.870	17.097	48.746
anthracene	3.089	6.593	11.264	4.416	3.121	1.101	.990	.897	n.d.
fluoranthene	13.244	136.943	227.957	37.798	26.550	16.545	12.081	14.457	20.149
pyrene	17.210	108.713	199.634	37.086	24.577	12.086	14.003	16.662	25.512
benzo(a)anthracene	12.815	39.680	108.298	21.455	7.818	3.055	n.d.	2.653	n.d.
chrysene	12.946	138.436	258.172	86.925	19.842	8.801	7.491	11.349	33.383
benzo(b)fluoranthene	15.293	118.607	282.670	72.587	19.305	6.748	7.901	10.434	63.298
benzo(k)fluoranthene	10.571	122.957	252.678	45.599	13.927	4.109	4.636	4.598	n.d.
benzo(e)pyrene	10.413	106.646	229.789	69.987	16.523	7.023	8.826	8.345	35.634
benzo(a)pyrene	6.477	48.973	170.597	21.270	10.353	3.117	1.822	2.883	4.693
indeno(1,2,3-cd)pyrene	n.d.	85.299	205.855	25.445	11.243	4.319	3.398	5.657	7.004
dibenzo(a,h)anthracene	8.099	21.744	31.646	6.850	1.942	.973	.726	1.739	2.057
benzo(g,h,i)perylene	12.488	97.422	223.031	65.399	14.442	5.510	6.661	5.848	11.527

PAH	10-28-94	12-01-94	01-13-95	01-27-95	02-23-95	04-06-95	05-01-95	05-22-95
naphthalene	73.824	N.Q.	N.Q.	47.736	46.492	N.Q.	N.Q.	N.Q.
acenaphthylene	3.999	n.d.	.541	6.909	8.283	2.278	n.d.	2.639
acenaphthene	3.952	n.d.	.891	n.d.	n.d.	N.Q.	N.Q.	N.Q.
fluorene	15.901	3.750	N.Q.	9.890	12.044	4.768	N.Q.	3.558
phenanthrene	205.168	59.855	10.499	124.374	173.210	48.086	N.Q.	31.549
anthracene	7.473	4.305	n.d.	7.309	8.167	n.d.	n.d.	2.604
fluoranthene	152.213	90.511	7.555	202.873	218.824	96.263	2.335	49.257
pyrene	149.591	67.363	7.530	166.673	153.065	60.623	1.512	36.161
benzo(a)anthracene	56.979	31.850	n.d.	84.251	53.118	13.286	1.627	12.328
chrysene	413.691	72.050	11.572	201.870	156.003	77.419	2.211	37.856
benzo(b)fluoranthene	322.224	116.755	8.993	306.389	190.353	102.188	1.962	38.805
benzo(k)fluoranthene	222.406	87.332	6.237	265.667	151.233	72.411	1.390	27.149
benzo(e)pyrene	254.591	81.282	6.313	213.795	128.535	71.228	1.266	26.320
benzo(a)pyrene	81.514	55.222	3.113	174.100	100.862	26.738	.833	20.766
indeno(1,2,3-cd)pyrene	116.552	83.171	5.766	229.410	127.890	48.807	n.d.	21.473
dibenzo(a,h)anthracene	16.395	11.719	.838	28.642	16.986	3.975	n.d.	3.197
benzo(g,h,i)perylene	135.948	79.027	6.818	220.831	131.981	56.387	n.d.	24.121

TABLE E-7: PAH Atmospheric particulate Concentrations measured at the York River, VIMS, Gloucester Pt., VA. for paired York River water samples

York River Site

PAH Atmospheric Particulate Concentrations (pg/m³)

PAH	08-12-94	10-06-94	12-06-94	12-07-94	12-09-94	02-10-95	04-12-95	05-24-95
naphthalene	30.539	168.798	77.159	N.Q.	66.486	N.Q.	N.Q.	210.693
acenaphthylene	2.707	12.960	23.545	5.287	6.202	4.109	1.442	20.369
acenaphthene	2.344	20.599	16.506	5.821	17.899	2.528	N.Q.	N.Q.
fluorene	4.001	33.787	13.905	4.910	7.030	4.495	N.Q.	15.278
phenanthrene	29.484	282.348	108.587	51.958	86.516	65.786	19.892	82.177
anthracene	3.115	19.191	13.905	3.334	6.543	4.162	1.063	6.277
fluoranthene	32.765	203.452	98.235	55.919	135.613	119.632	24.635	105.852
pyrene	20.058	157.649	94.720	43.647	126.910	86.654	15.626	109.704
benzo(a)anthracene	6.518	75.405	62.300	20.143	56.771	26.381	5.199	n.d.
chrysene	18.034	166.363	136.365	53.127	156.929	87.392	14.094	79.359
benzo(b)fluoranthene	17.752	292.194	386.033	80.040	165.008	116.123	13.453	51.104
benzo(k)fluoranthene	12.714	221.273	332.469	66.081	131.444	85.991	9.678	29.249
benzo(e)pyrene	17.795	234.671	358.517	64.860	133.200	77.324	9.171	60.762
benzo(a)pyrene	7.353	125.562	138.628	37.374	89.722	41.656	6.098	22.264
indeno(1,2,3-cd)pyrene	20.425	196.521	584.253	75.998	139.859	88.177	7.172	24.444
dibenzo(a,h)anthracene	3.407	25.043	36.655	6.635	14.765	9.574	1.682	n.d.
benzo(g,h,i)perylene	29.530	261.975	746.305	90.836	186.523	88.744	8.638	48.817

TABLE E-8: PAH Atmospheric particulate concentrations measured at Haven Beach, Mathews Co., VA. for paired Haven Beach Water Samples.

Haven Beach Site

PAH Atmospheric Particulate Concentrations (pg/m³)

PAH	05-10-94	05-22-94	06-26-94	06-28-94	06-29-94	11-05-94	11-08-94
naphthalene	36.525	N.Q.	44.829	N.Q.	N.Q.	N.Q.	45.667
acenaphthylene	2.337	1.676	.871	1.297	1.019	1.161	5.401
acenaphthene	n.d.	1.581	2.443	2.624	1.341	1.386	2.183
fluorene	4.757	3.302	2.340	3.339	1.548	3.446	4.684
phenanthrene	42.833	32.010	14.953	28.781	13.196	24.101	42.327
anthracene	4.703	2.802	1.237	2.821	1.173	1.559	2.432
fluoranthene	47.474	43.728	11.406	25.359	13.055	16.101	51.709
pyrene	40.760	35.818	9.524	22.778	9.644	13.809	76.827
benzo(a)anthracene	17.539	13.286	3.207	7.948	3.939	6.672	52.259
chrysene	46.751	36.720	8.227	16.748	9.475	19.495	122.188
benzo(b)fluoranthene	83.156	35.105	7.937	14.150	9.124	30.932	64.173
benzo(k)fluoranthene	69.140	24.431	5.506	10.290	6.324	23.166	36.751
benzo(e)pyrene	77.831	28.713	7.703	13.321	8.852	22.596	61.696
benzo(a)pyrene	39.360	15.296	3.595	8.134	4.451	8.216	23.995
indeno(1,2,3-cd)pyrene	74.710	22.485	5.415	9.151	7.155	18.009	43.548
dibenzo(a,h)anthracene	10.876	3.980	1.228	1.881	1.416	3.060	5.406
benzo(g,h,i)perylene	81.975	28.505	6.813	11.433	8.606	17.821	55.657

TABLE E-9: PAH Atmospheric particulate concentrations measured at the Elizabeth River, Portsmouth Coast Guard Station, Portsmouth, VA. for paired Elizabeth River water samples

Elizabeth River Site

PAH Atmospheric Particulate Concentrations (pg/m³)

PAH	07-15-94	09-08-94	11-12-94	01-09-95	03-11-95	05-04-95
naphthalene	154.054	81.917	N.Q.	232.285	N.Q.	N.Q.
acenaphthylene	4.168	6.703	5.481	38.747	5.173	7.532
acenaphthene	6.499	n.d.	5.170	78.300	7.440	9.110
fluorene	7.020	11.013	10.203	20.671	8.870	14.098
phenanthrene	43.053	96.969	91.788	302.056	169.838	130.250
anthracene	3.340	14.045	5.202	36.721	8.170	8.561
fluoranthene	20.530	96.673	125.574	533.524	205.687	229.606
pyrene	16.898	66.061	96.971	631.710	142.532	184.695
benzo(a)anthracene	6.263	25.930	29.994	200.210	52.584	59.183
chrysene	21.719	74.070	82.156	864.645	136.250	350.255
benzo(b)fluoranthene	17.122	76.709	87.384	433.885	155.686	150.210
benzo(k)fluoranthene	8.885	59.517	71.376	332.971	117.906	91.493
benzo(e)pyrene	13.190	55.687	65.189	387.036	107.813	122.232
benzo(a)pyrene	6.539	33.368	48.235	271.294	81.861	60.028
indeno(1,2,3-cd)pyrene	10.645	48.811	68.601	365.048	116.611	88.778
dibenzo(a,h)anthracene	n.d.	7.321	10.669	43.623	13.676	29.596
benzo(g,h,i)perylene	18.206	54.589	89.452	513.626	140.102	143.076

TABLE E-10: PAH Atmospheric particulate concentrations measured at the Hampton site, Grandview and Dandy Point, Hampton, VA for paired Hampton water samples.

Hampton Site

PAH Atmospheric Particulate Concentrations (pg/m³)

PAH	07-15-94	09-09-94	11-12-94	01-09-95	03-11-95	05-04-95
naphthalene	93.970	59.897	N.Q.	94.681	53.01	N.Q.
acenaphthylene	3.491	3.737	6.144	11.432	6.319	1.262
acenaphthene	6.249	11.877	5.102	18.235	5.061	N.Q.
fluorene	11.708	21.773	11.029	15.120	7.845	N.Q.
phenanthrene	70.994	155.231	81.170	167.214	111.240	16.709
anthracene	5.270	15.271	3.569	11.042	9.082	.826
fluoranthene	57.130	89.400	138.903	214.940	156.416	12.088
pyrene	34.809	47.818	135.126	146.144	105.690	10.363
benzo(a)anthracene	10.268	13.121	21.559	78.023	47.569	n.d.
chrysene	31.083	43.043	79.058	192.490	121.683	11.097
benzo(b)fluoranthene	23.428	53.833	72.988	259.754	169.004	10.918
benzo(k)fluoranthene	16.209	41.084	44.208	208.361	119.757	7.865
benzo(e)pyrene	16.592	38.778	52.897	171.040	106.809	7.827
benzo(a)pyrene	9.910	19.241	32.684	131.059	77.120	4.953
indeno(1,2,3-cd)pyrene	10.125	20.923	38.230	193.042	101.563	7.393
dibenzo(a,h)anthracene	n.d.	n.d.	6.285	29.495	14.160	1.985
benzo(g,h,i)perylene	16.677	20.750	46.531	183.864	113.417	10.486

Appendix F: Auxiliary Surface Water Data

TABLE F-1: PAH Dissolved Water Concentrations measured at the Wolftrap site, Chesapeake Bay

WOLFTRAP SITE

PAH Dissolved Water Concentrations (ng/l)

PAH	10-07-93	01-11-94	01-31-94	03-24-94	04-29-94	06-30-94	07-28-94	08-25-94	09-26-94
naphthalene	13.7768	21.6447	27.3563	24.0362	15.1764	10.1626	9.7054	10.4806	10.8403
acenaphthylene	n.d.	.3039	.3416	.8017	.1829	.1771	.2207	.1933	.1541
acenaphthene	.7452	.5816	.7294	1.1220	.6779	.7030	.7767	.7209	.5444
fluorene	2.2459	2.3994	2.9055	3.8991	3.2721	3.8688	4.0107	3.2615	2.0521
phenanthrene	4.3059	3.9165	4.1167	5.4140	4.0458	5.3993	6.0043	4.6786	3.0868
anthracene	n.d.	n.d.	n.d.	.1437	.1431	.1806	.1994	.1536	n.d.
fluoranthene	.2254	.3785	.3289	.3312	.1548	.3044	.3098	.2074	.2611
pyrene	.1734	.1937	.1544	.2284	.1932	.3345	.3813	.2740	.2787
benzo(a)anthracene	.0085	n.d.	n.d.	.0419	.0302	.0502	.0509	n.d.	n.d.
chrysene	.0636	.0636	.0502	.0424	.0306	.0437	.0443	.0564	.0776
benzo(b)fluoranthene	n.d.	n.d.	.0058	.0442	.0302	.0265	.0183	.0280	.0464
benzo(k)fluoranthene	n.d.	n.d.	n.d.	n.d.	n.d.	.0086	.0093	n.d.	.0305
benzo(e)pyrene	.0209	n.d.	.0064	.0219	.0147	.0192	.0171	.0173	.0342
benzo(a)pyrene	.0054	n.d.	n.d.	.0091	n.d.	.0123	.0116	n.d.	.0085
indeno(1,2,3-cd)pyrene	n.d.	n.d.	n.d.	n.d.	n.d.	n.d.	n.d.	n.d.	.0117
dibenzo(a,h)anthracene	n.d.	n.d.	n.d.	n.d.	n.d.	n.d.	n.d.	n.d.	.0157
benzo(g,h,i)perylene	.0121	.0092	n.d.	n.d.	n.d.	n.d.	n.d.	n.d.	.0188

PAH	10-28-94	12-01-94	01-13-95	01-27-95	02-23-95	04-06-95	05-01-95	05-22-95
naphthalene	13.4932	21.2167	24.2637	17.6734	17.3987	14.4477	13.4637	12.2808
acenaphthylene	.2769	.4904	.4262	.2073	.1844	.2381	.0826	.3812
acenaphthene	.5110	.5549	1.1126	.6031	.4456	.5814	.2246	.7424
fluorene	1.7353	2.0522	2.4618	2.4901	1.1709	1.9789	.6159	3.2159
phenanthrene	3.0177	2.9898	4.3376	3.8948	2.0108	3.4184	1.1071	4.5333
anthracene	.1088	.1131	.0969	.0988	.0460	.0635	.0313	.1194
fluoranthene	.1830	.2694	.7087	.2450	.2464	.2145	.2175	.1663
pyrene	.2055	.2436	.3058	.2130	.1166	.3322	.1104	.1597
benzo(a)anthracene	n.d.	n.d.	n.d.	n.d.	n.d.	n.d.	n.d.	n.d.
chrysene	.0283	.0372	.0809	.0232	.0387	.0346	n.d.	.0215
benzo(b)fluoranthene	.0099	n.d.	n.d.	.0119	.0143	.0488	.0193	.0052
benzo(k)fluoranthene	.0077	n.d.	n.d.	n.d.	n.d.	n.d.	n.d.	n.d.
benzo(e)pyrene	.0099	.0119	n.d.	.0193	.0114	.0526	.0128	.0052
benzo(a)pyrene	n.d.	n.d.	n.d.	.0160	.0048	.0470	n.d.	n.d.
indeno(1,2,3-cd)pyrene	n.d.	n.d.	n.d.	n.d.	.0052	.0553	n.d.	n.d.
dibenzo(a,h)anthracene	n.d.	n.d.	n.d.	n.d.	n.d.	n.d.	n.d.	n.d.
benzo(g,h,i)perylene	n.d.	n.d.	n.d.	.0515	.0074	n.d.	n.d.	n.d.

TABLE F-6: PAH particle-associated Water Concentrations measured at the Wolftrap site, Chesapeake Bay

WOLFTRAP SITE

PAH Particulate Water Concentrations (ng/l)

PAH	10-07-93	01-11-94	01-31-94	03-24-94	04-29-94	06-30-94	07-28-94	08-25-94	09-26-94
naphthalene	N.Q.	N.Q.	N.Q.	N.Q.	N.Q.	5.1817	2.0180	N.Q.	.5421
acenaphthylene	.0255	.0301	.0321	.0311	.0247	.0594	.0083	.0256	.0078
acenaphthene	.0478	n.d.	.0429	.0387	.0283	.1607	.0434	n.d.	n.d.
fluorene	.1074	.1254	.4809	.1153	.0881	.4791	.0846	.0746	.0518
phenanthrene	.4513	.4473	.5010	.3133	.2427	1.2770	.3703	.2233	.2154
anthracene	.0823	.0543	.0559	.0284	.0206	.0922	.0341	.0203	.0245
fluoranthene	.1451	.2693	.2557	.1959	.1018	.2954	.1445	.0887	.1316
pyrene	.1336	.2517	.2165	.1517	.1150	.6657	.1345	.0841	.2070
benzo(a)anthracene	.0769	.1064	.1066	.0801	.0636	.1240	.0596	.0186	.0451
chrysene	.1074	.1798	.1808	.1156	.0572	.1817	.0810	.0489	.0744
benzo(b)fluoranthene	.1399	.0621	.1680	.1352	.0642	.2505	.1112	.0583	.0989
benzo(k)fluoranthene	.1216	n.d.	.1546	.1167	.0495	.2252	.1012	.0679	.0955
benzo(e)pyrene	.1005	.1546	.1577	.1165	.0512	.2066	.0913	.0501	.0882
benzo(a)pyrene	.0985	.1492	.1546	.0976	.0392	.1669	.0714	.0340	.0699
indeno(1,2,3-cd)pyrene	.1615	.1752	.1778	.0156	.0591	.1635	.0724	n.d.	.0834
dibenzo(a,h)anthracene	n.d.	n.d.	.0311	n.d.	.0675	.0347	n.d.	n.d.	n.d.
benzo(g,h,i)perylene	.1151	.1488	.1646	.0203	.0617	.1773	.0862	.0433	.1054

PAH	10-28-94	12-01-94	01-13-95	01-27-95	02-23-95	04-06-95	05-01-95	05-22-95
naphthalene	N.Q.	.6500	.4690	.7463	N.Q.	.8432	N.Q.	N.Q.
acenaphthylene	.0083	.0154	.0058	.0141	.0136	.0216	N.Q.	.0151
acenaphthene	.0421	.0383	.0227	.0392	N.Q.	.0538	N.Q.	N.Q.
fluorene	.0451	.0856	.0560	.1311	.1029	.1935	N.Q.	.0977
phenanthrene	.1996	.3470	.2054	.5793	.3013	.6662	.1694	.3099
anthracene	.0218	.0358	.0157	.0759	.0280	.0736	.0244	.0258
fluoranthene	.1036	.1902	.0922	.3590	.1551	.3149	.1151	.1080
pyrene	.1060	.1619	.0673	.3014	.1171	.2877	.1001	.0993
benzo(a)anthracene	.0276	.0757	.0417	.1410	.0756	.1414	.0671	.0511
chrysene	.0733	.1191	.0414	.1846	.1048	.1968	.0911	.0658
benzo(b)fluoranthene	.0941	.1595	.0456	.2239	.1274	.2619	.1252	.0881
benzo(k)fluoranthene	.0837	.1516	.0339	.1799	.1091	.2101	.0986	.0710
benzo(e)pyrene	.0746	.1247	.0325	.1687	.0813	.1632	.0729	.0621
benzo(a)pyrene	.0534	.1191	.0321	.1829	.0256	.1669	.0652	.0593
indeno(1,2,3-cd)pyrene	.0519	.1085	.0508	.2575	.1064	.2342	.0958	.0777
dibenzo(a,h)anthracene	n.d.	n.d.	n.d.	.0337	.0156	.0382	.0177	.0107
benzo(g,h,i)perylene	.0623	.1117	.0452	.2223	.1081	.2615	.0956	.1062

TABLE F-7: PAH Particulate Water Concentrations measured at the York River Site

YORK RIVER SITE

PAH Particulate Water Concentrations (ng/l)

PAH	tank2								
	08-12-94	10-06-94	12-06-94	12-06-94	12-07-94	12-09-94	02-10-95	04-12-95	05-24-95
naphthalene	1.2296	.9574	.7981	.6203	1.5517	.7415	.9807	N.Q.	.7218
acenaphthylene	.0250	.0495	.0191	.0105	.0204	.0119	.0345	.0120	.0278
acenaphthene	.1364	.0699	.0709	.0522	.1336	.0349	.0422	N.Q.	.0429
fluorene	.1214	.1815	.1093	.0742	.1673	.0785	.0780	.0637	.1214
phenanthrene	.5528	.7786	.4755	.5184	.7062	.3600	.3133	.2364	.4790
anthracene	.0794	.1994	.0579	.0620	.0784	.0689	.0512	.0331	.2067
fluoranthene	.7691	1.4098	.5039	1.1162	.8644	.5264	.3070	.2029	.6965
pyrene	.5690	1.6790	.4305	.8490	.6682	.4841	.2558	.1891	.6483
benzo(a)anthracene	.2042	.5864	.1623	.2097	.2485	.2024	.1660	.1128	.3555
chrysene	.4975	.7801	.2753	.5420	.7121	.3799	.2296	.1629	.4706
benzo(b)fluoranthene	.4520	1.0790	.2960	.5301	.5593	.3733	.3193	.2452	.7161
benzo(k)fluoranthene	.3265	.7818	.2440	.4023	.3718	.3139	.2396	.1893	.6095
benzo(e)pyrene	.3760	1.0287	.2228	.3558	.3625	.2886	.1995	.1487	.5038
benzo(a)pyrene	.2440	.8134	.1967	.2679	.3223	.2828	.1949	.1362	.5130
indeno(1,2,3-cd)pyrene	.2859	.9459	.2198	.2818	.3544	.3022	.1129	.1737	.5683
dibenzo(a,h)anthracene	.0690	.1702	n.d.	.0338	.0621	.0485	.0458	.0471	.0976
benzo(g,h,i)perylene	.3421	1.2304	.27833	.3119	.3871	.2953	.1403	.1951	.5377

TABLE F-8: PAH Particulate Water Concentrations measured at the Haven Beach Site, Chesapeake Bay

HAVEN BEACH SITE

PAH Particulate Water Concentrations (ng/l)

PAH	tank2							
	05-10-94	05-22-94	06-26-94	06-28-94	06-29-94	11-05-94	11-08-94	
naphthalene	N.Q.	N.Q.	1.3763	2.4781	1.6212	N.Q.	N.Q.	.5826
acenaphthylene	n.d.	n.d.	.0402	.0750	.0402	.0148	.0133	.0176
acenaphthene	n.d.	n.d.	.0939	.1153	.1397	.0187	.0169	.0608
fluorene	.0885	1.1431	.1010	.1427	.9937	.0523	.0500	.0647
phenanthrene	.2511	1.1559	.5205	.7158	1.9598	.1798	.1812	.2851
anthracene	.0258	.7221	.0758	.1223	.1005	.0220	.0234	.0456
fluoranthene	.2463	.3361	1.1262	.9517	.6573	.2448	.2865	.4188
pyrene	.2670	.2851	.9646	.8999	.7191	.2464	.2894	.3851
benzo(a)anthracene	.1100	.6174	.3134	.3342	.4257	.0930	.0922	.1569
chrysene	.1618	.1767	.6435	.6342	.3292	.1622	.1611	.2745
benzo(b)fluoranthene	.1703	.1921	.7911	.9685	.3227	.1617	.1578	.3271
benzo(k)fluoranthene	.1943	.1782	.7697	.9359	.2640	.1369	.1398	.3337
benzo(e)pyrene	.1833	.2242	.6115	.7406	.3173	.1539	.1547	.2727
benzo(a)pyrene	.1572	.1947	.5105	.5639	.2445	.1329	.1448	.2130
indeno(1,2,3-cd)pyrene	n.d.	.1847	.4475	.5230	.2732	.1380	.1343	.2185
dibenzo(a,h)anthracene	n.d.	.0477	.1097	n.d.	.0743	.0279	.0991	n.d.
benzo(g,h,i)perylene	.2106	.1932	.4715	.5613	.2939	.1357	.1310	.2092

TABLE F-9: PAH particle-associated Water Concentrations measured at the Elizabeth River site

Elizabeth River Site

PAH particle-associated Water Concentrations (ng/l)

PAH	07-15-94	09-08-94	11-12-94	01-09-95	03-11-95	05-04-95
naphthalene	1.6764	1.8933	1.4611	n.a.	2.0389	1.4409
acenaphthylene	.0367	.0459	.0238	n.a.	.0860	.0504
acenaphthene	.2670	.2728	.1594	n.a.	.5390	.2826
fluorene	.3856	.3904	.2403	n.a.	.6227	.4309
phenanthrene	1.2856	1.2803	.8825	n.a.	2.3046	1.3092
anthracene	.3596	.3557	.2503	n.a.	.6389	.4486
fluoranthene	3.1682	2.3629	1.5932	n.a.	10.1574	3.0817
pyrene	2.2745	1.9935	1.6403	n.a.	8.5667	2.9722
benzo(a)anthracene	1.1584	.8145	.5553	n.a.	2.5708	1.2300
chrysene	2.3925	1.3209	.8987	n.a.	3.9513	1.9010
benzo(b)fluoranthene	2.3177	1.5761	1.1603	n.a.	4.2762	2.6772
benzo(k)fluoranthene	1.6115	1.1650	.8530	n.a.	3.5148	2.0348
benzo(e)pyrene	2.0135	1.4847	.9022	n.a.	2.9003	1.8571
benzo(a)pyrene	.9299	.9708	.7228	n.a.	2.3693	1.4081
indeno(1,2,3-cd)pyrene	.9900	.9871	.6885	n.a.	2.4355	1.4006
dibenzo(a,h)anthracene	.2349	.2307	.1231	n.a.	.5178	.2943
benzo(g,h,i)perylene	1.0235	1.0167	.6926	n.a.	2.3556	1.3673

TABLE F-10: PAH particle-associated Water concentrations measured at the Hampton site, Chesapeake Bay

HAMPTON SITE

PAH Particle-associated Water Concentrations (ng/l)

PAH	07-15-94	09-09-94	11-12-94	01-09-95	03-11-95	05-04-95
naphthalene	1.3149	.6527	2.1873	.6125	N.Q.	N.Q.
acenaphthylene	.0164	.0259	.0454	.0079	.0156	.0136
acenaphthene	.0418	.0306	.0934	.0204	N.Q.	N.Q.
fluorene	.0672	.0822	.1208	.0503	.0759	N.Q.
phenanthrene	.2540	.3638	.5132	.2432	.3228	.2063
anthracene	.0347	.0783	.0942	.0324	.0286	.0251
fluoranthene	.3083	.5379	.5483	.2292	.2803	.2211
pyrene	.2586	.4830	.4814	.1594	.1835	.2068
benzo(a)anthracene	.1070	.2265	.2536	.0754	.0953	.1241
chrysene	.1854	.3986	.3756	.1210	.1476	.1830
benzo(b)fluoranthene	.2028	.3965	.4907	.1362	.1696	.2488
benzo(k)fluoranthene	.1578	.3135	.4158	.1016	.1470	.2134
benzo(e)pyrene	.1848	.3648	.3533	.0965	.1208	.1629
benzo(a)pyrene	.1432	.2833	.3570	.0906	.1202	.1662
indeno(1,2,3-cd)pyrene	.1770	.3248	.4763	.1220	.1700	.2194
dibenzo(a,h)anthracene	.0438	.0490	.0689	.0261	.0257	.0342
benzo(g,h,i)perylene	.1825	.3632	.4170	.1098	.1494	.2113

Appendix G: Instantaneous Gaseous Flux Data for PAHs Across the Air-water Interface of Southern Chesapeake Bay

TABLE G-1: PAH Gas Exchange Fluxes across the Air-Water Interface, Wolftrap Site, Chesapeake Bay

WOLFTRAP SITE

PAH Gas Exchange Flux (ng/m²*day)

PAH	10-07-93	01-11-94	01-31-94	03-24-94	04-29-94	06-30-94	07-28-94	08-25-94	09-26-94
naphthalene	1526.099	1885.140	8120.446	4281.805	2719.581	2000.702	1865.129	1380.870	1630.307
acenaphthylene	n.q.	-76.205	-444.881	104.406	n.q.	29.710	36.518	22.348	18.676
acenaphthene	69.770	4.003	-165.499	142.420	97.498	117.990	128.513	83.527	68.819
fluorene	135.429	-34.771	-269.353	393.349	400.358	602.576	616.907	354.855	221.926
phenanthrene	-50.999	-322.258	-2195.630	64.821	-77.221	435.786	525.180	249.430	207.188
anthracene	n.q.	n.q.	n.q.	n.q.	n.q.	17.228	19.852	9.863	n.q.
fluoranthene	-52.416	-75.440	-232.044	-61.420	-82.803	-33.194	-29.422	-31.007	4.904
pyrene	-76.108	-75.650	-181.514	-89.221	-181.593	-49.145	-40.648	-41.074	2.357
benzo(a)anthracene	n.q.	n.q.	n.q.	n.q.	n.q.	n.q.	n.q.	n.q.	n.q.
chrysene	-696	n.q.	-5.677	-1.458	-1.737	2.407	2.649	2.802	6.050
benzo(b)fluoranthene	n.q.	n.q.	-.543	-.625	-.560	n.q.	n.q.	n.q.	-.554
benzo(k)fluoranthene	n.q.	n.q.	n.q.	n.q.	n.q.	n.q.	n.q.	n.q.	n.q.
benzo(e)pyrene	N.Q.	n.q.	n.q.	N.Q.	N.Q.	n.q.	n.q.	n.q.	N.Q.
benzo(a)pyrene	n.q.	n.q.	n.q.	-.174	n.q.	n.q.	n.q.	n.q.	n.q.
indeno(1,2,3-cd)pyrene	n.q.	n.q.	n.q.	n.q.	n.q.	n.q.	n.q.	n.q.	n.q.
dibenzo(a,h)anthracene	n.q.	n.q.	n.q.	n.q.	n.q.	n.q.	n.q.	n.q.	n.q.
benzo(g,h,i)perylene	-1.833	n.q.	n.q.	n.q.	n.q.	n.q.	n.q.	n.q.	n.q.

PAH	10-28-94	12-01-94	01-13-95	01-27-95	02-23-95	04-06-95	05-01-95	05-22-95
naphthalene	1335.226	4802.371	2993.234	3055.539	4596.334	2475.835	3783.023	1850.821
acenaphthylene	21.625	83.817	37.814	-24.356	2.555	24.901	n.q.	48.770
acenaphthene	41.529	96.090	95.860	28.307	-23.277	43.413	40.229	94.432
fluorene	101.281	219.184	98.145	39.759	-153.314	144.146	71.834	369.345
phenanthrene	21.135	190.579	-130.020	-218.445	-366.367	105.867	45.994	310.194
anthracene	n.q.	n.q.	n.q.	n.q.	n.q.	n.q.	n.q.	8.336
fluoranthene	-37.961	-8.199	-40.644	-69.578	-152.601	-27.132	-8.905	-43.834
pyrene	-55.235	-10.948	-90.533	-49.230	-74.571	-20.191	-15.615	-28.909
benzo(a)anthracene	n.q.	n.q.	n.q.	n.q.	n.q.	n.q.	n.q.	n.q.
chrysene	-7.114	-1.897	-1.694	-.311	-2.407	-.321	n.q.	-.049
benzo(b)fluoranthene	-1.508	n.q.	n.q.	n.q.	-.352	-.468	-.486	-.321
benzo(k)fluoranthene	-.770	n.q.	n.q.	n.q.	n.q.	n.q.	n.q.	n.q.
benzo(e)pyrene	N.Q.	N.Q.	n.q.	n.q.	N.Q.	N.Q.	N.Q.	N.Q.
benzo(a)pyrene	n.q.	n.q.	n.q.	n.q.	n.q.	n.q.	n.q.	n.q.
indeno(1,2,3-cd)pyrene	n.q.	n.q.	n.q.	n.q.	n.q.	n.q.	n.q.	n.q.
dibenzo(a,h)anthracene	n.q.	n.q.	n.q.	n.q.	n.q.	n.q.	n.q.	n.q.
benzo(g,h,i)perylene	n.q.	n.q.	n.q.	n.q.	n.q.	n.q.	n.q.	n.q.

